Forum of Mathematics, Sigma (2025), **Vol. 13**:e133 1–68
doi:10.1017/fms.2025.10069

CAMBRIDGE UNIVERSITY PRESS

RESEARCH ARTICLE

Metallic mean Wang tiles I: self-similarity, aperiodicity and minimality

Sébastien Labbé

CNRS, LaBRI, UMR 5800, Université de Bordeaux, 351, cours de la Libération, F-33400, Talence, France;
E-mail: sebastien.labbe@labri.fr.

Received: 11 March 2024; **Revised:** 11 April 2025; **Accepted:** 8 May 2025

2020 Mathematics Subject Classification: *Primary* – 52C23; *Secondary* – 37B51, 11B39

Abstract

For every positive integer n, we introduce a set $\mathcal{T}_n$ made of $(n+3)^2$ Wang tiles (unit squares with labeled edges). We represent a tiling by translates of these tiles as a configuration $\mathbb{Z}^2 \to \mathcal{T}_n$. A configuration is valid if the common edge of adjacent tiles has the same label. For every $n \geq 1$, we show that the Wang shift Ω_n, defined as the set of valid configurations over the tiles $\mathcal{T}_n$, is self-similar, aperiodic and minimal for the shift action. We say that $\{\Omega_n\}_{n\geq 1}$ is a family of metallic mean Wang shifts, since the inflation factor of the self-similarity of Ω_n is the positive root of the polynomial $x^2 - nx - 1$. This root is sometimes called the n-th metallic mean, and in particular, the golden mean when $n = 1$, and the silver mean when $n = 2$. When $n = 1$, the set of Wang tiles $\mathcal{T}_1$ is equivalent to the Ammann aperiodic set of 16 Wang tiles.

Contents

1. Introduction

One of the most well-known aperiodic tilings was discovered by Penrose. In its original version, four shapes derived from the regular pentagon can be used to tile the plane, and none of the allowed tilings are periodic [48]. Penrose tilings were soon given an equivalent description in terms of multigrids or cut and project schemes [12]; see also [24, §10] and [5, §6.2]. The aperiodic structure of Penrose tilings is explained by the properties of a specific irrational number: the positive root φ of the polynomial $x^2 - x - 1$, also known as the golden ratio or golden mean. For example, in the kite-and-dart version of the Penrose tilings, the ratio of kites to darts is equal to the golden ratio [49].

Recently, the discovery of an aperiodic monotile [58] attracted a lot of attention [60, 6, 2]. Smith and coauthors presented a single shape, a 13-edge polygon called the hat, whose isometric copies tile the plane but never periodically. Again, the golden ratio appears in tilings by the hat. In a tiling by isometric copies of the hat, both the hat and its mirror image appear (up to orientation preserving isometries – that is, translations and rotations). The frequency of the hat and its mirror image in a tiling are not equal. The ratio of the most frequent orientation of the hat to the least frequent one is equal to the fourth power of the golden ratio.[1] Two months later, the same authors discovered another aperiodic tile called Spectre, which does not need its mirror image to tile the plane [59]. Tilings by the Spectre are not all combinatorially equivalent to tilings by the hat: some are periodic (if the reflected tile is allowed). But every tiling by the hat tile is combinatorially equivalent to some Spectre tiling.

Other examples of aperiodic tilings are related to the golden mean, including Ammann A2 L-shaped tiles [4] (also studied in [1, 15]); see Figure 1. The golden mean also appears in the description of tilings generated by the Jeandel–Rao aperiodic set of 11 Wang tiles [26]: the frequency of the tiles [34], the

[1]The figure [58, Fig. 2.11] shows a substitution where the image of a shape H_7 contains 5 shapes H_8 and 1 shape H_7 and the image of the shape H_8 contains 6 shapes H_8 and 1 shape H_7. Shape H_7 contains 6 hats and 1 anti-hats; shape H_8 contains 7 hats and 1 anti-hats. We compute that the Perron–Frobenius dominant right-eigenvector $\begin{pmatrix} -3\varphi+5 \\ 3\varphi-4 \end{pmatrix}$ of the incidence matrix $\left(\begin{smallmatrix} 1 & 1 \\ 5 & 6 \end{smallmatrix}\right)$ of the substitution is mapped to $\begin{pmatrix} \varphi^4 \\ 1 \end{pmatrix}$ by the matrix $\left(\begin{smallmatrix} 6 & 7 \\ 1 & 1 \end{smallmatrix}\right)$.

https://doi.org/10.1017/fms.2025.10069 Published online by Cambridge University Press

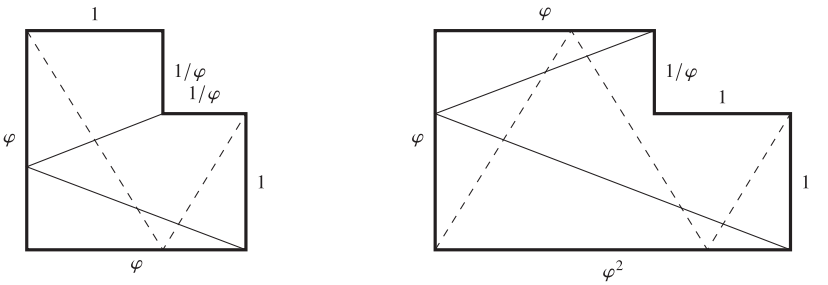

Figure 1. *Two shapes belonging to the Ammann A2 family. The matching conditions are given by what are called Ammann bars appearing as dashed and solid lines in the interior of the tiles and which must continue straight across the edges of the tiling. This is a reproduction of Figure 10.4.1 from [24]. See also Figure 12 from [1].*

inflation factor of its self-similarity [33, 35], and the slopes of its nonexpansive directions [36] are all expressed in $\mathbb{Q}(\phi)$.

It is then natural to ask whether there are aperiodic tilings out there such that the ratios of tile frequencies are not in $\mathbb{Q}(\varphi)$. It turns out that there are many. Recall that the first examples of aperiodic tilings provided by Berger [8], simplified by Knuth [30] and Robinson [53], are described by substitutions whose inflation factor is an integer (2 in this case). Many other substitutive and aperiodic planar tilings have an integer inflation factor and are listed in [5, §6.4]. It includes the chair tiling [52], the sphinx tiling [63], the $(1+\varepsilon+\varepsilon^2)$-tiling [50] and the Taylor and Socolar-Taylor tilings [61].

Many substitution tilings with non-integer inflation factor are known. Various types of planar aperiodic substitution tilings with n-fold rotational symmetry involving cyclotomic numbers were described in recent years [22, 29, 17, 47, 28]; see the sections [18, §1.7] and [5, §7.3]. Examples of algebraic non-Pisot aperiodic tilings were portrayed in [5, §6.5]. Moreover, substitution tilings with transcendental inflation factor were recently proposed in [19] using compact alphabets.

Closer to golden mean are other algebraic integers, starting with those of degree two, for which aperiodic tilings exist. In Ammann A4 and A5 aperiodic tilings [24], the ratio of frequency of the two involved tiles is $\sqrt{2}$ [4, p. 22]. Nowadays these tilings are known as Ammann–Beenker tilings [5, §6.1] since their algebraic properties were independently described in [7]. In [4], the question whether there exist sets of aperiodic prototiles associated with irrational numbers other than $\sqrt{2}$ and the golden ratio was mentioned. But they had '*no conjecture concerning the characterization of all numbers that are possible for such ratios*' of frequencies of tiles.

The inflation factor of Ammann–Beenker substitution tilings is $1+\sqrt{2}$ [5, Prop. 6.2]. This number is sometimes called the silver mean because its continued fraction expansion is $[2;2,2,\dots]$, where that of the golden mean is $[1;1,1,\dots]$. The golden mean and the silver mean belong to a larger family made of the positive root of the polynomial x^2-nx-1, where n is a positive integer:

$$\beta_n = \frac{n+\sqrt{n^2+4}}{2} = n + \cfrac{1}{n + \cfrac{1}{n + \cfrac{1}{\dots}}}.$$

We refer to this root as the n^{th} **metallic mean** [46]. These numbers were called silver means [56] and noble means in [5, §4.4] (note that noble numbers was already defined in [56, Appendix B, p. 392–394] for a different meaning). Observe also that the definition of metallic means from [13] is larger, as it contains all positive roots of polynomial x^2-px-q, where p and q are positive integers. In this contribution, we consider only the metallic means, in the sense of de Spinadel, which are algebraic units; that is, $p \geq 1$ and $q = 1$.

https://doi.org/10.1017/fms.2025.10069 Published online by Cambridge University Press

When a tiling space is preserved by a substitution, it is also preserved by powers of this substitution. Since odd-powers of metallic means are metallic means, we know substitution tilings for infinitely many other metallic means. In particular, the inflation factor of the third power of the substitution for Penrose tilings is the 4^{th} metallic mean $\beta_1^3 = \beta_4$. Also, the inflation factor of the third power of the substitution for Ammann–Beenker tilings is the cube of the silver ratio, which is the 14^{th} metallic mean $\beta_2^3 = \beta_{14}$, etc. For more information, we refer the reader to the OEIS [45] where indices of metallic means that are powers of other metallic means are listed as sequence A352403.

In recent years, new discoveries were made in the theory of quasicrystals related to metallic mean numbers. A self-similar hexagonal quasicrystal whose inflation factor is the 3^{rd} metallic mean (also called bronze-mean) was described in [14]. It is given by a substitution rule involving a small and a large equilateral triangles and a rectangle; see [20]. Their construction was further extended to every $(3n)^{th}$ metallic mean in [44] where $n \geq 1$ is a positive integer.

Our contribution

In this contribution, we introduce a new family of aperiodic tiles using the oldest known shape for aperiodic tiles: the unit square. Unit squares with labeled edges and tilings of the plane by infinitely many translated copies of them were considered by Wang [66] with the condition that adjacent tiles must share the same label on the common edge. Such tiles are nowadays called **Wang tiles**. A set of Wang tiles is **aperiodic** if it admits at least one valid tiling, and none of them is periodic. The first known aperiodic set of tiles was discovered by Berger [8]: a set of 20426 Wang tiles. Many smaller examples were discovered thereafter, and we refer the reader to [26] for an overview of these developments leading to the discovery of the smallest possible size (= 11) for an aperiodic set of Wang tiles.

For every positive integer n, we construct a set $\mathcal{T}_n$ made of $(n+3)^2$ Wang tiles, and we consider the subshift Ω_n defined as the set of valid configurations $\mathbb{Z}^2 \to \mathcal{T}_n$ over these tiles. We also say that Ω_n is a **Wang shift** because it is a subshift defined from a set of Wang tiles. The set $\mathcal{T}_n$ is the disjoint union of 5 sets of tiles:

- n^2 white tiles,
- n yellow horizontal stripe tiles and n yellow vertical stripe tiles,
- n blue horizontal stripe tiles and n blue vertical stripe tiles,
- $n+1$ green horizontal overlap tiles and $n+1$ green vertical overlap tiles,
- 7 junction tiles.

We observe that the sum of cardinalities of the five subsets is $n^2 + 2n + 2n + 2(n+1) + 7 = (n+3)^2$. The sets $\mathcal{T}_n$ of Wang tiles for $n = 1, 2, 3, 4, 5$ are shown in Figure 2, and rectangular valid tilings over the sets $\mathcal{T}_n$ for $n = 1, 2, 3, 4$ are shown in Figure 3, Figure 4, Figure 5 and Figure 6.

The family of Wang shift $(\Omega_n)_{n\geq 1}$ has too many nice properties to hold in one article. In this first article dedicated to its study, we focus on its substitutive properties. Its dynamical properties and the consideration of $\mathcal{T}_n$ as the set of instances of a computer chip will be considered separately in a follow-up contribution.

The main result of the current contribution is to prove that the Wang shift Ω_n is self-similar for every integer $n \geq 1$. The self-similarity is given by a 2-dimensional substitution over an alphabet of size $(n+3)^2$. The self-similarity is not a bijection, but informally it is essentially one. This is formalized with the terminology of recognizability (one-to-one up to a shift) and surjectivity up to a shift. See Section 2 for the definition of Wang shifts and Section 3 for the definition of 2-dimensional substitutions, self-similarity and recognizability.

Theorem A. *For every integer $n \geq 1$, the set $\mathcal{T}_n$ containing $(n+3)^2$ Wang tiles defines a Wang shift Ω_n which is self-similar. More precisely, there exists an expansive and recognizable 2-dimensional substitution $\omega_n : \Omega_n \to \Omega_n$ which is onto up to a shift – that is, such that $\Omega_n = \overline{\omega_n(\Omega_n)}^{\sigma}$.*

https://doi.org/10.1017/fms.2025.10069 Published online by Cambridge University Press

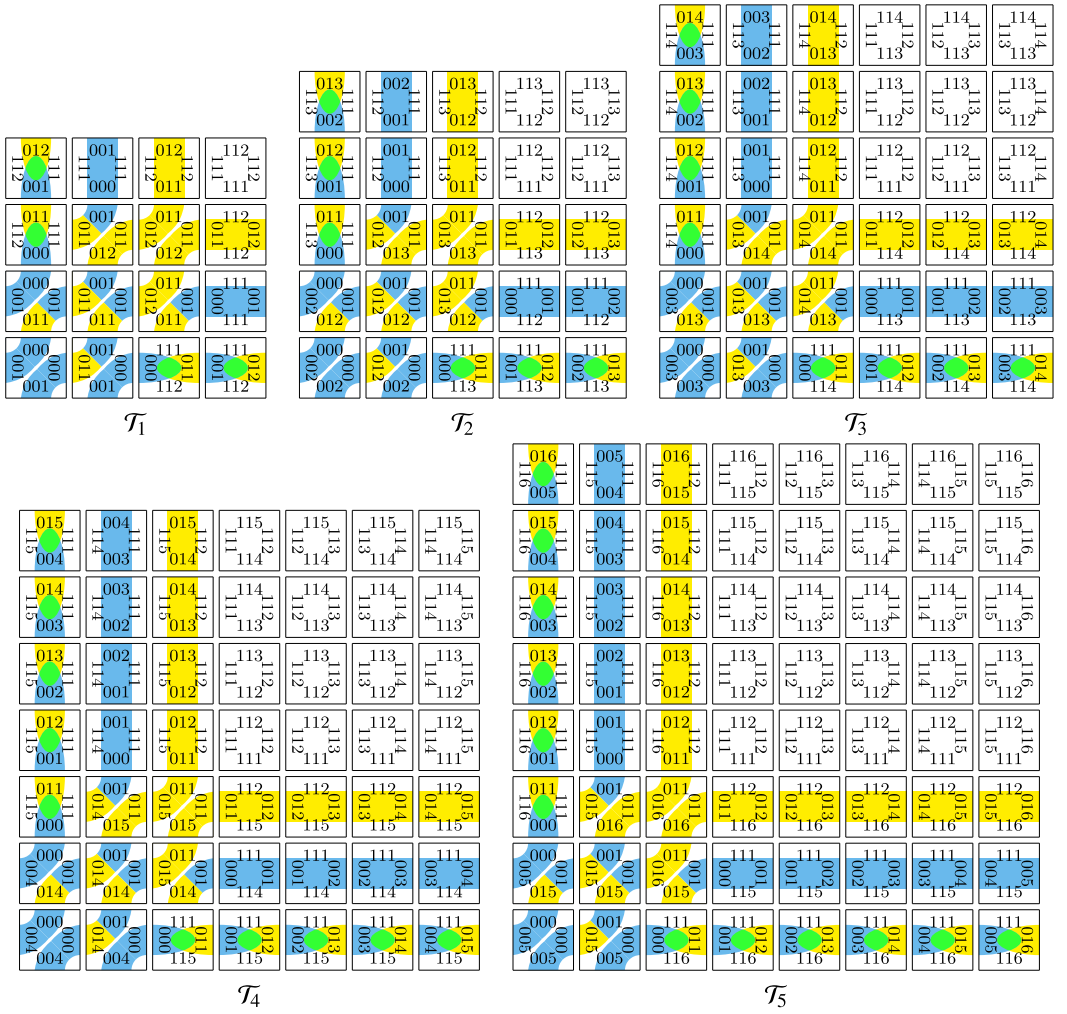

Figure 2. *Metallic mean Wang tile sets $\mathcal{T}_n$ for $n = 1, 2, 3, 4, 5$.*

The proof of Theorem A is the same for every integer $n \geq 1$. Indeed, we show that every configuration in Ω_n can be decomposed uniquely into rectangular blocks that we call return blocks. These return blocks and their right, top, left and bottom labels are in bijection with an extended set $\mathcal{T}_n' \supset \mathcal{T}_n$ of Wang tiles. Then we show that in the extended Wang shift $\Omega_n' \supseteq \Omega_n$ defined from the extended set $\mathcal{T}_n'$ of Wang tiles, only the tiles in $\mathcal{T}_n$ appear. Thus, $\Omega_n' \subseteq \Omega_n$. This shows that $\Omega_n = \Omega_n'$ and that Ω_n is self-similar.

As a corollary, we deduce that the Wang shift Ω_n is aperiodic.

Corollary B. *For every integer $n \geq 1$, the Wang shift Ω_n is aperiodic.*

Our second result is that the self-similarity is primitive. As in the 1-dimensional case, we say that a 2-dimensional substitution ω is primitive if there exists $m \in \mathbb{N}$ such that, for every $a, b \in \mathcal{A}$, the letter b occurs in $\omega^m(a)$.

Theorem C. *For every integer $n \geq 1$, the 2-dimensional substitution $\omega_n : \Omega_n \to \Omega_n$ is primitive. The Perron–Frobenius dominant eigenvalue of the incidence matrix of ω_n is β_n^2, the square of the n^{th} metallic mean number, and the inflation factor of ω_n is β_n.*

https://doi.org/10.1017/fms.2025.10069 Published online by Cambridge University Press

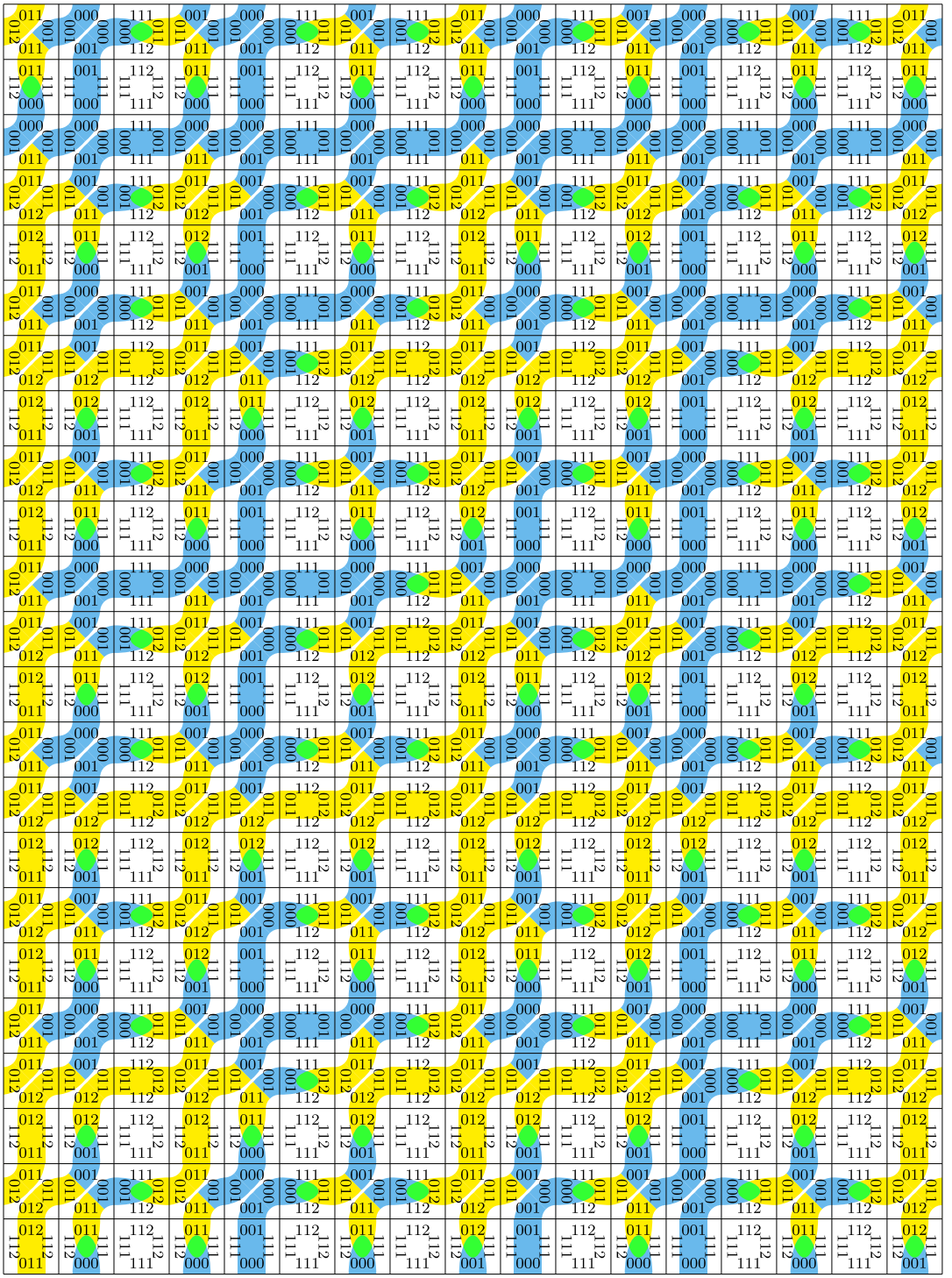

Figure 3. *A valid* 17×23 *pattern with Wang tile set* $\mathcal{T}_1$.

https://doi.org/10.1017/fms.2025.10069 Published online by Cambridge University Press

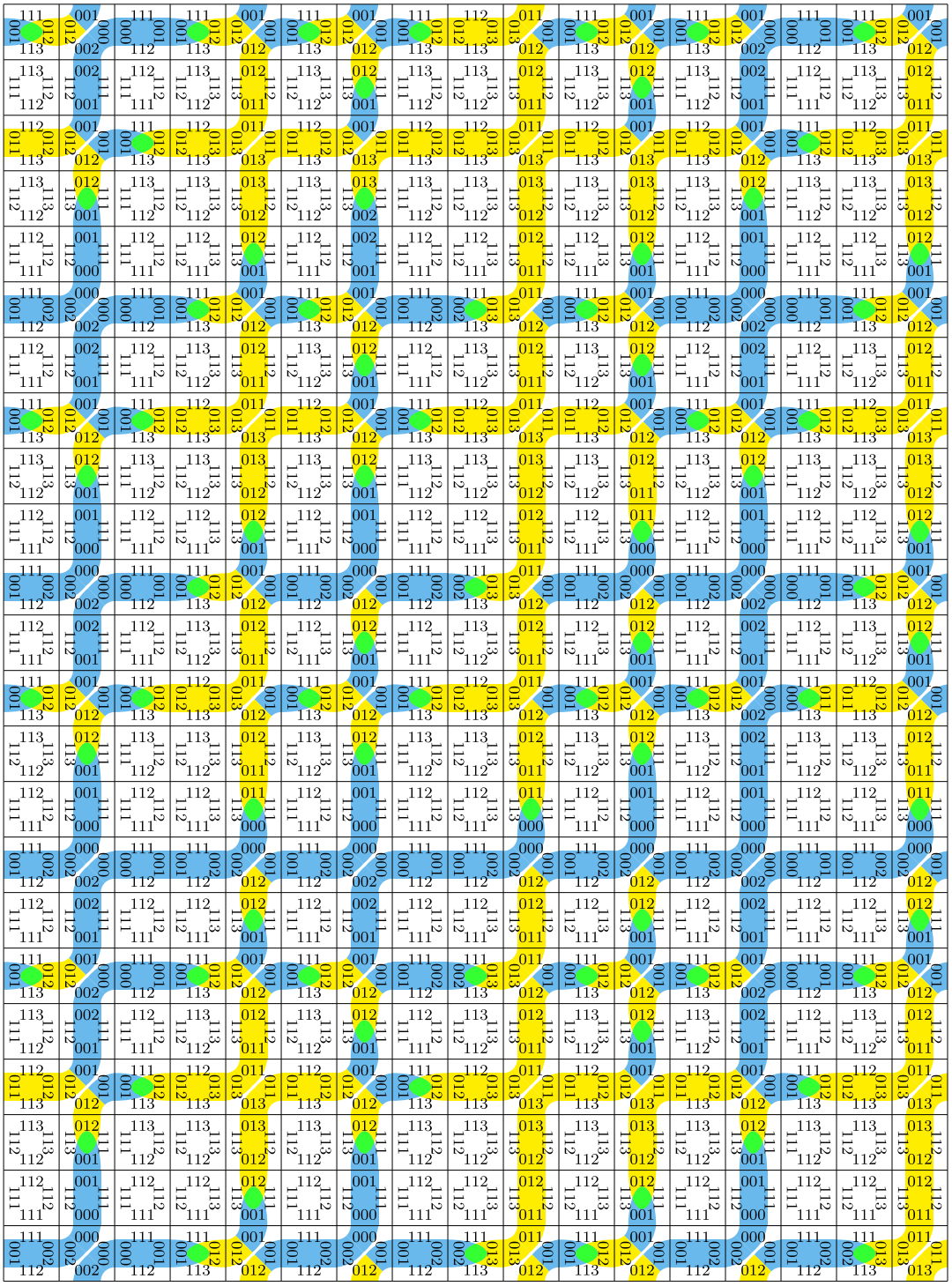

Figure 4. *A valid* 17×23 *pattern with Wang tile set* $\mathcal{T}_2$.

https://doi.org/10.1017/fms.2025.10069 Published online by Cambridge University Press

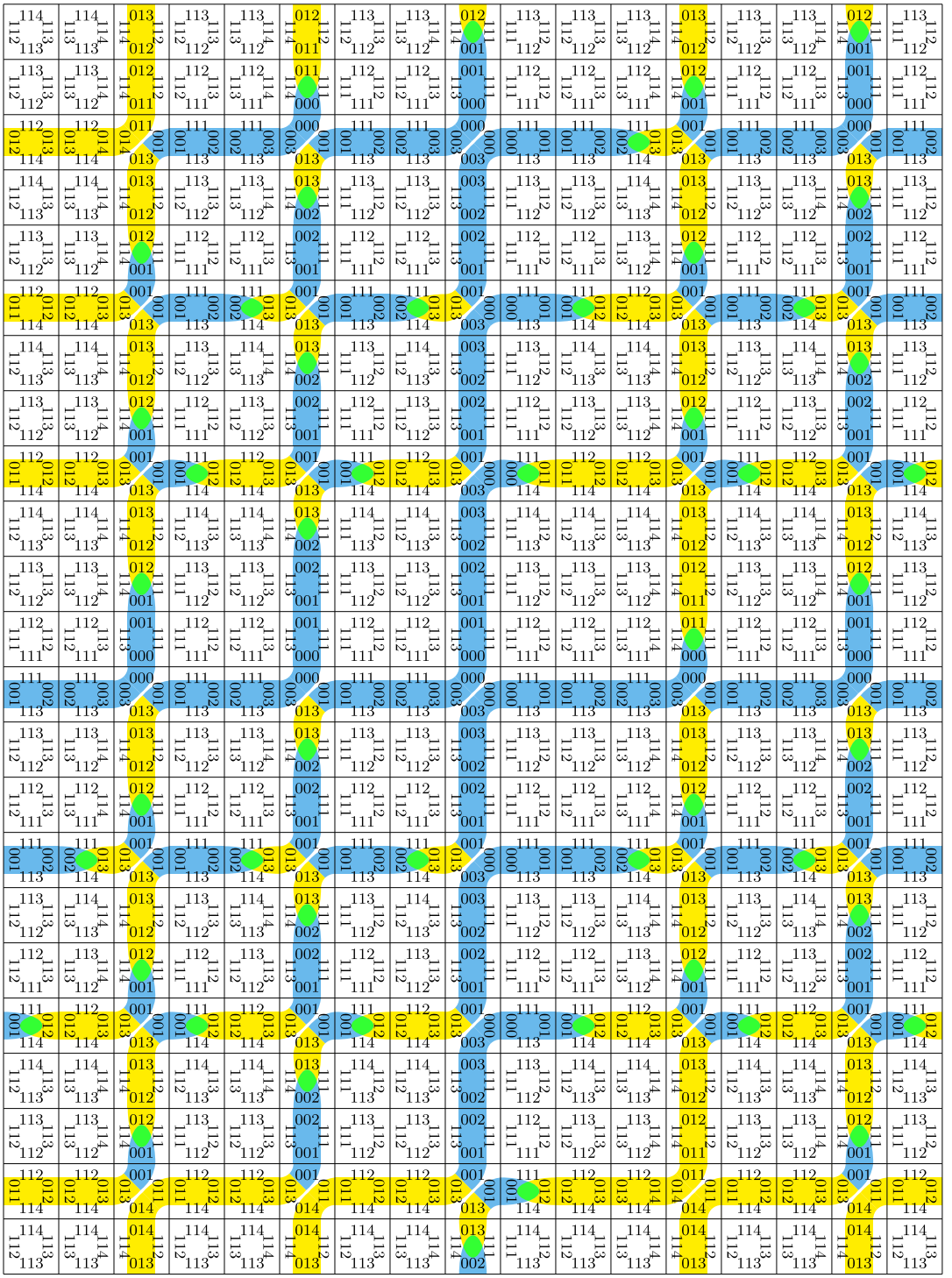

Figure 5. *A valid* 17×23 *pattern with Wang tile set* $\mathcal{T}_3$.

https://doi.org/10.1017/fms.2025.10069 Published online by Cambridge University Press

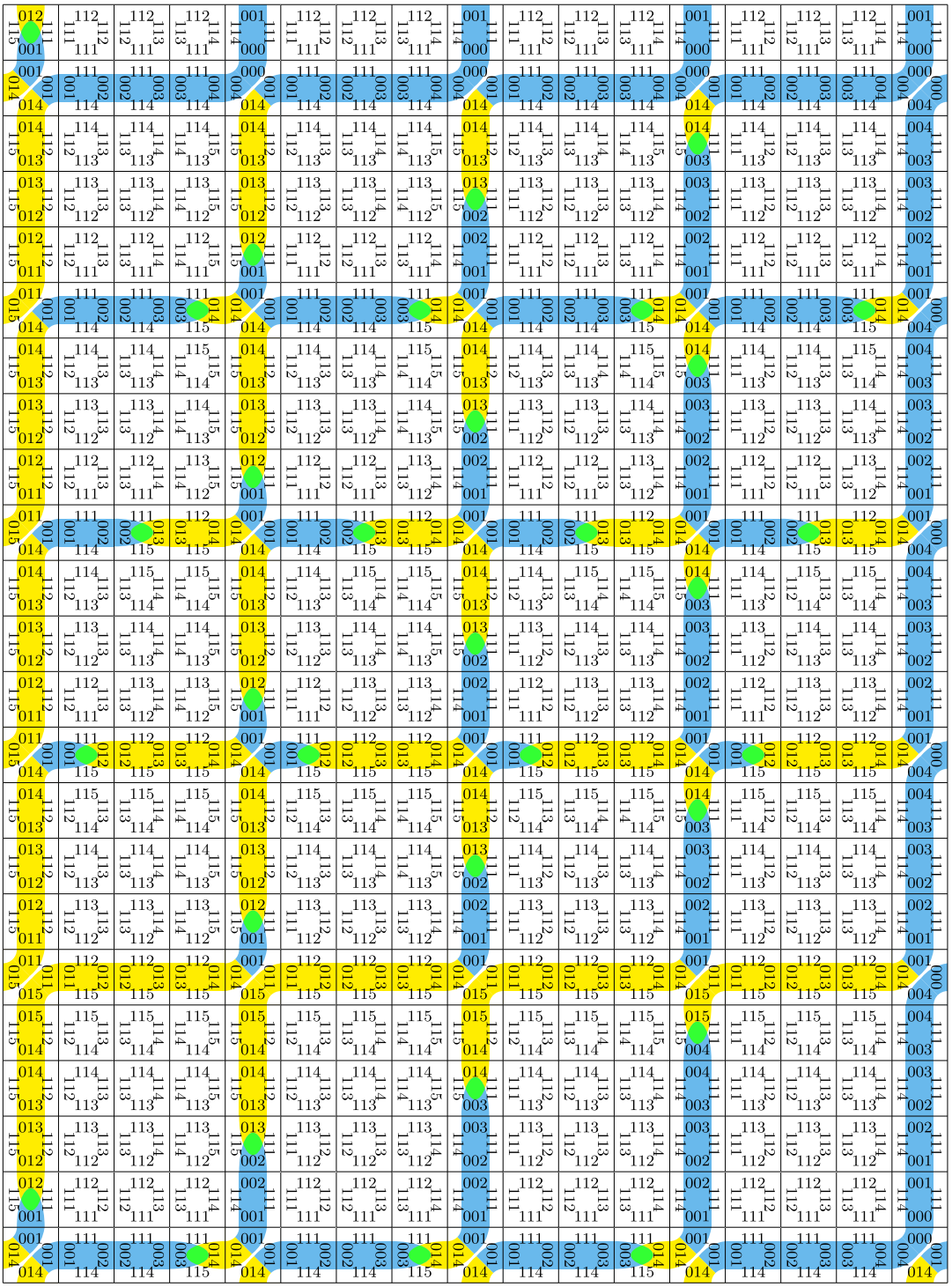

Figure 6. *A valid* 17×23 *pattern with Wang tile set* $\mathcal{T}_4$.

https://doi.org/10.1017/fms.2025.10069 Published online by Cambridge University Press

Our third result is that the Wang shift Ω_n is minimal; that is, if $X \subseteq \Omega_n$ is a nonempty closed shift-invariant subset, then $X = \Omega_n$. Equivalently, every shift orbit is dense, which implies that every configuration in ω_n is uniformly recurrent. Every small set of aperiodic Wang tiles does not satisfy this property. For instance, the Robinson Wang shift is not minimal [21], and neither is the Jeandel–Rao Wang shift [35]. The proof of minimality is based on a criterion involving the patterns of shapes 1×2, 2×1 and 2×2 and their images under the substitution; see Lemma 10.4.

Theorem D. *For every integer $n \geq 1$, the Wang shift Ω_n is minimal and is equal to the substitutive subshift $\Omega_n = \mathcal{X}_{\omega_n}$.*

In a tiling of the plane by the two shapes shown in Figure 1 respecting the matching condition, there appear what are called Ammann bars. In this case, the slopes of the Ammann bars take four different values: two slope values for the dashed Ammann bars and two slope values for the solid Ammann bars. As explained in [24, p.594–598], the solid bars can be regarded as the edges of a new tiling by rhombs and parallelograms, for which the dashed bars can be regarded as markings on the tiles specifying the matching conditions. Sixteen parallelogram tiles arise from this construction which can be recoded as 16 Wang tiles. As we show in Theorem E, the Ammann 16 Wang tiles are equivalent to $\mathcal{T}_1$, the first member of the family $\mathcal{T}_n$ when $n = 1$.

Theorem E. *When $n = 1$, the set $\mathcal{T}_n$ is equal, up to symbol relabeling, to the Ammann set of 16 Wang tiles.*

Thus, the family $(\mathcal{T}_n)_{n\geq 1}$ can be considered as an extension of the Ammann set of Wang tiles to the metallic mean numbers.

Structure of the article

In Section 2, we present preliminaries on dynamical systems, subshifts and Wang shifts. In Section 3, we recall definitions of 2-dimensional substitutions. In Section 4, we introduce two Wang shifts $\Omega_n \subseteq \Omega'_n$ defined by the sets $\mathcal{T}_n \subseteq \mathcal{T}'_n$ of Wang tiles. In Section 5, we define two substitutions $\omega'_n : \Omega'_n \to \Omega'_n$ and $\omega_n : \Omega_n \to \Omega_n$. In Section 6, we describe the return blocks in the Wang shifts Ω_n and Ω'_n, and we prove that every configuration in the Wang shift Ω_n can be desubstituted into a configuration from Ω'_n. In Section 7, we prove that tiles in $\mathcal{T}'_n \setminus \mathcal{T}_n$ do not appear in configurations of Ω'_n. Thus, $\Omega'_n \subseteq \Omega_n$. Observe that Section 7 depends on the results from Section 5 and Section 6. In Section 8, we prove that Ω_n is self-similar and aperiodic. In Section 9, we prove that the self-similarity is primitive. In Section 10, we prove that Ω_n is minimal. In Section 11, we state some questions raised by the current work. The article finishes with two appendices. Section A (Appendix A) gathers pictures of the substitutions ω_n for $1 \leq n \leq 5$. In Section B (Appendix B), we prove the self-similarity of Ω_n when $n = 2$ using computer explorations.

2. Preliminaries on Wang shifts

This section follows the preliminary section of the chapter [37].

2.1. Topological dynamical systems

Most of the notions introduced here can be found in [65]. A **dynamical system** is a triple (X, G, T), where X is a topological space, G is a topological group and T is a continuous function $G \times X \to X$ defining a left action of G on X: if $x \in X$, e is the identity element of G and $g, h \in G$, then using additive notation for the operation in G, we have $T(e, x) = x$ and $T(g + h, x) = T(g, T(h, x))$. In other words, if one denotes the transformation $x \mapsto T(g, x)$ by T^g, then $T^{g+h} = T^g T^h$. In this work, we consider the Abelian group $G = \mathbb{Z} \times \mathbb{Z}$.

If $Y \subset X$, let $\overline{Y}$ denote the topological closure of Y and let $\overline{Y}^T := \cup_{g\in G} T^g(Y)$ denote the T-closure of Y. A subset $Y \subset X$ is **T-invariant** if $\overline{Y}^T = Y$. A dynamical system (X, G, T) is called **minimal** if X

https://doi.org/10.1017/fms.2025.10069 Published online by Cambridge University Press

does not contain any nonempty, proper, closed T-invariant subset. The left action of G on X is **free** if $g = e$ whenever there exists $x \in X$ such that $T^g(x) = x$.

Let (X, G, T) and (Y, G, S) be two dynamical systems with the same topological group G. A **homomorphism** $\theta : (X, G, T) \to (Y, G, S)$ is a continuous function $\theta : X \to Y$ satisfying the commuting property that $S^g \circ \theta = \theta \circ T^g$ for every $g \in G$. A homomorphism $\theta : (X, G, T) \to (Y, G, S)$ is called an **embedding** if it is one-to-one, a **factor map** if it is onto, and a **topological conjugacy** if it is both one-to-one and onto and its inverse map is continuous. If $\theta : (X, G, T) \to (Y, G, S)$ is a factor map, then (Y, G, S) is called a **factor** of (X, G, T) and (X, G, T) is called an **extension** of (Y, G, S). Two dynamical systems are **topologically conjugate** if there is a topological conjugacy between them.

2.2. Subshifts and shifts of finite type

In this section, we introduce multidimensional subshifts, a particular type of dynamical systems [40, §13.10], [55, 39, 25]. Let $\mathcal{A}$ be a finite set, $d \geq 1$, and let $\mathcal{A}^{\mathbb{Z}^d}$ be the set of all maps $x : \mathbb{Z}^d \to \mathcal{A}$, equipped with the compact product topology. An element $x \in \mathcal{A}^{\mathbb{Z}^d}$ is called **configuration**, and we write it as $x = (x_{\boldsymbol{m}}) = (x_{\boldsymbol{m}} : \boldsymbol{m} \in \mathbb{Z}^d)$, where $x_{\boldsymbol{m}} \in \mathcal{A}$ denotes the value of x at $\boldsymbol{m}$. The topology on $\mathcal{A}^{\mathbb{Z}^d}$ is compatible with the metric defined for all configurations $x, x' \in \mathcal{A}^{\mathbb{Z}^d}$ by $\operatorname{dist}(x, x') = 2^{-\min\{\|\boldsymbol{n}\| : x_{\boldsymbol{n}} \neq x'_{\boldsymbol{n}}\}}$ where $\|\boldsymbol{n}\| = |n_1| + \cdots + |n_d|$. The **shift action** $\sigma : \boldsymbol{n} \mapsto \sigma^{\boldsymbol{n}}$ of the additive group $\mathbb{Z}^d$ on $\mathcal{A}^{\mathbb{Z}^d}$ is defined by

$$(\sigma^{\boldsymbol{n}}(x))_{\boldsymbol{m}} = x_{\boldsymbol{m}+\boldsymbol{n}} \tag{2.1}$$

for every $x = (x_{\boldsymbol{m}}) \in \mathcal{A}^{\mathbb{Z}^d}$ and $\boldsymbol{n} \in \mathbb{Z}^d$. If $X \subset \mathcal{A}^{\mathbb{Z}^d}$, let $\overline{X}$ denote the topological closure of X and let $\overline{X}^{\sigma} := \{\sigma^{\boldsymbol{n}}(x) \mid x \in X, \boldsymbol{n} \in \mathbb{Z}^d\}$ denote the shift-closure of X. A subset $X \subset \mathcal{A}^{\mathbb{Z}^d}$ is **shift-invariant** if $\overline{X}^{\sigma} = X$. A closed, shift-invariant subset $X \subset \mathcal{A}^{\mathbb{Z}^d}$ is a **subshift**. If $X \subset \mathcal{A}^{\mathbb{Z}^d}$ is a subshift, we write $\sigma = \sigma^X$ for the restriction of the shift action (2.1) to X. When X is a subshift, the triple $(X, \mathbb{Z}^d, \sigma)$ is a dynamical system and the notions presented in the previous section hold.

A configuration $x \in X$ is **periodic** if there is a nonzero vector $\boldsymbol{n} \in \mathbb{Z}^d \setminus \{\boldsymbol{0}\}$ such that $x = \sigma^{\boldsymbol{n}}(x)$, and otherwise it is **nonperiodic**. We say that a nonempty subshift X is **aperiodic** if the shift action σ on X is free.

For any subset $S \subset \mathbb{Z}^d$ let $\pi_S : \mathcal{A}^{\mathbb{Z}^d} \to \mathcal{A}^S$, denote the projection map which restricts every $x \in \mathcal{A}^{\mathbb{Z}^d}$ to S. A **pattern** is a function $p \in \mathcal{A}^S$ for some finite subset $S \subset \mathbb{Z}^d$. To every pattern $p \in \mathcal{A}^S$ corresponds a subset $\pi_S^{-1}(p) \subset \mathcal{A}^{\mathbb{Z}^d}$ called **cylinder**. A nonempty set $X \subset \mathcal{A}^{\mathbb{Z}^d}$ is a **subshift** if and only if there exists a set $\mathcal{F}$ of **forbidden** patterns such that

$$X = \{x \in \mathcal{A}^{\mathbb{Z}^d} \mid \pi_S \circ \sigma^{\boldsymbol{n}}(x) \notin \mathcal{F} \text{ for every } \boldsymbol{n} \in \mathbb{Z}^d \text{ and } S \subset \mathbb{Z}^d\}; \tag{2.2}$$

see [25, Prop. 9.2.4]. A subshift $X \subset \mathcal{A}^{\mathbb{Z}^d}$ is a **subshift of finite type** (SFT) if there exists a finite set $\mathcal{F}$ such that (2.2) holds. In this article, we consider shifts of finite type on $\mathbb{Z} \times \mathbb{Z}$ – that is, the case $d = 2$.

2.3. Wang shifts

A **Wang tile** is a tuple of four colors $(a, b, c, d) \in I \times J \times I \times J$ where I is a finite set of vertical colors and J is a finite set of horizontal colors; see [66, 53]. A Wang tile is represented as a unit square with colored edges:

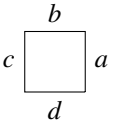

https://doi.org/10.1017/fms.2025.10069 Published online by Cambridge University Press

Figure 7. *The set of 3 Wang tiles introduced in [66] using letters $\{A, B, C, D, E\}$ instead of numbers from the set $\{1, 2, 3, 4, 5\}$ for labeling the edges. Each tile is identified uniquely by an index from the set $\{0, 1, 2\}$ written at the center each tile.*

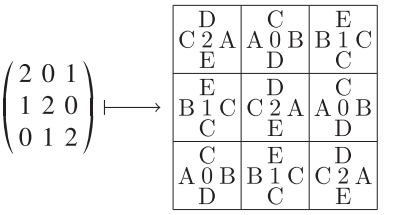

Figure 8. *A finite 3×3 pattern on the left is valid with respect to the Wang tiles since it respects Equations (2.3) and (2.4). Validity can be verified on the tiling shown on the right.*

For each Wang tile $\tau = (a, b, c, d)$, let $\textsc{Right}(\tau) = a$, $\textsc{Top}(\tau) = b$, $\textsc{Left}(\tau) = c$, $\textsc{Bottom}(\tau) = d$ denote respectively the **colors** or **labels** of the right, top, left and bottom edges of τ.

Let $\mathcal{T} = \{t_0, \dots, t_{m-1}\}$ be a set of Wang tiles as the one shown in Figure 7. A configuration $x : \mathbb{Z}^2 \to \{0, \dots, m-1\}$ is **valid** with respect to $\mathcal{T}$ if it assigns a tile in $\mathcal{T}$ to each position of $\mathbb{Z}^2$, so that contiguous edges of adjacent tiles have the same color; that is,

$$\textsc{Right}(t_{x(\boldsymbol{n})}) = \textsc{Left}(t_{x(\boldsymbol{n}+\boldsymbol{e}_1)}) \tag{2.3}$$

$$\textsc{Top}(t_{x(\boldsymbol{n})}) = \textsc{Bottom}(t_{x(\boldsymbol{n}+\boldsymbol{e}_2)}) \tag{2.4}$$

for every $\boldsymbol{n} \in \mathbb{Z}^2$ where $\boldsymbol{e}_1 = (1, 0)$ and $\boldsymbol{e}_2 = (0, 1)$. A finite pattern which is valid with respect to $\mathcal{U}$ is shown in Figure 8.

Let $\Omega_{\mathcal{T}} \subset \{0, \dots, m-1\}^{\mathbb{Z}^2}$ denote the set of all valid configurations with respect to $\mathcal{T}$, called the **Wang shift** of $\mathcal{T}$. To a configuration $x \in \Omega_{\mathcal{T}}$ corresponds a tiling of the plane $\mathbb{R}^2$ by the tiles $\mathcal{T}$ where the unit square Wang tile $t_{x(\boldsymbol{n})}$ is placed at position $\boldsymbol{n}$ for every $\boldsymbol{n} \in \mathbb{Z}^2$, as in Figure 8. Together with the shift action σ of $\mathbb{Z}^2$, $\Omega_{\mathcal{T}}$ is a SFT of the form (2.2) since there exists a finite set of forbidden patterns made of all horizontal and vertical dominoes of two tiles that do not share an edge of the same color.

A configuration $x \in \Omega_{\mathcal{T}}$ is **periodic** if there exists $\boldsymbol{n} \in \mathbb{Z}^2 \setminus \{0\}$ such that $x = \sigma^{\boldsymbol{n}}(x)$. A set $\mathcal{T}$ of Wang tiles is **periodic** if there exists a periodic configuration $x \in \Omega_{\mathcal{T}}$. Originally, Wang thought that every set $\mathcal{T}$ of Wang tiles is periodic as soon as $\Omega_{\mathcal{T}}$ is nonempty [66]. Wang noticed that if this statement were true, it would imply the existence of an algorithm solving the *domino problem* – that is, taking as input a set of Wang tiles and returning *yes* or *no* whether there exists a valid configuration with these tiles. Berger, a student of Wang, later proved that the domino problem is undecidable and he also provided a first example of an aperiodic set of Wang tiles [8]. A set $\mathcal{T}$ of Wang tiles is **aperiodic** if the Wang shift $\Omega_{\mathcal{T}}$ is a nonempty aperiodic subshift.

2.4. Directional determinism

A set $\mathcal{T}$ of Wang tiles is called **SW-deterministic** if there do not exist two different tiles in $\mathcal{T}$ that would have the same colors on their bottom and left edges, respectively [27]. In other words, for all colors C_1 and C_2, there exists at most one tile in $\mathcal{T}$ whose bottom and left edges have colors C_1 and C_2, respectively.

Let $S = \{a_1, a_1 + 1, \dots, b_1\} \times \{a_2, a_2 + 1, \dots, b_2\}$ be a rectangular support where a_1, b_1, a_2, b_2 are integers such that $a_1 \le b_1$ and $a_2 \le b_2$. Let $p : S \to \mathcal{T}$ be a valid rectangular pattern over the tiles $\mathcal{T}$. We say that the **bottom labels of** p and **top labels of** p are, respectively, the sequences

https://doi.org/10.1017/fms.2025.10069 Published online by Cambridge University Press

$$\textsc{Bottom}(p_{a_1,a_2}), \textsc{Bottom}(p_{a_1+1,a_2}), \dots, \textsc{Bottom}(p_{b_1,a_2}) \text{ and}$$
$$\textsc{Top}(p_{a_1,b_2}), \textsc{Top}(p_{a_1+1,b_2}), \dots, \textsc{Top}(p_{b_1,b_2})$$

read on the pattern from left to right. Also, we say that the **left labels of** p and **right labels of** p are, respectively, the sequences

$$\textsc{Left}(p_{a_1,a_2}), \textsc{Left}(p_{a_1,a_2+1}), \dots, \textsc{Left}(p_{a_1,b_2}) \text{ and}$$
$$\textsc{Right}(p_{b_1,a_2}), \textsc{Right}(p_{b_1,a_2+1}), \dots, \textsc{Right}(p_{b_1,b_2})$$

read on the pattern from bottom to top.

As shown in the next lemma, the local definition of SW-deterministic sets of Wang tiles extends into a wider property on rectangular patterns.

Lemma 2.1. *Let $\mathcal{T}$ be a SW-deterministic set of Wang tiles. If p and q are two rectangular valid patterns with the same shape, the same sequence of bottom labels and the same sequence of left labels, then $p = q$.*

Proof. By contradiction, suppose that there are two distinct rectangular patterns p and q whose sequence of bottom labels is X and sequence of left labels is Y. Since p and q are distinct, there exists a position $k \in \mathbb{N}^2$ such that $p_k \neq q_k$. Consider such a position in the support of p and q which minimizes the norm $\|k\|_1$. Since the position is minimal, every tile at position smaller in norm is the same in both patterns. In particular, it implies that $\textsc{Left}(p_k) = \textsc{Left}(q_k)$ and $\textsc{Bottom}(p_k) = \textsc{Bottom}(q_k)$. The set of Wang tile $\mathcal{T}_n$ is SW-deterministic. This implies that $\textsc{Top}(p_k) = \textsc{Top}(q_k)$ and $\textsc{Right}(p_k) = \textsc{Right}(q_k)$. Since the four labels of the Wang tiles are the same, we must have $p_k = q_k$, a contradiction. We conclude the uniqueness of the rectangular pattern. □

NW-, **NE-** and **SE-deterministic** sets of Wang tiles are defined analogously. Recall that it was shown in [27] that there exist aperiodic tile sets that are deterministic in all four directions simultaneously.

3. Preliminaries on 2-dimensional substitutions

Rectangular 2-dimensional substitutions and their symbolic dynamical systems were considered in [43]. For a certain class of 2-dimensional substitution systems, it was shown how to construct a set of Wang tiles such that the associated Wang shift is an almost everywhere one-to-one extension of the substitution system [43, Theorem 4.5]. This result was generalized later for geometrical substitutions over polygonal tiles [23].

In this section, we introduce 2-dimensional substitutions. Our definition and the one presented in [43] are incomparable. On the one hand, we restrict to the deterministic case (every letter has a unique image). On the other hand, we extend to different alphabets $\mathcal{A}$ and $\mathcal{B}$ for the domain and codomain. The section follows the preliminary section of the chapter [37].

3.1. d-dimensional word

We denote by $\{\boldsymbol{e}_k | 1 \leq k \leq d\}$ the canonical basis of $\mathbb{Z}^d$ where $d \geq 1$ is an integer. If $i \leq j$ are integers, then $[\![i, j]\!]$ denotes the interval of integers $\{i, i+1, \dots, j\}$. Let $\boldsymbol{n} = (n_1, \dots, n_d) \in \mathbb{N}^d$ and $\mathcal{A}$ be an alphabet. We denote by $\mathcal{A}^{\boldsymbol{n}}$ the set of functions

$$u : [\![0, n_1 - 1]\!] \times \cdots \times [\![0, n_d - 1]\!] \to \mathcal{A}.$$

An element $u \in \mathcal{A}^{\boldsymbol{n}}$ is called a **d-dimensional word** of **size** $\boldsymbol{n} = (n_1, \dots, n_d) \in \mathbb{N}^d$ on the alphabet $\mathcal{A}$. We use the notation $\textsc{size}(u) = \boldsymbol{n}$ when necessary. The set of all finite d-dimensional words is $\mathcal{A}^{*^d} = \bigcup_{\boldsymbol{n} \in \mathbb{N}^d} \mathcal{A}^{\boldsymbol{n}}$. A d-dimensional word of size $\boldsymbol{e}_k + \sum_{i=1}^{d} \boldsymbol{e}_i$ is called a **domino in the direction** $\boldsymbol{e}_k$. When the context is clear, we write $\mathcal{A}$ instead of $\mathcal{A}^{(1,\dots,1)}$. When $d = 2$, we represent a d-dimensional word u of size (n_1, n_2) as a matrix with Cartesian coordinates:

https://doi.org/10.1017/fms.2025.10069 Published online by Cambridge University Press

$$u = \begin{pmatrix} u_{0,n_2-1} & \cdots & u_{n_1-1,n_2-1} \\ \cdots & \cdots & \cdots \\ u_{0,0} & \cdots & u_{n_1-1,0} \end{pmatrix}.$$

Let $\boldsymbol{n}, \boldsymbol{m} \in \mathbb{N}^d$ and $u \in \mathcal{A}^{\boldsymbol{n}}$ and $v \in \mathcal{A}^{\boldsymbol{m}}$. If there exists an index i such that $n_j = m_j$ for all $j \in \{1, \ldots, d\} \setminus \{i\}$, then the **concatenation** of u and v in the direction $\boldsymbol{e}_i$ is defined: it is the d-dimensional word $u \odot^i v$ of size $(n_1, \ldots, n_{i-1}, n_i + m_i, n_{i+1}, \ldots, n_d) \in \mathbb{N}^d$ given as

$$(u \odot^i v)(\boldsymbol{a}) = \begin{cases} u(\boldsymbol{a}) & \text{if} \quad 0 \le a_i < n_i, \\ v(\boldsymbol{a} - n_i \boldsymbol{e}_i) & \text{if} \quad n_i \le a_i < n_i + m_i. \end{cases}$$

The notation $u \odot^i v$ was used in [11].

The following equation illustrates the concatenation of 2-dimensional words in the direction $\boldsymbol{e}_2$:

$$\begin{pmatrix} 4 & 5 \\ 10 & 5 \end{pmatrix} \odot^2 \begin{pmatrix} 3 & 10 \\ 9 & 9 \\ 0 & 0 \end{pmatrix} = \begin{pmatrix} 3 & 10 \\ 9 & 9 \\ 0 & 0 \\ 4 & 5 \\ 10 & 5 \end{pmatrix}$$

and in the direction $\boldsymbol{e}_1$:

$$\begin{pmatrix} 2 & 8 & 7 \\ 7 & 3 & 9 \\ 1 & 1 & 0 \\ 6 & 6 & 7 \\ 7 & 4 & 3 \end{pmatrix} \odot^1 \begin{pmatrix} 3 & 10 \\ 9 & 9 \\ 0 & 0 \\ 4 & 5 \\ 10 & 5 \end{pmatrix} = \begin{pmatrix} 2 & 8 & 7 & 3 & 10 \\ 7 & 3 & 9 & 9 & 9 \\ 1 & 1 & 0 & 0 & 0 \\ 6 & 6 & 7 & 4 & 5 \\ 7 & 4 & 3 & 10 & 5 \end{pmatrix}.$$

Let $\boldsymbol{n}, \boldsymbol{m} \in \mathbb{N}^d$ and $u \in \mathcal{A}^{\boldsymbol{n}}$ and $v \in \mathcal{A}^{\boldsymbol{m}}$. We say that u **occurs in** v **at position** $\boldsymbol{p} \in \mathbb{N}^d$ if v is large enough; that is, $\boldsymbol{m} - \boldsymbol{p} - \boldsymbol{n} \in \mathbb{N}^d$ and

$$v(\boldsymbol{a} + \boldsymbol{p}) = u(\boldsymbol{a})$$

for all $\boldsymbol{a} = (a_1, \ldots, a_d) \in \mathbb{N}^d$ such that $0 \le a_i < n_i$ with $1 \le i \le d$. If u occurs in v at some position, then we say that u is a d-dimensional **subword** or **factor** of v.

3.2. d-dimensional language

A subset $L \subseteq \mathcal{A}^{*^d}$ is called a d-dimensional **language**. A language $L \subseteq \mathcal{A}^{*^d}$ is called **factorial** if for every $v \in L$ and every d-dimensional subword u of v, we have $u \in L$. All languages considered in this contribution are factorial. Given a configuration $x \in \mathcal{A}^{\mathbb{Z}^d}$, the **language** $\mathcal{L}(x)$ defined by x is

$$\mathcal{L}(x) = \{u \in \mathcal{A}^{*^d} \mid u \text{ is a } d\text{-dimensional subword of } x\}.$$

The **language** of a subshift $X \subseteq \mathcal{A}^{\mathbb{Z}^d}$ is $\mathcal{L}_X = \cup_{x \in X} \mathcal{L}(x)$. Conversely, given a factorial language $L \subseteq \mathcal{A}^{*^d}$, we define the subshift

$$\mathcal{X}_L = \{x \in \mathcal{A}^{\mathbb{Z}^d} \mid \mathcal{L}(x) \subseteq L\}.$$

A d-dimensional subword $u \in \mathcal{A}^{*^d}$ is **legal** (or **allowed**) in a subshift $X \subset \mathcal{A}^{\mathbb{Z}^d}$ if $u \in \mathcal{L}_X$, and it is **illegal** in X if $u \notin \mathcal{L}_X$ [5]. A language $L \subseteq \mathcal{A}^{*^d}$ is **illegal** in a subshift $X \subset \mathcal{A}^{\mathbb{Z}^d}$ if $L \cap \mathcal{L}_X = \varnothing$.

https://doi.org/10.1017/fms.2025.10069 Published online by Cambridge University Press

3.3. d-dimensional morphisms

Let $\mathcal{A}$ and $\mathcal{B}$ be two alphabets. Let $L \subseteq \mathcal{A}^{*^d}$ be a factorial language. A function $\omega : L \to \mathcal{B}^{*^d}$ is a **d-dimensional morphism** if for every i with $1 \leq i \leq d$, and every $u, v \in L$ such that $u \odot^i v$ is defined and $u \odot^i v \in L$, we have that the concatenation $\omega(u) \odot^i \omega(v)$ in direction $\boldsymbol{e}_i$ is defined and

$$\omega(u \odot^i v) = \omega(u) \odot^i \omega(v).$$

Note that the left-hand side of the equation is defined since $u \odot^i v$ belongs to the domain of ω. A d-dimensional morphism $L \to \mathcal{B}^{*^d}$ is thus completely defined from the image of the letters in $\mathcal{A}$, so we sometimes denote a d-dimensional morphism as a rule $\mathcal{A} \to \mathcal{B}^{*^d}$ when the language L is unspecified.

As noticed by [43, p.144], the images under the morphism of any two letters appearing in the same row of a word from L have the same height. Symmetrically, the images under the morphism of any two letters appearing in the same column of a word from L have the same width.

Let $L \subseteq \mathcal{A}^{*^d}$ be a factorial language and $\mathcal{X}_L \subseteq \mathcal{A}^{\mathbb{Z}^d}$ be the subshift generated by L. A d-dimensional morphism $\omega : L \to \mathcal{B}^{*^d}$ can be extended to a continuous map $\omega : \mathcal{X}_L \to \mathcal{B}^{\mathbb{Z}^d}$ (over the topology of subshifts, as defined in Section 2.2) in such a way that the origin of $\omega(x)$ is at position $\mathbf{0}$ in the word $\omega(x_{\mathbf{0}})$ for all $x \in \mathcal{X}_L$. More precisely, the image under ω of the configuration $x \in \mathcal{X}_L$ is

$$\omega(x) = \lim_{n \to \infty} \sigma^{f(n)} \omega\left(\sigma^{-n\mathbf{1}}(x|_{[\![-n\mathbf{1}, n\mathbf{1}[\![})\right) \in \mathcal{B}^{\mathbb{Z}^d},$$

where $\mathbf{1} = (1, \ldots, 1) \in \mathbb{Z}^d$, $f(n) = \text{SIZE}\left(\omega(\sigma^{-n\mathbf{1}}(x|_{[\![-n\mathbf{1}, \mathbf{0}[\![}))\right)$ for all $n \in \mathbb{N}$ and $[\![\boldsymbol{m}, \boldsymbol{n}[\![= [\![m_1, n_1 - 1]\!] \times \cdots \times [\![m_d, n_d - 1]\!]$. We say that the map $\omega : \mathcal{X}_L \to \mathcal{B}^{\mathbb{Z}^d}$ is a **d-dimensional substitution**.

In general, the image of a subshift under a d-dimensional substitution might not be closed under the shift. But the closure under the shift of the image of a subshift $X \subseteq \mathcal{A}^{\mathbb{Z}^d}$ under ω is the subshift

$$\overline{\omega(X)}^{\sigma} = \{\sigma^{\boldsymbol{k}} \omega(x) \in \mathcal{B}^{\mathbb{Z}^d} \mid \boldsymbol{k} \in \mathbb{Z}^d, x \in X\} \subseteq \mathcal{B}^{\mathbb{Z}^d}.$$

This motivates the following definition.

Definition 3.1. Let X, Y be two subshifts and $\omega : X \to Y$ be a d-dimensional substitution. If $Y = \overline{\omega(X)}^{\sigma}$, then we say that ω is **onto up to a shift**.

3.4. Self-similar subshifts

In this section, we consider languages and subshifts defined from morphisms leading to self-similar structures. In this situation, the domain and codomain of morphisms are defined over the same alphabet. Formally, we consider the case of d-dimensional morphisms $\mathcal{A} \to \mathcal{B}^{*^d}$ where $\mathcal{A} = \mathcal{B}$.

The definition of self-similarity depends on the notion of expansiveness. It avoids the presence of lower-dimensional self-similar structure by having expansion in all directions.

Definition 3.2. We say that a d-dimensional morphism $\omega : \mathcal{A} \to \mathcal{A}^{*^d}$ is **expansive** if for every $a \in \mathcal{A}$ and $K \in \mathbb{N}$, there exists $m \in \mathbb{N}$ such that $\min(\text{SIZE}(\omega^m(a))) > K$.

Definition 3.3. A subshift $X \subseteq \mathcal{A}^{\mathbb{Z}^d}$ is **self-similar** if there exists an expansive d-dimensional morphism $\omega : \mathcal{A} \to \mathcal{A}^{*^d}$ such that $X = \overline{\omega(X)}^{\sigma}$.

Self-similar subshifts can be constructed by iterative application of a morphism ω starting with the letters. The **language** $\mathcal{L}_\omega$ defined by an expansive d-dimensional morphism $\omega : \mathcal{A} \to \mathcal{A}^{*^d}$ is

https://doi.org/10.1017/fms.2025.10069 Published online by Cambridge University Press

$$\mathcal{L}_\omega = \{u \in \mathcal{A}^{*^d} \mid u \text{ is a } d\text{-dimensional subword of } \omega^n(a) \text{ for some } a \in \mathcal{A} \text{ and } n \in \mathbb{N}\}.$$

The **substitutive shift** $\mathcal{X}_\omega = \mathcal{X}_{\mathcal{L}_\omega}$ defined from the language of ω is a self-similar subshift since $\mathcal{X}_\omega = \overline{\omega(\mathcal{X}_\omega)}^\sigma$ holds.

A d-dimensional morphism $\omega : \mathcal{A} \to \mathcal{A}^{*^d}$ is **primitive** if there exists $m \in \mathbb{N}$ such that for every $a, b \in \mathcal{A}$, the letter b occurs in $\omega^m(a)$. Note that if ω is primitive, then the Perron–Frobenius theorem applies for its **incidence matrix** $M_\omega = (|\omega(a)|_b)_{(b,a)\in\mathcal{A}\times\mathcal{A}}$; see [51].

3.5. *d-dimensional recognizability*

The definition of recognizability dates back to the work of Host, Quéffelec and Mossé [42]. The definition introduced below is based on some work of Berthé et al. [9] on the recognizability in the case of S-adic systems where more than one substitution is involved.

Definition 3.4 (recognizable). Let $X \subseteq \mathcal{A}^{\mathbb{Z}^d}$ and $\omega : X \to \mathcal{B}^{\mathbb{Z}^d}$ be a d-dimensional substitution. If $y \in \overline{\omega(X)}^\sigma$ (i.e., $y = \sigma^{\boldsymbol{k}}\omega(x)$ for some $x \in X$ and $\boldsymbol{k} \in \mathbb{Z}^d$, where σ is the d-dimensional shift map), we say that $(\boldsymbol{k}, x)$ is an **ω-representation of** y. We say that it is **centered** if $y_{\mathbf{0}}$ lies inside of the image of $x_{\mathbf{0}}$ (i.e., if $\mathbf{0} \le \boldsymbol{k} < \text{SIZE}(\omega(x_{\mathbf{0}}))$ coordinate-wise). We say that ω is **recognizable in** $X \subseteq \mathcal{A}^{\mathbb{Z}^d}$ if each $y \in \mathcal{B}^{\mathbb{Z}^d}$ has at most one centered ω-representation $(\boldsymbol{k}, x)$ with $x \in X$.

The self-similarity of Ω_n allows us to conclude aperiodicity of the Wang shift using well-known arguments (see [62, 42], who showed that recognizability and aperiodicity are equivalent for primitive substitutive sequences).

The following statement corresponds to only one of the directions (the easy one) of the equivalence which does not need the notion of primitivity. It was proved for 2-dimensional substitutions in [33]; see also [37, Proposition 3.6].

Proposition 3.5 [33, Proposition 6]. *Let $\omega : \mathcal{A} \to \mathcal{A}^{*^d}$ be an expansive d-dimensional morphism. Let $X \subseteq \mathcal{A}^{\mathbb{Z}^d}$ be a self-similar subshift such that $\overline{\omega(X)}^\sigma = X$. If ω is recognizable in X, then X is aperiodic.*

4. The family of metallic mean Wang tiles

For every integer $n \in \mathbb{Z}$, we write $\overline{n}$ to denote $n + 1$ and $\underline{n}$ to denote $n - 1$:

$$\overline{n} := n + 1,$$
$$\underline{n} := n - 1.$$

For every Wang tile $\tau = (a, b, c, d)$, we define its symmetric image under the positive diagonal as $\widehat{\tau} = (b, a, d, c)$:

if $\tau =$ 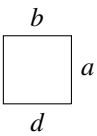

, then $\widehat{\tau} =$ 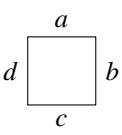

.

4.1. *The tiles*

For every integer $n \ge 1$, let

$$V_n = \{(v_0, v_1, v_2) \in \mathbb{Z}^3 : 0 \le v_0 \le v_1 \le 1 \text{ and } v_1 \le v_2 \le n + 1\}$$

be a set of vectors having non-decreasing entries with an upper bound of 1 on the middle entry and an upper bound of $n + 1$ on the last entry. The label of the edges of the Wang tiles considered in this

https://doi.org/10.1017/fms.2025.10069 Published online by Cambridge University Press

article are vectors in V_n. To lighten the figures and the presentation of the Wang tiles, it is convenient to denote the vector $(v_0, v_1, v_2) \in V_n$ more compactly as a word $v_0v_1v_2$. For instance, the vector $(1, 1, 1)$ is represented as 111.

For every integer $n \geq 1$, we define the following set of Wang tiles whose labels belong to the set V_n. We have n^2 white tiles whose labels all start with 11:

$$W_n = \left\{ w_n^{i,j} := \begin{array}{ccc} & 11\bar{j} & \\ 11i & \square & 11\bar{i} \\ & 11j & \end{array} \;\middle|\; \begin{array}{l} 1 \leq i \leq n, \\ 1 \leq j \leq n \end{array} \right\} \qquad (n^2 \text{ white tiles}).$$

We have horizontal stripe tiles whose top and bottom labels all start with 11 and whose left and right labels start with 0. These are divided into four sets according to the first two digits of the left and right labels which can be 00 (associated with color blue) or 01 (associated with color yellow).

$$B'_n = \left\{ b_n^i := \begin{array}{ccc} & 111 & \\ 00i & \square & 00\bar{i} \\ & 11n & \end{array} \;\middle|\; 0 \leq i \leq n \right\} \qquad (n+1 \text{ horizontal blue stripe tiles}),$$

$$G_n = \left\{ g_n^i := \begin{array}{ccc} & 111 & \\ 00i & \square & 01\bar{i} \\ & 11\bar{n} & \end{array} \;\middle|\; 0 \leq i \leq n \right\} \qquad (n+1 \text{ horizontal green stripe tiles}),$$

$$Y_n = \left\{ y_n^i := \begin{array}{ccc} & 112 & \\ 01i & \square & 01\bar{i} \\ & 11\bar{n} & \end{array} \;\middle|\; 1 \leq i \leq n \right\} \qquad (n \text{ horizontal yellow stripe tiles}),$$

$$A_n = \left\{ a_n^i := \begin{array}{ccc} & 112 & \\ 01i & \square & 00\bar{i} \\ & 11n & \end{array} \;\middle|\; 1 \leq i \leq n \right\} \qquad (n \text{ horizontal antigreen tiles}).$$

The set B'_n of horizontal blue tiles are those such that both left and right labels start with 00 and are identified with a horizontal blue stripe. The set Y_n of horizontal yellow tiles are those such that both left and right labels start with 01 and are identified with a horizontal yellow stripe. The set G_n of horizontal green tiles are those such that the left label starts with 00 and right label starts with 01 and are identified with a green region intersecting blue and yellow horizontal stripes. The set A_n of horizontal antigreen tiles contains the tiles whose left label starts with 01 and whose right label starts with 00. They are identified with non-intersecting blue and yellow horizontal stripes and no green intersecting region.

The tiles in A_n are called 'antigreen' because they are 'against the system' as shown later in Lemma 7.2. Antigreen tiles do not appear in any valid configuration, but they are needed as they play an important role in the description of the substitutive structure of the valid configurations allowed by these tiles; see Proposition 5.9 and Proposition 6.7.

We also have vertical stripe tiles which are the symmetric images of the horizontal stripe tiles under a reflection over the positive diagonal:

https://doi.org/10.1017/fms.2025.10069 Published online by Cambridge University Press

$$\widehat{B'_n} = \left\{ \widehat{b^i_n} := \begin{array}{c} 00\bar{i} \\ 11n \square 111 \\ 00i \end{array} \;\middle|\; 0 \le i \le n \right\} \quad (n+1 \text{ vertical blue stripe tiles}),$$

$$\widehat{G_n} = \left\{ \widehat{g^i_n} := \begin{array}{c} 01\bar{i} \\ 11\overline{n} \square 111 \\ 00i \end{array} \;\middle|\; 0 \le i \le n \right\} \quad (n+1 \text{ vertical green stripe tiles}),$$

$$\widehat{Y_n} = \left\{ \widehat{y^i_n} := \begin{array}{c} 01\bar{i} \\ 11\overline{n} \square 112 \\ 01i \end{array} \;\middle|\; 1 \le i \le n \right\} \quad (n \text{ vertical yellow stripe tiles}),$$

$$\widehat{A_n} = \left\{ \widehat{a^i_n} := \begin{array}{c} 00\bar{i} \\ 11n \square 112 \\ 01i \end{array} \;\middle|\; 1 \le i \le n \right\} \quad (n \text{ vertical antigreen tiles}).$$

Finally, we have 9 junction tiles (the gray region is drawn in blue or yellow color depending on the specific values of k, ℓ, r, s):

$$J'_n = \left\{ j^{k,\ell,r,s}_n := \begin{array}{c} (0,r,s) \\ (0,s,r+n) \square (0,k,\ell) \\ (0,\ell,k+n) \end{array} \;\middle|\; \begin{array}{l} 0 \le k \le \ell \le 1, \\ 0 \le r \le s \le 1 \end{array} \right\}$$

$$= \left\{ \begin{array}{ccc} 000 & 001 & 011 \\ 00n & 01n & 01\overline{n} \end{array} \right\} \times \left\{ \begin{array}{ccc} 000 & 001 & 011 \\ 00n & 01n & 01\overline{n} \end{array} \right\}$$

$$= \left\{ \begin{array}{ccc} \begin{array}{c} 000 \\ 00n \times 011 \\ 01\overline{n} \end{array} & \begin{array}{c} 001 \\ 01n \square 011 \\ 01\overline{n} \end{array} & \begin{array}{c} 011 \\ 01\overline{n} \square 011 \\ 01\overline{n} \end{array} \\ \begin{array}{c} 000 \\ 00n \square 001 \\ 01n \end{array} & \begin{array}{c} 001 \\ 01n \square 001 \\ 01n \end{array} & \begin{array}{c} 011 \\ 01\overline{n} \square 001 \\ 01n \end{array} \\ \begin{array}{c} 000 \\ 00n \square 000 \\ 00n \end{array} & \begin{array}{c} 001 \\ 01n \square 000 \\ 00n \end{array} & \begin{array}{c} 011 \\ 01\overline{n} \times 000 \\ 00n \end{array} \end{array} \right\} \quad (9 \text{ junction tiles}).$$

We may observe that white tiles and junction tiles are closed under the reflection over the positive diagonal:

$$\widehat{W_n} = W_n \text{ and } \widehat{J'_n} = J'_n.$$

Junction tiles play a similar role to junction tiles in [43]; thus, we reuse the same vocabulary.

https://doi.org/10.1017/fms.2025.10069 Published online by Cambridge University Press

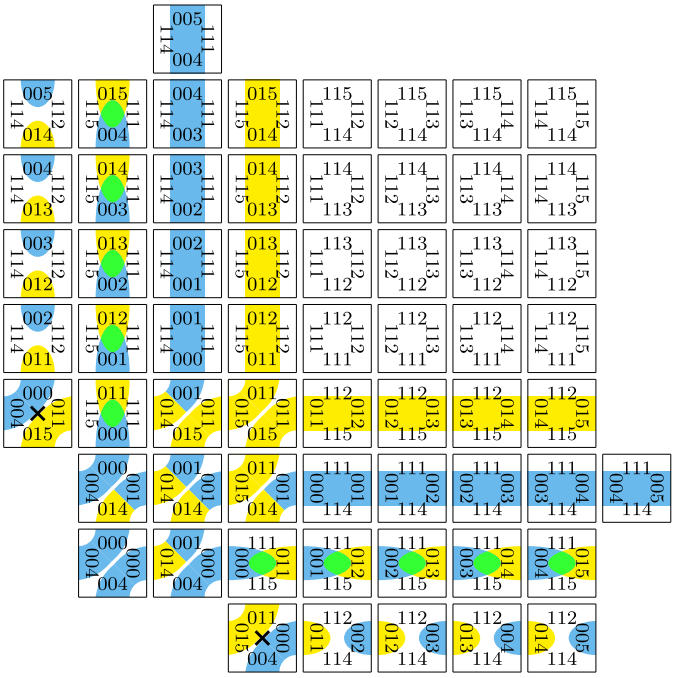

Figure 9. *Extended metallic mean Wang tile sets $\mathcal{T}'_n$ for $n = 4$. The junction tiles in $\mathcal{D}$ are shown with a $\times$-mark in their center.*

4.2. The extended set $\mathcal{T}'_n$ of metallic mean Wang tiles

For every integer $n \geq 1$, the **extended set of metallic mean Wang tiles** is the union of all of the tiles defined above:

$$\mathcal{T}'_n = W_n \cup B'_n \cup G_n \cup Y_n \cup A_n \cup \widehat{B'_n} \cup \widehat{G_n} \cup \widehat{Y_n} \cup \widehat{A_n} \cup J'_n.$$

The set $\mathcal{T}'_n$ of tiles defines the **extended metallic mean Wang shift**

$$\Omega'_n = \Omega_{\mathcal{T}'_n}.$$

The set $\mathcal{T}'_n$ contains $n^2 + 2(n + 1 + n + 1 + n + n) + 9 = n^2 + 8n + 13$ Wang tiles. The set $\mathcal{T}'_n$ of Wang tiles for $n = 4$ is shown in Figure 9.

4.3. The subset $\mathcal{T}_n$ of metallic mean Wang tiles

We need to define an important subset of the extended metallic mean Wang tiles $\mathcal{T}'_n$ because some of the tiles are not necessary as they do not appear in any valid configurations of Ω'_n. For example, we can observe that no tile of $\mathcal{T}'_n$ has label $00\overline{n}$ on the left or bottom. Therefore, the last horizontal blue tile and last vertical blue tile which use label $00\overline{n}$ on their top or right edge admit no immediate surroundings with tiles in $\mathcal{T}'_n$. As shown in Section 7 using results proved in Section 5 and Section 6, other tiles from $\mathcal{T}'_n$ do not admit arbitrarily large surroundings. Therefore, it is convenient to remove them.

https://doi.org/10.1017/fms.2025.10069 Published online by Cambridge University Press

Let

$$\mathcal{D} = \{b_n^n,\ \widehat{b_n^n},\ j_n^{0,0,1,1},\ j_n^{1,1,0,0}\}$$

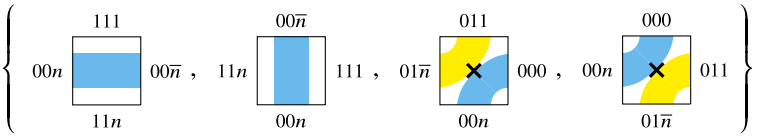

be the set containing the last blue horizontal and vertical tiles as well as two of the junction tiles. For every positive integer n, we delete the four tiles of $\mathcal{D}$ from $\mathcal{T}_n'$ as well as all of the antigreen tiles. We obtain the following **subset of metallic mean Wang tiles**

$$\begin{aligned}\mathcal{T}_n &= \mathcal{T}_n' \setminus \left(A_n \cup \widehat{A_n} \cup \mathcal{D}\right)\\ &= W_n \cup B_n \cup G_n \cup Y_n \cup \widehat{B_n} \cup \widehat{G_n} \cup \widehat{Y_n} \cup J_n,\end{aligned}$$

where $B_n = B_n' \setminus \mathcal{D}$ is the remaining set of n horizontal blue stripe tiles and $J_n = J_n' \setminus \mathcal{D} = \left\{j_n^{0,0,0,0}, j_n^{0,1,0,0}, j_n^{0,0,0,1}, j_n^{0,1,0,1}, j_n^{1,1,0,1}, j_n^{0,1,1,1}, j_n^{1,1,1,1}\right\}$ is the remaining set of 7 junction tiles. The set $\mathcal{T}_n$ contains $n^2 + 2(n+n+1+n) + 7 = (n+3)^2$ Wang tiles. It is shown in Figure 2 for $n = 1, 2, 3, 4, 5$.

The set $\mathcal{T}_n$ of tiles defines the **Metallic mean Wang shift**

$$\Omega_n = \Omega_{\mathcal{T}_n},$$

which is a subshift of Ω_n' because $\mathcal{T}_n \subset \mathcal{T}_n'$.

Remark 4.1. The reader may wonder why we need to introduce the extended set $\mathcal{T}_n'$ if only the tiles in the subset $\mathcal{T}_n$ appear in configurations of Ω_n'. This is because the extended set is needed to describe and prove the self-similarity of $\mathcal{T}_n$ in Theorem A. In the proof (using the vocabulary of supertiles from the only article published by Ammann [4]), we show that if the markings of the supertiles at level k are in bijection with the tiles in $\mathcal{T}_n$, then the markings of the supertiles at level $k+1$ are in bijection with tiles in $\mathcal{T}_n'$ (not $\mathcal{T}_n$!). In other words, we cannot get rid of the ghost tiles in $\mathcal{T}_n' \setminus \mathcal{T}_n$ because they keep reappearing at the next level of the hierarchy in bigger sizes.

4.4. The Ammann aperiodic set of 16 Wang tiles

A reproduction of the Ammann aperiodic set of 16 Wang tiles [24, p.595, Figure 11.1.13] is shown in Figure 10. The Ammann set of 16 Wang tiles corresponds to $\mathcal{T}_1$.

Theorem E. *When $n = 1$, the set $\mathcal{T}_n$ is equal, up to symbol relabeling, to the Ammann set of 16 Wang tiles.*

Proof. The following is a bijection from the labels of the Ammann set of 16 Wang tiles and the labels of the tiles in $\mathcal{T}_1$:

$$1 \mapsto 112, \quad 2 \mapsto 111, \quad 3 \mapsto 001, \quad 4 \mapsto 011, \quad 5 \mapsto 012, \quad 6 \mapsto 000.$$

See Figure 10 (note that the order of the tiles is not the same). □

Thus, the family $(\mathcal{T}_n)_{n\geq 1}$ can be considered as a generalization of the Ammann aperiodic set of 16 Wang tiles.

https://doi.org/10.1017/fms.2025.10069 Published online by Cambridge University Press

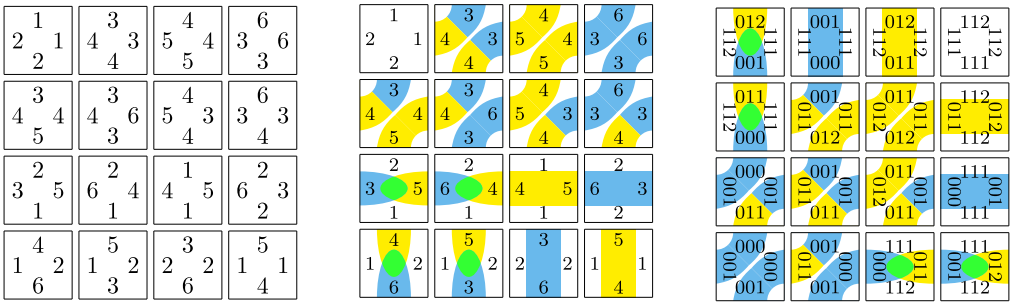

Figure 10. *Left: a reproduction of the Ammann aperiodic set of 16 Wang tiles [24, p.595, Figure 11.1.13]. Middle: the Ammann aperiodic set of 16 Wang tiles in the same order but with coloring corresponding to the white, yellow, green, blue and junction tiles of the set $\mathcal{T}_1$. Right: The set $\mathcal{T}_1$ of Wang tiles whose edge labels are vectors in $\mathbb{N}^3$. The sets are equivalent up to a bijection of the edge labels.*

4.5. Symmetric properties

The set $\mathcal{T}_n$ has nice symmetric properties. The first being that it is closed under the mirror image through the positive diagonal; that is, $\widehat{\mathcal{T}_n} = \mathcal{T}_n$. Another less evident observation is that the set $\mathcal{T}_n$ is equivalent to its image under a half-turn rotation up to the application of an involution of $V_n \setminus \{(0,0,\overline{n})\}$ applied on the edge labels of the Wang tiles.

Lemma 4.2. *Let $\sigma : (i,j,k) \mapsto (i, 1+i-j, n+1+i-k)$ (an involution on $V_n \setminus \{(0,0,\overline{n})\}$). Then,*

$$\mathcal{T}_n = \left\{ \begin{array}{c} \sigma(v) \\ \sigma(\alpha) \square \sigma(u) \\ \sigma(\beta) \end{array} \;\middle|\; \begin{array}{c} \beta \\ u \square \alpha \\ v \end{array} \in \mathcal{T}_n \right\}$$

Proof. When rotating the tiles of $\mathcal{T}_n$ by half a turn and applying the map σ on the resulting labels, we may observe that yellow tiles become blue tiles and vice versa, white tiles are mapped to white tiles, junction tiles are mapped to junction tiles and green tiles are mapped to green tiles. □

This translates into the existence of nontrivial reflection symmetry and rotational symmetry for the Wang shift Ω_n. As we show in this article, it has no translational symmetries.

4.6. Directional determinism

We show in this section that the sets $\mathcal{T}_n$ and $\mathcal{T}'_n$ are SW- and NE-deterministic.

Lemma 4.3. *The sets $\mathcal{T}_n$ and $\mathcal{T}'_n$ are SW- and NE-deterministic. However, the sets $\mathcal{T}_n$ and $\mathcal{T}'_n$ are neither NW- nor SE-deterministic.*

Proof. Let us show that $\mathcal{T}'_n$ is SW-deterministic. Let $s,t \in \mathcal{T}'_n$ be such that $\textsc{Left}(s) = u = \textsc{Left}(t)$ and $\textsc{Bottom}(s) = v = \textsc{Bottom}(t)$ for some vectors $u = (u_0,u_1,u_2), v = (v_0,v_1,v_2) \in V_n$.

- If $u_0 = 0$, $v_0 = 0$, then $s,t \in J'_n$.
- If $u_0 = 1$, $v_0 = 1$, then $s,t \in W_n$.
- If $u_0 = 0$, $v_0 = 1$, $u_1 = 0$ and $v_2 = n$, then $s,t \in B'_n$.
- If $u_0 = 0$, $v_0 = 1$, $u_1 = 0$ and $v_2 = \overline{n}$, then $s,t \in G_n$.
- If $u_0 = 0$, $v_0 = 1$, $u_1 = 1$ and $v_2 = n$, then $s,t \in A_n$.
- If $u_0 = 0$, $v_0 = 1$, $u_1 = 1$ and $v_2 = \overline{n}$, then $s,t \in Y_n$.
- If $u_0 = 1$, $v_0 = 0$, $v_1 = 0$ and $u_2 = n$, then $s,t \in \widehat{B'_n}$.
- If $u_0 = 1$, $v_0 = 0$, $v_1 = 0$ and $u_2 = \overline{n}$, then $s,t \in \widehat{G_n}$.

https://doi.org/10.1017/fms.2025.10069 Published online by Cambridge University Press

- If $u_0 = 1$, $v_0 = 0$, $v_1 = 1$ and $u_2 = n$, then $s, t \in \widehat{A_n}$.
- If $u_0 = 1$, $v_0 = 0$, $v_1 = 1$ and $u_2 = \overline{n}$, then $s, t \in \widehat{Y_n}$.

One can observe that each of the subsets W_n, B'_n, G_n, Y_n, A_n, J'_n is SW-deterministic. By symmetry, $\widehat{B'_n}$, $\widehat{G_n}$, $\widehat{Y_n}$ and $\widehat{A_n}$ are SW-deterministic. We conclude that $s = t$. Thus, $\mathcal{T}'_n$ is SW-deterministic. Using a similar argument, one can observe that $\mathcal{T}'_n$ is NE-deterministic. By restriction, the subset $\mathcal{T}_n \subset \mathcal{T}'_n$ is SW- and NE-deterministic.

However, $\mathcal{T}_n$ is neither NW- nor SE-deterministic because the subset J_n is neither NW- nor SE-deterministic. By extension, the extended set $\mathcal{T}'_n$ is neither NW- nor SE-deterministic. □

5. A substitution $\Omega_n \to \Omega_n$

The goal of this section is twofold. First, we introduce a 2-dimensional substitution $\Omega_n \to \Omega_n$ deduced from a substitution $\tau_n : V_n \to (V_n)^*$ defined on the boundary labels of the Wang tiles. Then, we characterize the possible valid rectangular tilings with external labels in the image of τ_n; see Proposition 5.9.

5.1. A 1-dimensional substitution for the boundary

It is convenient to define, for every integer $n \geq 1$, the following map:

$$\begin{aligned} \tau_n : V_n &\to (V_n)^* \\ xyz &\mapsto \begin{cases} 0(x-y+1)n \cdot (11n)^{z-x-1} \cdot (11\overline{n})^{n+1-z} & \text{if } x \neq z, \\ 0(x-y+1)\overline{n} \cdot (11\overline{n})^{n-z} & \text{if } x = z. \end{cases} \end{aligned}$$

The above formula declines into the following five cases:

$$\begin{aligned} \tau_n(000) &= 01\overline{n} \cdot (11\overline{n})^n, \\ \tau_n(111) &= 01\overline{n} \cdot (11\overline{n})^{n-1}, \\ \tau_n(00\bar{i}) &= 01n \cdot (11n)^i \cdot (11\overline{n})^{n-i} && \text{if } 0 \leq i \leq n, \\ \tau_n(01\bar{i}) &= 00n \cdot (11n)^i \cdot (11\overline{n})^{n-i} && \text{if } 0 \leq i \leq n, \\ \tau_n(11\bar{i}) &= 01n \cdot (11n)^{i-1} \cdot (11\overline{n})^{n-i} && \text{if } 1 \leq i \leq n. \end{aligned} \tag{5.1}$$

For example, when $n = 1$, $n = 2$ or $n = 4$, we have

$$\tau_1 \begin{cases} 000 \mapsto 012, 112 \\ 001 \mapsto 011, 112 \\ 002 \mapsto 011, 111 \\ 011 \mapsto 001, 112 \\ 012 \mapsto 001, 111 \\ 111 \mapsto 012 \\ 112 \mapsto 011 \end{cases}, \quad \tau_2 \begin{cases} 000 \mapsto 013, 113, 113 \\ 001 \mapsto 012, 113, 113 \\ 002 \mapsto 012, 112, 113 \\ 003 \mapsto 012, 112, 112 \\ 011 \mapsto 002, 113, 113 \\ 012 \mapsto 002, 112, 113 \\ 013 \mapsto 002, 112, 112 \\ 111 \mapsto 013, 113 \\ 112 \mapsto 012, 113 \\ 113 \mapsto 012, 112 \end{cases}, \quad \tau_4 \begin{cases} 000 \mapsto 015, 115, 115, 115, 115 \\ 001 \mapsto 014, 115, 115, 115, 115 \\ 002 \mapsto 014, 114, 115, 115, 115 \\ 003 \mapsto 014, 114, 114, 115, 115 \\ 004 \mapsto 014, 114, 114, 114, 115 \\ 005 \mapsto 014, 114, 114, 114, 114 \\ 011 \mapsto 004, 115, 115, 115, 115 \\ 012 \mapsto 004, 114, 115, 115, 115 \\ 013 \mapsto 004, 114, 114, 115, 115 \\ 014 \mapsto 004, 114, 114, 114, 115 \\ 015 \mapsto 004, 114, 114, 114, 114 \\ 111 \mapsto 015, 115, 115, 115 \\ 112 \mapsto 014, 115, 115, 115 \\ 113 \mapsto 014, 114, 115, 115 \\ 114 \mapsto 014, 114, 114, 115 \\ 115 \mapsto 014, 114, 114, 114 \end{cases}. $$

The map τ_n was discovered during computer explorations. It appears naturally when searching for a self-similarity for the tilings in Ω_n; see Appendix B in Section B and in particular the output of the computation performed at line 84.

https://doi.org/10.1017/fms.2025.10069 Published online by Cambridge University Press

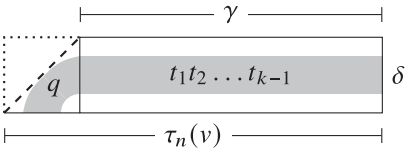

Figure 11. *A horizontal strip of tiles from $\mathcal{T}'_n$ made of a bottom right part q of a junction tile and a sequence $t_1t_2\ldots t_{k-1}$ of horizontal stripe tiles. The bottom labels of the strip is $\tau_n(v)$ for some $v \in V_n$. The top labels of the horizontal stripe tiles is $\gamma \in (V_n)^*$ and its right-most right label is $\delta \in V_n$.*

Lemma 5.1. *For every $(x, y, z) \in V_n$, the map τ_n satisfies the following:*

- *the length of $\tau_n(xyz) \in (V_n)^*$ is $n + 1 - x$;*
- *the first item of $\tau_n(xyz)$ is $0(x{-}y{+}1)n$ or $0(x{-}y{+}1)\overline{n}$;*
- *there are $z - x$ occurrences of ${**}n$ in the image of $\tau_n(xyz)$.*

In particular, τ_n is injective.

Proof. The three items follow from the definition. We prove that τ_n is injective. Assume that $xyz \neq x'y'z'$. We want to show that $\tau_n(xyz) \neq \tau_n(x'y'z')$. If $x \neq x'$, then the images are distinct because their lengths are different. If $x = x'$ and $y \neq y'$, then the images are distinct because the second digit of their first item satisfies $x{-}y{+}1 \neq x{-}y'{+}1$. If $x = x'$, $y = y'$ and $z \neq z'$, then the images are distinct because there are $z - x$ occurrences of $**n$ in the image of $\tau_n(xyz)$. □

5.2. A substitution ω'_n for the tiles in $\mathcal{T}'_n$

Let

$$Q_n = \left\{ \begin{array}{ccc} 000 & 001 & 011 \\ 00n & 01n & 01\overline{n} \end{array} \right\}$$

be the set of possible values for the bottom right part of a junction tile in J'_n.

Lemma 5.2. *Let $n \geq 1$ be an integer. For every $v \in V_n$, there exist a unique bottom right part $q \in Q_n$ and a unique sequence $t_1t_2\ldots t_{k-1}$ of tiles in $\mathcal{T}'_n$ such that $q\,t_1t_2\ldots t_{k-1}$ is a valid horizontal strip of tiles from left to right whose sequence of bottom labels is $\tau_n(v)$ where $k = |\tau_n(v)|$.*

Moreover, if γ is the sequence of top labels of $t_1t_2\ldots t_{k-1}$ and δ is its right-most right label – that is, the right label of t_{k-1} (see Figure 11) – then the following statements hold.

- *If $v = 00i$ with $0 \leq i \leq \overline{n}$, then*
  - *if $0 \leq i \leq n$, then $\gamma = (111)^i \cdot (112)^{n-i}$ and $\delta = 01\overline{n}$,*
  - *if $i = n + 1$, then $\gamma = (111)^n$ and $\delta = 00\overline{n}$.*
- *If $v = 01i$ with $1 \leq i \leq \overline{n}$, then*
  - *if $1 \leq i \leq n$, then $\gamma = (111)^i \cdot (112)^{n-i}$ and $\delta = 01n$,*
  - *if $i = n + 1$, then $\gamma = (111)^n$ and $\delta = 00n$.*
- *If $v = 11i$ with $1 \leq i \leq \overline{n}$, then*
  - *if $1 \leq i \leq n$, then $\gamma = (111)^{i-1} \cdot (112)^{n-i}$ and $\delta = 01n$,*
  - *if $i = n + 1$, then $\gamma = (111)^{n-1}$ and $\delta = 00n$.*

In particular, no antigreen tiles appear in the horizontal strip. Also, if $v \in V_n \setminus \{00\overline{n}\}$, then the last blue tile does not appear in the strip.

https://doi.org/10.1017/fms.2025.10069 Published online by Cambridge University Press

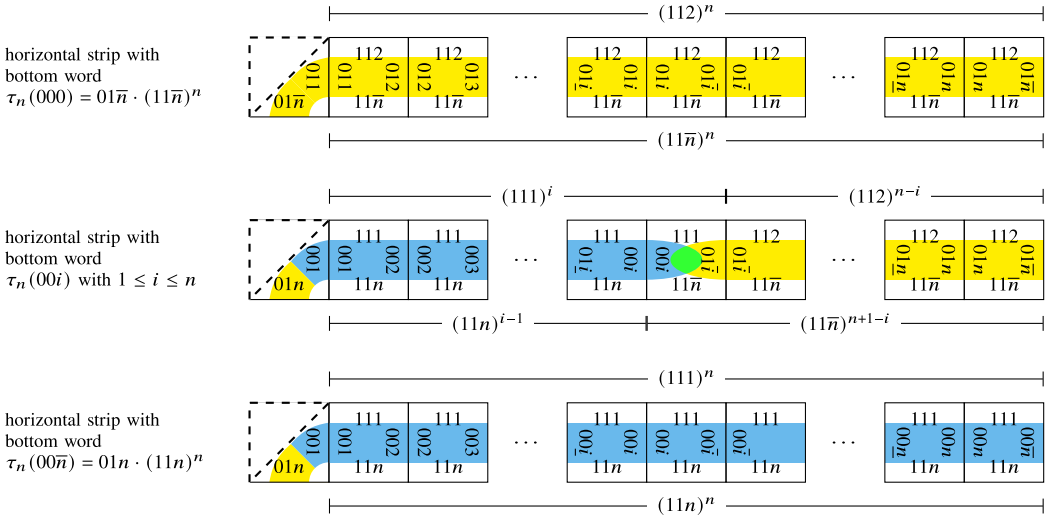

Figure 12. *Horizontal strip with bottom word $\tau_n(00i)$ with $0 \le i \le n$.*

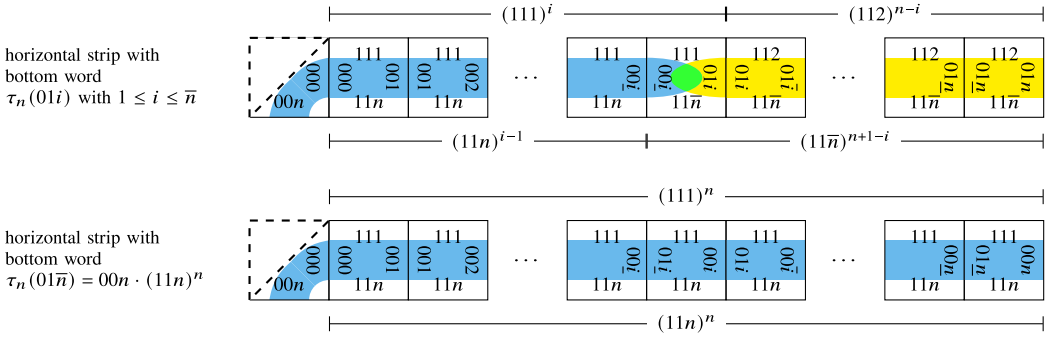

Figure 13. *Horizontal strip with bottom word $\tau_n(01i)$ with $1 \le i \le n+1$.*

Proof. Assume $v = 00i$ with $0 \le i \le \overline{n}$. The following three cases occur.

- If $i = 0$, then the sequence of bottom labels is $\tau_n(000) = 01\overline{n} \cdot (11\overline{n})^n$, the sequence of top labels is $(112)^n$ and the right-most right label is $01\overline{n}$.
- If $1 \le i \le n$, then the sequence of bottom labels is $\tau_n(00i) = 01n \cdot (11n)^{i-1} \cdot (11\overline{n})^{n+1-i}$, the sequence of top labels is $(111)^i \cdot (112)^{n-i}$ and the right-most right label is $01\overline{n}$.
- If $i = n+1$, then the sequence of bottom labels is $\tau_n(00i) = 01n \cdot (11n)^n$, the sequence of top labels is $(111)^n$ and the right-most right label is $00\overline{n}$.

The $n+1$ tiles of the strip for the three cases are illustrated in Figure 12. We observe that the last blue tile (the blue horizontal stripe tile with left label $00n$) is used in the strip only when $i = n+1$.

Assume $v = 01i$ with $1 \le i \le \overline{n}$. The following two cases occur.

- If $1 \le i \le n$, then the sequence of bottom labels is $\tau_n(01i) = 00n \cdot (11n)^{i-1} \cdot (11\overline{n})^{n+1-i}$, the sequence of top labels is $(111)^i \cdot (112)^{n-i}$ and the right-most right label is $01n$.
- If $i = n+1$, then the sequence of bottom labels is $\tau_n(00i) = 00n \cdot (11n)^n$, the sequence of top labels is $(111)^n$ and the right-most right label is $00n$.

The $n+1$ tiles of the strip for the two cases are illustrated in Figure 13.

https://doi.org/10.1017/fms.2025.10069 Published online by Cambridge University Press

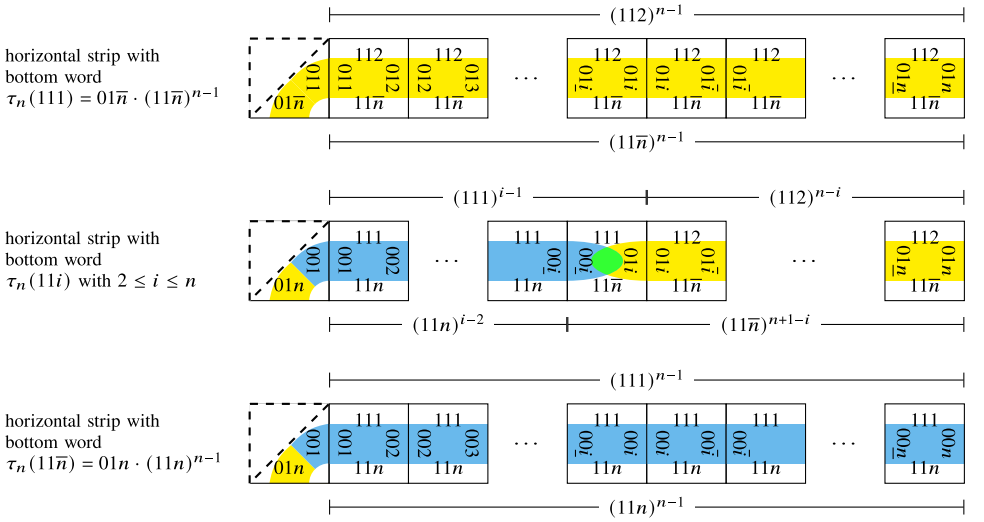

Figure 14. *Horizontal strip with bottom word $\tau_n(11i)$ with $1 \le i \le n+1$.*

Assume $v = 11i$ with $1 \le i \le \overline{n}$. The following three cases occur.

- If $i = 1$, then the sequence of bottom labels is $\tau_n(111) = 01\overline{n} \cdot (11\overline{n})^{n-1}$, the sequence of top labels is $(112)^{n-1}$ and the right-most right label is $01n$.
- If $2 \le i \le n$, then the sequence of bottom labels is $\tau_n(11i) = 01n \cdot (11n)^{i-2} \cdot (11\overline{n})^{n+1-i}$, the sequence of top labels is $(111)^{i-1} \cdot (112)^{n-i}$ and the right-most right label is $01n$.
- If $i = n+1$, then the sequence of bottom labels is $\tau_n(11i) = 01n \cdot (11n)^{n-1}$, the sequence of top labels is $(111)^{n-1}$ and the right-most right label is $00n$.

The n tiles of the strip for the three cases are illustrated in Figure 14. □

Since $\mathcal{T}_n = \widehat{\mathcal{T}_n}$, Lemma 5.2 has a symmetric version describing the vertical strip of tiles from $\mathcal{T}'_n$ with left labels equal to $\tau_n(u)$ for some $u \in V_n$. Lemma 5.2 and its symmetric version can be used together to construct valid rectangular patterns with external boundaries given by the images under the map τ_n; see Figure 16.

Lemma 5.3. *Let $\alpha, \beta, u, v \in V_n$. If* $\begin{array}{ccc} & \beta & \\ u & \square & \alpha \\ & v & \end{array} \in \mathcal{T}'_n$, *then there exists a unique valid rectangular pattern with tiles in $\mathcal{T}'_n$ whose right, top, left and bottom labels are respectively $\tau_n(\alpha)$, $\tau_n(\beta)$, $\tau_n(u)$ and $\tau_n(v)$.*

Proof. Let $u, v \in V_n$. For every tile in $\mathcal{T}'_n$, the left label starts with 0 if and only if the right label starts with 0, and, symmetrically, the bottom label starts with 0 if and only if the top label starts with 0. Since we have $\tau_n(V_n) \subset \{00n, 01n, 01\overline{n}\} \cdot \{11n, 11\overline{n}\}^*$, any valid rectangular pattern with tiles in $\mathcal{T}'_n$ whose sequence of bottom labels is $\tau_n(v)$ and sequence of left labels is $\tau_n(u)$ can be split into four disjoint regions: a junction tile at the bottom left corner, a row of horizontal stripe tiles at the bottom, a column of vertical stripe tiles on the left and a rectangular pattern of white tiles for the remaining rectangle; see Figure 15.

(Existence) Let $u, v, \alpha, \beta \in V_n$ be such that $t = \begin{array}{ccc} & \beta & \\ u & \square & \alpha \\ & v & \end{array} \in \mathcal{T}'_n$. First, we show that the junction tile at the bottom left corner of the rectangular pattern with bottom labels $\tau_n(v)$ and left labels $\tau_n(u)$ is one of the 9 junction tile in $\mathcal{T}'_n$. For every $u, v \in V_n$, we have $\tau_n(u), \tau_n(v) \in \{00n, 01n, 01\overline{n}\} \cdot (V_n)^*$. For every $x, y \in \{00n, 01n, 01\overline{n}\}$, there exists a unique junction tile in $\mathcal{T}'_n$ with bottom label x and left label y.

https://doi.org/10.1017/fms.2025.10069 Published online by Cambridge University Press

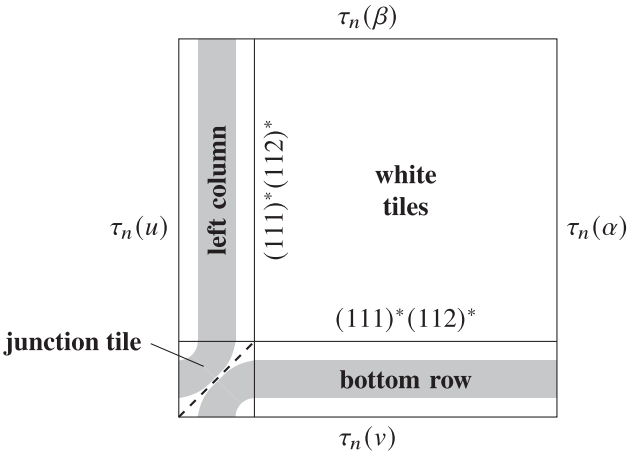

Figure 15. *The global shape of a rectangular pattern whose sequence of bottom labels is $\tau_n(v)$ and sequence of left labels is $\tau_n(u)$. The pattern is split into four disjoint parts: the junction tile, the left column, the bottom row and the white tiles.*

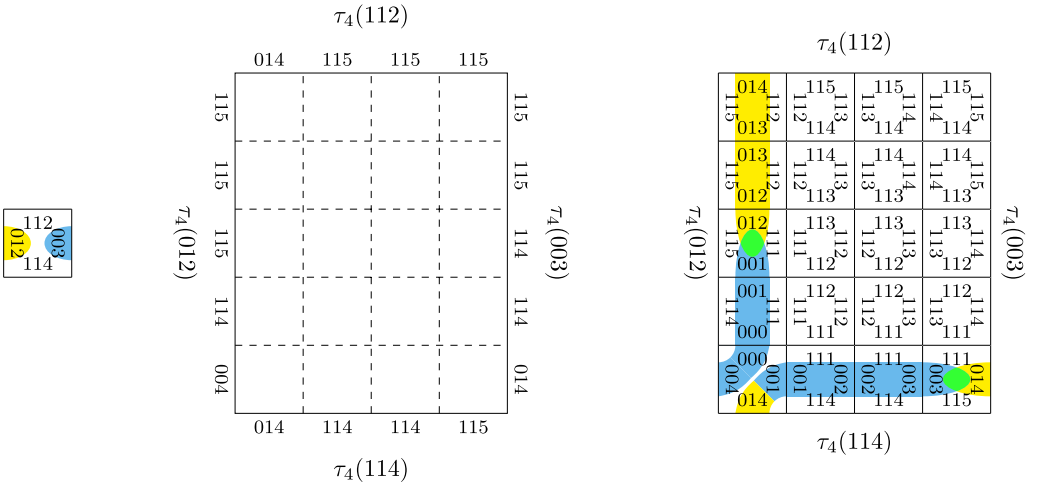

Figure 16. *Left: some antigren tile in $\mathcal{T}_4'$. Middle: the images under τ_4 of the labels of the tile form the boundary labels of a rectangle. Right: there is a unique rectangular pattern with such boundary words and tiles in $\mathcal{T}_4'$. As shown in Lemma 5.3, this holds for every $n \geq 1$ and for every tile in $\mathcal{T}_n'$ allowing to define the map ω_n'.*

It remains to show the existence of tiles from $\mathcal{T}_n'$ to cover the bottom row, the left column and the region of white tiles while respecting the label constraints; see Figure 15. Again, we proceed case by case.

Suppose that t is a junction tile in $\mathcal{T}_n'$; that is, $u, v \in \{00n, 01n, 01\overline{n}\}$. We have $|\tau_n(u)| = |\tau_n(v)| = n+1$. In order to formalize the argument that follows, it is practical to define the following two maps on the subset $\{00n, 01n, 01\overline{n}\} \subset V_n$:

$$\sigma : \begin{array}{ll} \{00n, 01n, 01\overline{n}\} & \to V_n \\ 00n & \mapsto 01\overline{n}, \\ 01n & \mapsto 01n, \\ 01\overline{n} & \mapsto 00n, \end{array} \quad \text{and} \quad \mu : \begin{array}{ll} \{00n, 01n, 01\overline{n}\} & \to V_n \\ 00n & \mapsto 000, \\ 01n & \mapsto 001, \\ 01\overline{n} & \mapsto 011. \end{array}$$

https://doi.org/10.1017/fms.2025.10069 Published online by Cambridge University Press

Notice that $\alpha = \mu(v)$ and $\beta = \mu(u)$ and σ is an involution. Also, if $v \in \{00n, 01n, 01\overline{n}\}$, then $\tau_n \circ \mu(v) = \sigma(v) \cdot (11\overline{n})^n$. From Lemma 5.2, there exists a unique choice of tiles for the bottom row whose sequence of top labels is $(111)^n$ and right-most right label is $01\overline{n}$ if $v = 00n, 01n$ if $v = 01n, 00n$ if $v = 01\overline{n}$. In other words, the right-most right label of the bottom row is $\sigma(v)$. Symmetrically, there exists a unique choice of tiles for the left column whose sequence of right labels is $(111)^n$ and top-most top label is $\sigma(u)$. Since the bottom row is of length n, and white tiles increase the last digit by one, the remaining region can be uniquely filled with white tiles such that the sequence of right labels of the rectangular pattern is $\sigma(v) \cdot (11\overline{n})^n = \tau_n \circ \mu(v) = \tau_n(\alpha)$. Symmetrically, the sequence of top labels of the rectangular pattern is $\sigma(u) \cdot (11\overline{n})^n = \tau_n \circ \mu(u) = \tau_n(\beta)$.

Suppose that $t = \begin{array}{ccc} & \beta & \\ u & \square & \alpha \\ & v & \end{array} = \begin{array}{ccc} & 11\overline{i} & \\ 11j & \square & 11\overline{j} \\ & 11i & \end{array}$ is a white tile in $\mathcal{T}'_n$; that is, $u = 11j$ with $1 \le j \le n$ and $v = 11i$ with $1 \le i \le n$. Also, $\alpha = 11\overline{j}$ and $\beta = 11\overline{i}$. We have $|\tau_n(u)| = |\tau_n(v)| = n$. From Lemma 5.2, there exists a unique choice of tiles for the bottom row whose sequence of top labels is $(111)^{i-1} \cdot (112)^{n-i}$ and right-most right label is $01n$. From a symmetric version of Lemma 5.2, there exists a unique choice of tiles for the left column whose sequence of right labels is $(111)^{j-1} \cdot (112)^{n-j}$ and top-most top label is $01n$. The remaining region can be uniquely filled with white tiles. In this case, the sequence of right labels of the rectangular pattern is $01n \cdot (11n)^{j-1} \cdot (11\overline{n})^{n-j} = \tau_n(11\overline{j}) = \tau_n(\alpha)$. Symmetrically, the sequence of top labels of the rectangular pattern is $01n \cdot (11n)^{i-1} \cdot (11\overline{n})^{n-i} = \tau_n(11\overline{i}) = \tau_n(\beta)$.

Suppose that t is a horizontal stripe tile in $\mathcal{T}'_n$. We have $u = 00j$ with $0 \le j \le n$ or $u = 01j$ with $1 \le j \le n$. Also $v \in \{11n, 11\overline{n}\}$. Let

$$\beta = \begin{cases} 111 & \text{if } u = 00j \text{ with } 0 \le j \le n, \\ 112 & \text{if } u = 01j \text{ with } 1 \le j \le n, \end{cases} \quad \text{and} \quad \alpha = \begin{cases} 00\overline{j} & \text{if } v = 11n, \\ 01\overline{j} & \text{if } v = 11\overline{n}. \end{cases}$$

Also, $|\tau_n(u)| = n + 1$ and $|\tau_n(v)| = n$. There are two cases for v:

- If $v = 11n$, then from Lemma 5.2, there exists a unique choice of tiles for the bottom row whose sequence of top labels is $(111)^{n-1}$ and right-most right label is $01n$.
- If $v = 11\overline{n}$, then from Lemma 5.2, there exists a unique choice of tiles for the bottom row whose sequence of top labels is $(111)^{n-1}$ and right-most right label is $00n$.

There are two cases for u:

- If $u = 00j$ with $0 \le j \le n$, then from the symmetric version of Lemma 5.2, there exists a unique choice of tiles for the left column whose sequence of right labels is $(111)^j \cdot (112)^{n-j}$ and top-most top label is $01\overline{n}$.
- If $u = 01j$ with $1 \le j \le n$, then from the symmetric version of Lemma 5.2, there exists a unique choice of tiles for the left column whose sequence of right labels is $(111)^j \cdot (112)^{n-j}$ and top-most top label is $01n$.

Thus, the remaining region can be uniquely filled with white tiles, and the sequence of right labels of the rectangular pattern is

$$\tau_n(\alpha) = \begin{cases} 01n \cdot (11n)^j \cdot (11\overline{n})^{n-j} = \tau_n(00\overline{j}) & \text{if } v = 11n, \\ 00n \cdot (11n)^j \cdot (11\overline{n})^{n-j} = \tau_n(01\overline{j}) & \text{if } v = 11\overline{n}. \end{cases}$$

Symmetrically, the sequence of top labels of the rectangular pattern is

$$\tau_n(\beta) = \begin{cases} 01\overline{n} \cdot (11\overline{n})^{n-1} = \tau_n(111) & \text{if } u = 00j \text{ with } 0 \le j \le n, \\ 01n \cdot (11\overline{n})^{n-1} = \tau_n(112) & \text{if } u = 01j \text{ with } 1 \le j \le n. \end{cases}$$

https://doi.org/10.1017/fms.2025.10069 Published online by Cambridge University Press

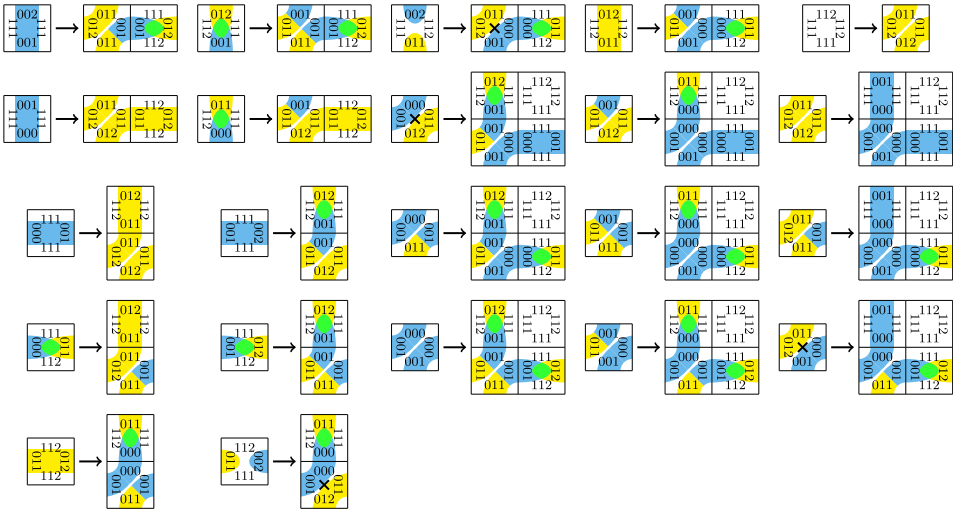

Figure 17. *The substitution ω'_1. An $\times$-mark indicates the tiles in $J'_1 \setminus J_1$.*

Suppose that t is a vertical stripe tile in $\mathcal{T}'_n$. A rectangular pattern respecting the constraints can be obtained by taking the image under reflection of the rectangular pattern constructed above for when t is a horizontal stripe tile in $\mathcal{T}'_n$.

(Uniqueness) Uniqueness follows from Lemma 2.1 and Lemma 4.3. □

Following Lemma 5.3, we define the following map:

$$\begin{array}{ccccc} \omega'_n : & \mathcal{T}'_n & \to & (\mathcal{T}'_n)^{*2} \\ & \begin{array}{ccc} & \beta & \\ u & \square & \alpha \\ & v & \end{array} & \mapsto & \begin{array}{l}\text{the unique rectangular}\\ \text{pattern with external labels}\end{array} & \begin{array}{ccc} & \tau_n(\beta) & \\ \tau_n(u) & \square & \tau_n(\alpha) \\ & \tau_n(v) & \end{array} . \end{array} \tag{5.2}$$

For example, the map ω'_1 is illustrated in Figure 17.

Lemma 5.4. *The map ω'_n defines a 2-dimensional substitution $\omega'_n : \Omega'_n \to \Omega'_n$.*

Proof. From Lemma 5.3, for every tile $t \in \mathcal{T}'_n$, the image $\omega'_n(t)$ is a valid rectangular pattern over the Wang tiles $\mathcal{T}'_n$. Moreover, if $s \odot^1 t \in (\mathcal{T}'_n)^{*^2}$ is a valid horizontal domino, then $\omega'_n(s \odot^1 t)$ is a valid rectangular pattern over the Wang tiles $\mathcal{T}'_n$. Similarly, if $s \odot^2 t \in (\mathcal{T}'_n)^{*^2}$ is a valid vertical domino, then $\omega'_n(s \odot^2 t)$ is a valid rectangular pattern over the Wang tiles $\mathcal{T}'_n$. Thus, if $y \in \Omega'_n$ is a valid configuration, then $\omega'_n(y)$ is also a valid configuration. Therefore, $\omega'_n(y) \in \Omega'_n$. □

5.3. A substitution ω_n for the tiles in $\mathcal{T}_n$

Not all tiles of $\mathcal{T}'_n$ appear in the image of a tile under the substitution ω'_n. For example, it follows from Lemma 5.2 that antigreen stripe tiles do not appear in the images of tiles under ω'_n. Therefore, the substitution ω'_n is not primitive.

As it can be observed in Figure 17, some tiles in $\mathcal{T}'_1 \setminus \mathcal{T}_1$ appear in the images of ω'_1. Namely, the images of the antigreen tiles under ω'_1 contain junction tiles in $J'_1 \setminus J_1 = \{j_1^{0,0,1,1}, j_1^{1,1,0,0}\}$. As shown in the next lemma, this is the only exception.

Lemma 5.5. *Let $n \geq 1$ be an integer and $t \in \mathcal{T}'_n$. The pattern $\omega'_n(t)$ contains a tile in $\mathcal{T}'_n \setminus \mathcal{T}_n$ if and only if $n = 1$ and t is an antigreen tile.*

https://doi.org/10.1017/fms.2025.10069 Published online by Cambridge University Press

Proof. Let $n \geq 1$ be an integer. ($\Longleftarrow$) If $n = 1$, the set of antigreen tiles in $\mathcal{T}_1'$ is $A_1 \cup \widehat{A_1} = \{a_1^1, \widehat{a_1^1}\}$. In Figure 17, we observe that $\omega_1'(a_1^1)$ contains the junction tile $j_1^{1,1,0,0} \in \mathcal{T}_1' \setminus \mathcal{T}_1$ and $\omega_1'(\widehat{a_1^1})$ contains the junction tile $j_1^{0,0,1,1} \in \mathcal{T}_1' \setminus \mathcal{T}_1$.

($\Longrightarrow$) Let $t = \begin{array}{ccc} & \beta & \\ u & \square & \alpha \\ & v & \end{array} \in \mathcal{T}_n'$. The labels of the boundary of $\omega_n'(t)$ are $\begin{array}{ccc} & \tau_n(\beta) & \\ \tau_n(u) & \square & \tau_n(\alpha) \\ & \tau_n(v) & \end{array}$.

Suppose that the pattern $\omega_n'(t)$ contains a tile in $\mathcal{T}_n' \setminus \mathcal{T}_n$. We have $v \in V_n \setminus \{00\overline{n}\}$. From Lemma 5.2, the bottom row of the pattern $\omega_n'(t)$ does not contain the last blue tile. Also, $u \in V_n \setminus \{00\overline{n}\}$. From the symmetric version of Lemma 5.2, the left column of the pattern $\omega_n'(t)$ does not contain the last blue tile. From Lemma 5.2, the pattern $\omega_n'(t)$ does not contain any antigreen (vertical or horizontal) stripe tile. Therefore, the pattern $\omega_n'(t)$ must contain a junction tile in $J_n' \setminus J_n = \{j_n^{1,1,0,0}, j_n^{0,0,1,1}\}$.

Suppose that $\omega_n'(t)$ contains the junction tile $j_n^{1,1,0,0}$. Therefore, we must have $\tau_n(v) \in 01\overline{n} \cdot (V_n)^*$ and $\tau_n(u) \in 00n \cdot (V_n)^*$. Thus, $v \in \{000, 111\}$ and $u = 01j$ with $1 \leq j \leq n$. We proceed case by case.

- Assume $v = 000$. The only tile $t \in \mathcal{T}_n'$ with bottom label $v = 000$ is a blue or green vertical stripe tile whose left label is $u = 11n$ or $u = 11\overline{n}$, a contradiction.
- Assume $v = 111$ and $n > 1$. The only tile $t \in \mathcal{T}_n'$ with bottom label $v = 111$ is a white tile whose left label is $u = 11i$ with $1 \leq i \leq n$, a contradiction.
- Assume $v = 111$ and $n = 1$. The only tile $t \in \mathcal{T}_1'$ with bottom label $v = 111$ is a white tile whose left label is $u = 111$, a blue horizontal stripe tile whose left label is 000 or 001, or an antigreen tile a_1^1 whose left label is 011. Only the antigreen tile does not yield a contradiction with the value of u given above. Thus, $t = a_1^1$.

Symmetrically, if $\omega_n'(t)$ contains the junction tile $j_n^{0,0,1,1}$, we conclude that $n = 1$ and $t = \widehat{a_1^1}$. □

A consequence of Lemma 5.5 is that if $n \geq 2$ and $t \in \mathcal{T}_n'$, then the pattern $\omega_n'(t)$ contains only tiles from $\mathcal{T}_n$. Also for every $n \geq 1$ and $t \in \mathcal{T}_n$, the pattern $\omega_n'(t)$ contains only tiles from $\mathcal{T}_n$. Thus, it becomes natural to restrict the substitution ω_n' to the set $\mathcal{T}_n$. We obtain the following map $\omega_n = \omega_n'|_{\mathcal{T}_n}$:

$$\begin{array}{ccccc} \omega_n : & \mathcal{T}_n & \to & (\mathcal{T}_n)^{*2} & \\ & \begin{array}{ccc} & \beta & \\ u & \square & \alpha \\ & v & \end{array} & \mapsto & \text{the unique rectangular pattern with external labels} & \begin{array}{ccc} & \tau_n(\beta) & \\ \tau_n(u) & \square & \tau_n(\alpha) \\ & \tau_n(v) & \end{array} \end{array} \tag{5.3}$$

The substitutions ω_n for $n = 1, \ldots, 5$ are illustrated in Figure 31, Figure 32, Figure 33, Figure 34 and Figure 35 (in the appendix).

Lemma 5.6. *The map ω_n defines a 2-dimensional substitution $\omega_n : \Omega_n \to \Omega_n$ such that $\overline{\omega_n(\Omega_n)}^{\sigma} \subset \Omega_n$.*

Proof. From Lemma 5.4, the map ω_n' defines a 2-dimensional substitution $\Omega_n' \to \Omega_n'$. From Lemma 5.5, $\omega_n'(x) \in \Omega_n$ for every configuration $x \in \Omega_n$. Thus, $\omega_n'(\Omega_n) \subseteq \Omega_n$. The restriction of ω_n' to Ω_n is ω_n, so that $\omega_n(\Omega_n) \subseteq \Omega_n$. Since Ω_n is a subshift, it is closed under the shift. Therefore, $\overline{\omega_n(\Omega_n)}^{\sigma} \subset \Omega_n$. □

The goal of the next section is to show that $\Omega_n = \overline{\omega_n(\Omega_n)}^{\sigma}$ – namely, that every configuration in Ω_n can be desubstituted using ω_n. The proof of this is completed in Section 8. Following the above discussion, the 2-dimensional substitution ω_n' is not primitive, but we show in Section 9 that the substitution ω_n is primitive.

https://doi.org/10.1017/fms.2025.10069 Published online by Cambridge University Press

5.4. *A sufficient and necessary condition*

The goal of this section is to show that the sufficiency in the statement of Lemma 5.3 is also a necessity – namely, that every rectangular pattern, with external boundary labeled by images under τ_n, is obtained from a tile in $\mathcal{T}_n'$. The precise statement is given in Proposition 5.9.

For every integer $n \geq 1$, let

$$Z_n = \{v_0v_1v_2 \in V_n \mid v_0 = 0\}$$

be the set of vectors of V_n such that the first entry is zero and let

$$M_n = \{v_0v_1v_2 \in V_n \mid v_2 \geq n\}$$

be the set of vectors of V_n such that the last entry is n or $\overline{n}$.

Lemma 5.7. *If*

$$\begin{aligned}(u,v) \in\ & (\{11\overline{n}\} \times V_n \setminus Z_n) \cup (V_n \setminus Z_n \times \{11\overline{n}\}) \\ & \cup (\{00\overline{n}\} \times M_n \cap Z_n) \cup (M_n \cap Z_n \times \{00\overline{n}\}) \\ & \cup (\{00\overline{n}, 01\overline{n}\} \times M_n \setminus Z_n) \cup (M_n \setminus Z_n \times \{00\overline{n}, 01\overline{n}\}),\end{aligned} \tag{5.4}$$

then there exists a unique valid rectangular pattern with tiles in $\mathcal{T}_n'$ whose right, top, left and bottom labels are respectively R, T, $\tau_n(u)$ and $\tau_n(v)$ for some $R, T \in (V_n)^*$, and there is no $(\alpha, \beta) \in V_n \times V_n$ such that $R = \tau_n(\alpha)$ and $T = \tau_n(\beta)$.

Proof. Suppose that $u \in V_n \setminus Z_n$ and $v = 11\overline{n}$. We have $|\tau_n(u)| = |\tau_n(v)| = n$. Since $v = 11\overline{n}$, then from Lemma 5.2, there exists a unique choice of tiles for the bottom row whose sequence of top labels is $(111)^{n-1}$ and right-most right label is $00n$. There are two cases to consider for u:

- If $u = 11j$ with $1 \leq j \leq n$, then from a symmetric version of Lemma 5.2, there exists a unique choice of tiles for the left column whose sequence of right labels is $(111)^{j-1} \cdot (112)^{n-j}$.
- If $u = 11\overline{n}$, then from a symmetric version of Lemma 5.2, there exists a unique choice of tiles for the left column whose sequence of right labels is $(111)^{n-1}$.

In both cases, the remaining region of the rectangular pattern can be uniquely filled with white tiles. The sequence of right labels of the rectangular pattern starts with $00n$. Such a sequence cannot be written as an image under the map τ_n because there is no $\alpha \in V_n$ such that $\tau_n(\alpha)$ starts with $00n$ and is of length n.

Suppose that $u \in M_n \cap Z_n = \{00n, 00\overline{n}, 01n, 01\overline{n}\}$ and $v = 00\overline{n}$. We have $|\tau_n(u)| = |\tau_n(v)| = n + 1$. From Lemma 5.2, there exists a unique choice of tiles for the bottom row whose sequence of top labels is $(111)^n$. Since $v = 00\overline{n}$, from a symmetric version of Lemma 5.2, there exists a unique choice of tiles for the left column whose sequence of right labels is $(111)^n$ and top-most top label is $00\overline{n}$. Since the bottom row is of length n, and white tiles increase the last digit by one, the remaining region can be uniquely filled with white tiles. Since the sequence of top labels of the rectangular pattern starts with $00\overline{n}$, it cannot be written as an image under the map τ_n.

Suppose that $u \in \{00\overline{n}, 01\overline{n}\}$ and $v \in M_n \setminus Z_n = \{11n, 11\overline{n}\}$. We have $|\tau_n(u)| = n+1$ and $|\tau_n(v)| = n$. From Lemma 5.2, there exists a unique choice of tiles for the bottom row whose sequence of top labels is $(111)^n$. Symmetrically, there exists a unique choice of tiles for the left column whose sequence of right labels is $(111)^n$ and top-most top label is in $\{00n, 00\overline{n}\}$. The remaining region can be uniquely filled with white tiles. The sequence of top labels is in $\{00n, 00\overline{n}\} \cdot (11\overline{n})^{n-1}$. Such a sequence cannot be written as an image under the map τ_n because there is no $\alpha \in V_n$ such that $\tau_n(\alpha)$ starts with $00n$ or $00\overline{n}$ and is of length n.

Suppose that $u = 11\overline{n}$ and $v \in V_n \setminus Z_n$, or $u = 00\overline{n}$ and $v \in M_n \cap Z_n$, or $u \in M_n \setminus Z_n$ and $v \in \{00\overline{n}, 01\overline{n}\}$. A rectangular pattern respecting the constraints can be obtained by taking the image under reflection of the rectangular pattern constructed above. □

https://doi.org/10.1017/fms.2025.10069 Published online by Cambridge University Press

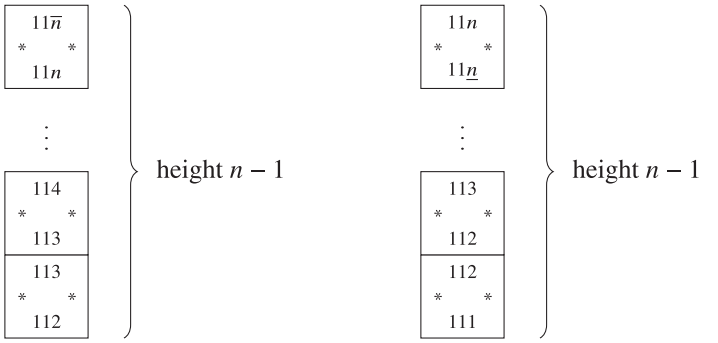

Figure 18. *The height of a valid vertical column made entirely of white tiles from $\mathcal{T}_n$ is at most $n-1$ if the bottom label of the bottom-most tile is* 112 *or if the top label of the top-most tile is* $11n$.

Proposition 5.8. *Let $u, v \in V_n$. There exists a valid rectangular pattern of tiles in $\mathcal{T}_n'$ whose sequence of bottom labels is $\tau_n(v)$ and sequence of left labels is $\tau_n(u)$ if and only if*

$$(u,v) \in (V_n \setminus Z_n \times V_n \setminus Z_n) \cup (M_n \cap Z_n \times M_n \cap Z_n) \cup (M_n \setminus Z_n \times Z_n) \cup (Z_n \times M_n \setminus Z_n). \quad (5.5)$$

Proof. Let $u, v \in V_n$. ($\Longrightarrow$) We show the contrapositive – namely, that if (5.5) does not hold, then there is no rectangular pattern with $\tau_n(u)$ as the sequence of labels on the left and $\tau_n(v)$ as the sequence of labels at the bottom. If (5.5) does not hold, then

$$\begin{aligned}(u,v) \in &\big((Z_n \times V_n \setminus Z_n) \cup (V_n \setminus Z_n \times Z_n) \cup (Z_n \times Z_n)\big) \\ &\setminus \big((M_n \cap Z_n \times M_n \cap Z_n) \cup (M_n \setminus Z_n \times Z_n) \cup (Z_n \times M_n \setminus Z_n)\big) \\ = &(Z_n \times V_n \setminus (M_n \cup Z_n)) \cup (V_n \setminus (M_n \cup Z_n) \times Z_n) \cup (Z_n \times Z_n \setminus M_n) \cup (Z_n \setminus M_n \times Z_n).\end{aligned}$$

There are four cases to consider:

- Assume $u \in Z_n$ and $v \in V_n \setminus (M_n \cup Z_n)$. We have $v = 11j$ with $1 \le j < n$. From Lemma 5.2, the bottom row of the rectangular pattern has at least one label 112 on its top. Since the difference between the last digit of the top label and the last digit of the bottom label of a white tile is 1 and the maximal last digit of a white tile in $\mathcal{T}_n$ is $\overline{n}$, the height of the white tile region is at most $n-1$; see Figure 18. Thus, $|\tau_n(u)| \le n$. This is incompatible with $u \in Z_n$ because $u \in Z_n$ implies that $|\tau_n(u)| = n+1$.
- Assume $u \in V_n \setminus (M_n \cup Z_n)$ and $v \in Z_n$. This case also leads to a contradiction following an argument symmetric to the previous one.
- Assume $u \in Z_n$ and $v \in Z_n \setminus M_n$. We have $v = 00j$ with $0 \le j < n$ or $v = 01j$ with $1 \le j < n$. In both cases, we have from Lemma 5.2 that the bottom row of the rectangular pattern has at least one label 112 on its top. For the same reason as in the first item, the height of the rectangular pattern is $|\tau_n(u)| \le n$. This is incompatible with $u \in Z_n$ because $u \in Z_n$ implies that $|\tau_n(u)| = n+1$.
- Assume $u \in Z_n \setminus M_n$ and $v \in Z_n$. This case also leads to a contradiction following an argument symmetric to the previous one.

($\Longleftarrow$) Let

$$P = (V_n \setminus Z_n \times V_n \setminus Z_n) \cup (M_n \cap Z_n \times M_n \cap Z_n) \cup (M_n \setminus Z_n \times Z_n) \cup (Z_n \times M_n \setminus Z_n),$$

$$Q = \left\{ (u,v) \in V_n \times V_n \;\middle|\; \text{there exists } \alpha, \beta \in V_n \text{ such that } \begin{array}{c} u \;\square^{\beta} \;\alpha \\ v \end{array} \in \mathcal{T}_n' \right\}.$$

https://doi.org/10.1017/fms.2025.10069 Published online by Cambridge University Press

Notice that $Q \subset P$ and

$$\begin{aligned} P \setminus Q = &(\{11\overline{n}\} \times V_n \setminus Z_n) \cup (V_n \setminus Z_n \times \{11\overline{n}\}) \\ &\cup (\{00\overline{n}\} \times M_n \cap Z_n) \cup (M_n \cap Z_n \times \{00\overline{n}\}) \\ &\cup (\{00\overline{n}, 01\overline{n}\} \times M_n \setminus Z_n) \cup (M_n \setminus Z_n \times \{00\overline{n}, 01\overline{n}\}). \end{aligned} \tag{5.6}$$

We assume that (5.5) holds; that is, $(u, v) \in P$. There are two cases to consider.

- If $(u, v) \in Q$, then, from Lemma 5.3, there exists a valid rectangular pattern with tiles in $\mathcal{T}'_n$ whose left and bottom labels are respectively $\tau_n(u)$ and $\tau_n(v)$.
- If $(u, v) \in P \setminus Q$, then using (5.6) and Lemma 5.7, there exists a valid rectangular pattern with tiles in $\mathcal{T}'_n$ whose left and bottom labels are respectively $\tau_n(u)$ and $\tau_n(v)$. □

Proposition 5.9. *Let $\alpha, \beta, u, v \in V_n$. There exists a valid rectangular pattern with tiles in $\mathcal{T}'_n$ whose right, top, left and bottom labels are respectively $\tau_n(\alpha)$, $\tau_n(\beta)$, $\tau_n(u)$ and $\tau_n(v)$ if and only if* $u \begin{smallmatrix} \beta \\ \square \\ v \end{smallmatrix} \alpha \in \mathcal{T}'_n$.

Proof. Let $\alpha, \beta, u, v \in V_n$. ($\Longleftarrow$) The existence of the rectangular pattern was proved in Lemma 5.3.

($\Longrightarrow$) Suppose that there exists a valid rectangular pattern with tiles in $\mathcal{T}'_n$ whose right, top, left and bottom labels are respectively $\tau_n(\alpha)$, $\tau_n(\beta)$, $\tau_n(u)$ and $\tau_n(v)$. From Proposition 5.8, (u, v) satisfies (5.5); that is $(u, v) \in P$. From Lemma 5.7, (u, v) does not satisfy (5.4) because all boundary words can be written as the image of τ_n. Thus, $(u, v) \notin P \setminus Q$ using (5.6). We conclude that $(u, v) \in Q$. Thus, there exists $\alpha', \beta' \in V_n$ such that $u \begin{smallmatrix} \beta' \\ \square \\ v \end{smallmatrix} \alpha' \in \mathcal{T}'_n$. From Lemma 5.3, there exists a valid rectangular pattern with tiles in $\mathcal{T}'_n$ whose right, top, left and bottom labels are respectively $\tau_n(\alpha')$, $\tau_n(\beta')$, $\tau_n(u)$ and $\tau_n(v)$. From Lemma 2.1, we must have $\tau_n(\alpha') = \tau_n(\alpha)$ and $\tau_n(\beta') = \tau_n(\beta)$ because $\mathcal{T}'_n$ is SW-deterministic from Lemma 4.3. Since τ_n is injective over the set V_n, we have $\alpha = \alpha'$ and $\beta = \beta'$. □

Proposition 5.9 is used in Lemma 6.6 in order to desubstitute configurations in Ω_n over tiles in $\mathcal{T}_n$. Nevertheless, considering tiles in $\mathcal{T}'_n$ is necessary for Proposition 5.9 to hold for every integer $n \geq 1$. Following Lemma 5.5, Proposition 5.9 can be restated as follows when $n \geq 2$.

Corollary 5.10. *Suppose that $n \geq 2$ is an integer and let $\alpha, \beta, u, v \in V_n$. There exists a valid rectangular pattern with tiles in $\mathcal{T}_n$ whose right, top, left and bottom labels are respectively $\tau_n(\alpha)$, $\tau_n(\beta)$, $\tau_n(u)$ and $\tau_n(v)$ if and only if* $u \begin{smallmatrix} \beta \\ \square \\ v \end{smallmatrix} \alpha \in \mathcal{T}'_n$.

Proof. Let $\alpha, \beta, u, v \in V_n$. ($\Longrightarrow$) follows from Proposition 5.9 since $\mathcal{T}_n \subset \mathcal{T}'_n$.

($\Longleftarrow$) From Lemma 5.5, for every tile $t \in \mathcal{T}'_n$, the rectangular pattern $\omega'_n(t)$ satisfies the boundary conditions, and it contains only the tiles from the set $\mathcal{T}_n$. □

6. A desubstitution $\Omega_n \leftarrow \Omega'_n$

In this section, we decompose configurations in Ω'_n and in Ω_n into rectangular blocks called return blocks. The external boundary labels of the return blocks within a configuration in Ω_n behave like a new set $\mathcal{T}'_n$ of Wang tiles which contains $\mathcal{T}_n$ as a subset.

6.1. Return blocks in the Wang shift Ω'_n

In this section, we study some properties of the Wang shift Ω'_n defined by the Wang tiles $\mathcal{T}'_n$. Since $\mathcal{T}_n \subset \mathcal{T}'_n$ for every $n \geq 1$, we have $\Omega_n \subset \Omega'_n$. Thus, the properties shown for Ω'_n also hold for Ω_n.

https://doi.org/10.1017/fms.2025.10069 Published online by Cambridge University Press

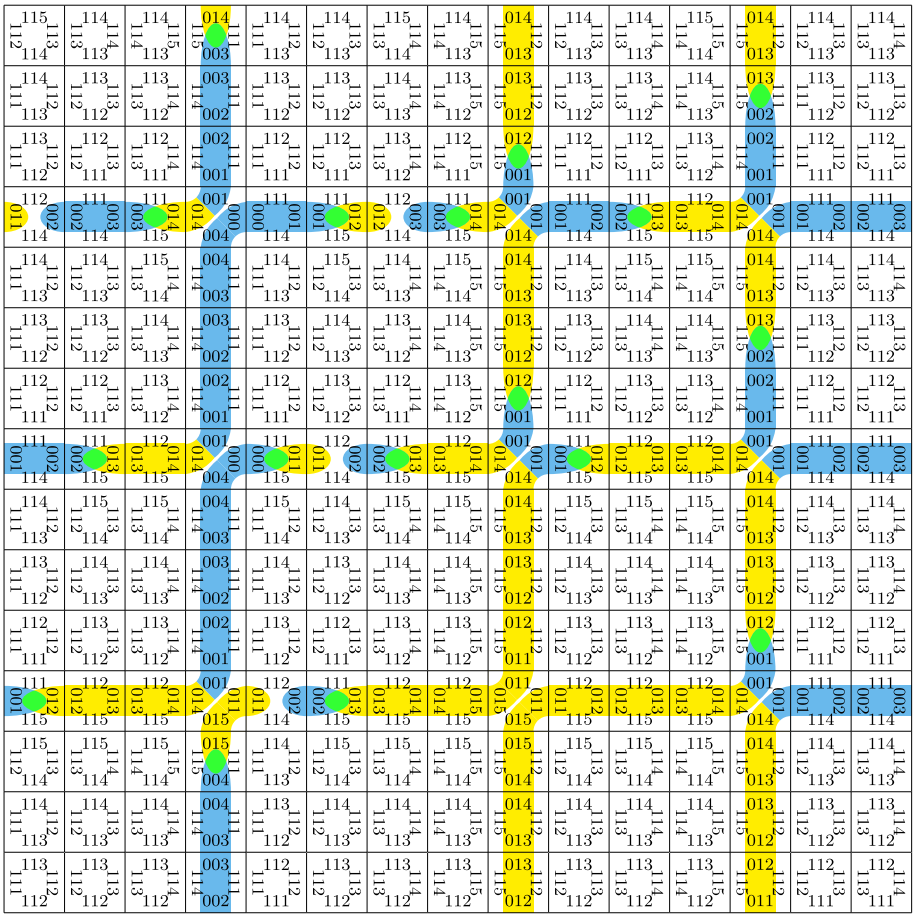

Figure 19. *A valid* 15×15 *pattern using the extended set* $\mathcal{T}_4'$ *of Wang tiles. Note that it contains some antigreen tiles.*

A tiling with the set $\mathcal{T}_4'$ is shown in Figure 19. We observe the presence of rows and columns of colored tiles. At the intersection of these colored rows and columns are junction tiles. In other words, the set of positions of junction tiles in the figure is the Cartesian product of two sets. Also, the distance between two consecutive junction tiles in the same row or column is 4 or 5. In the following lemmas, we prove that these observations hold in general.

Lemma 6.1. *Let* $n \geq 1$ *be an integer. For every valid configuration* $c \in \Omega_n'$*, the distance between two consecutive occurrences of junction tiles in the same row is* n*,* $n+1$ *or* $n+2$*.*

Also, the sequence of bottom labels of the tiles between two consecutive junction tiles (including the left junction tile but not the right one) belongs to $\{00n, 01n, 01\overline{n}\} \cdot \{11n, 11\overline{n}\}^*$*.*

Proof. The horizontal Rauzy graph restricted to tiles whose vertical edge labels are starting with zero is shown in Figure 20. An arc in the horizontal Rauzy graph links two tiles $s \to t$ if and only if the right label of tile s is equal to the left label of tile t. The graph allows to visualize the combinatorial structure between two consecutive junction tiles on the same horizontal row within a configuration of Ω_n'.

The right label of a junction tile is 000, 001 or 011, which implies that the last digit of the right label of a junction tile is 0 or 1. The left label of a junction tile is $00n$, $01n$ or $01\overline{n}$, which implies that the last digit of the left label of a junction tile is n or $\overline{n}$. Since the last digit increases by 1 from the left label to the right label of every intermediate tile (a tile appearing in between two consecutive junction tiles in

https://doi.org/10.1017/fms.2025.10069 Published online by Cambridge University Press

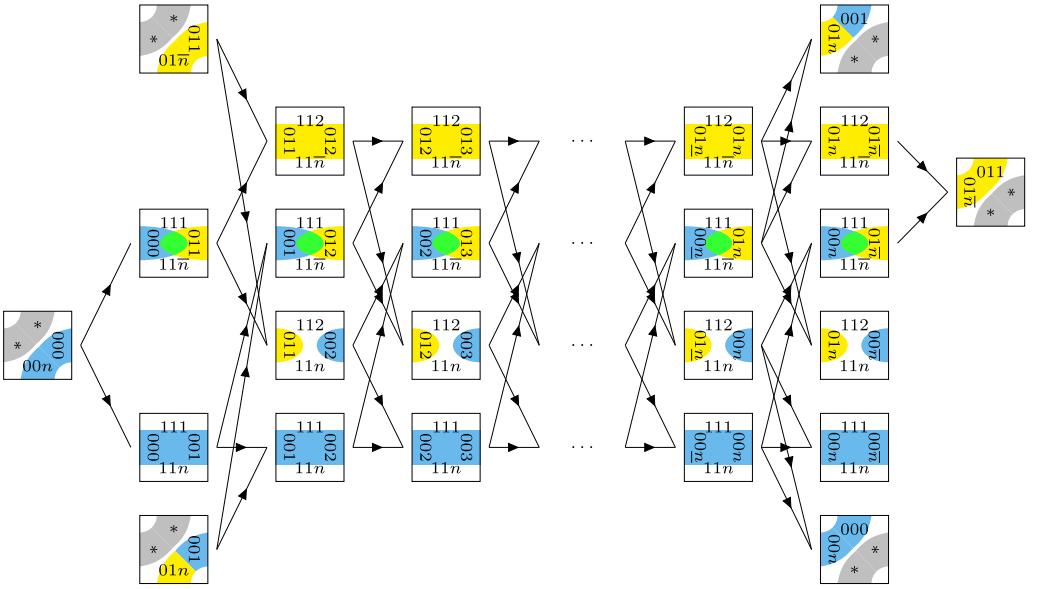

Figure 20. *Combinatorial structure between two consecutive junction tiles on the same horizontal row within a configuration of Ω'_n. The nodes of the graph are placed such that any two tiles appearing in the same column have the same last digit for its left or right labels. The length of a path from a junction tile to a junction tile is n, $n+1$ or $n+2$.*

the same row), the number of tiles in between two consecutive junction tiles on the same row is at least $n-1$ and at most $\overline{n}-0 = n+1$. We conclude that the distance (number of edges in the Rauzy graph) between two consecutive junction tiles in the same row is n, $n+1$ or $n+2$. In particular, it is at least n.

The bottom label of a junction tile is in the set $\{00n, 01n, 01\overline{n}\}$. The bottom label of every intermediate tile is $11n$ or $11\overline{n}$. Therefore, the sequence of bottom labels of the tiles between two consecutive junction tiles (including the left junction tile but not the right one) belongs to $\{00n, 01n, 01\overline{n}\} \cdot \{11n, 11\overline{n}\}^*$; see Figure 20. □

Lemma 6.2. *Let $n \geq 1$ be an integer. For every valid configuration $c \in \Omega'_n$, the distance between two consecutive occurrences of a vertical stripe tile (blue, green, yellow or antigreen) in the same row is $n-1$, n or $n+1$.*

Proof. The horizontal Rauzy graph restricted to vertical edge labels starting with 1 is shown in Figure 21. An arc in the horizontal Rauzy graph links two tiles $s \to t$ if and only if the right label of tile s is equal to the left label of tile t. The graph allows to visualize the combinatorial structure between two consecutive vertical stripe tiles on the same horizontal row within a configuration of Ω'_n.

The right label of a vertical stripe tile is 111 or 112, which implies that the last digit of the right label of a vertical stripe tile is 1 or 2. The left label of a vertical stripe tile is $11n$ or $11\overline{n}$, which implies that the last digit of the left label of a vertical stripe tile is n or $\overline{n}$. Since the last digit increases by 1 from the left label to the right label of every intermediate tile (a tile appearing in between two consecutive vertical stripe tiles in the same row), the number of tiles in between two consecutive vertical stripe tiles on the same row is at least $n-2$ and at most $\overline{n}-1 = n$. We conclude that the distance (number of edges in the Rauzy graph) between two consecutive vertical stripe tiles in the same row is $n-1$, n or $n+1$. In particular, it is at most $n+1$. □

Lemma 6.3. *Let $n \geq 1$ be an integer. For every valid configuration $c \in \Omega'_n$, there exist two strictly increasing sequences $A, B : \mathbb{Z} \to \mathbb{Z}$ such that the following hold.*

https://doi.org/10.1017/fms.2025.10069 Published online by Cambridge University Press

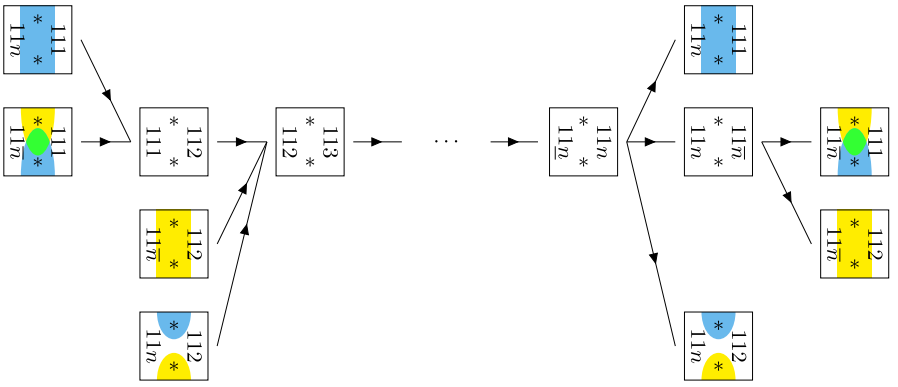

Figure 21. *Combinatorial structure between two consecutive vertical stripe tile on the same horizontal row within a configuration of Ω'_n. The length of a path from a vertical stripe tile to a vertical stripe tile is $n-1$, n or $n+1$.*

1. *The set of positions of junction tiles in the configuration c is the Cartesian product $c^{-1}(J'_n) = A(\mathbb{Z}) \times B(\mathbb{Z})$.*
2. *The distance between two consecutive occurrences of junction tiles in the same row is n or $n+1$; that is, $A(k+1) - A(k) \in \{n, n+1\}$ for every $k \in \mathbb{Z}$.*
3. *The distance between two consecutive occurrences of junction tiles in the same column is n or $n+1$; that is, $B(k+1) - B(k) \in \{n, n+1\}$ for every $k \in \mathbb{Z}$.*

Proof. (1) Let

$$E = \{(\alpha_1\alpha_2\alpha_3, \beta_1\beta_2\beta_3, \gamma_1\gamma_2\gamma_3, \delta_1\delta_2\delta_3) \in \mathcal{T}'_n \mid \alpha_1 = 0\} \subset \mathcal{T}'_n,$$
$$F = \{(\alpha_1\alpha_2\alpha_3, \beta_1\beta_2\beta_3, \gamma_1\gamma_2\gamma_3, \delta_1\delta_2\delta_3) \in \mathcal{T}'_n \mid \beta_1 = 0\} \subset \mathcal{T}'_n.$$

Tiles in E have zero as the first coordinate of their right and left edge labels since $\alpha_1 = \gamma_1$. Tiles in F have zero as the first coordinate of their top and bottom edge labels since $\beta_1 = \delta_1$. Notice that we have $E \cup F \subset Y_n \cup \widehat{Y_n} \cup G_n \cup \widehat{G_n} \cup B'_n \cup \widehat{B'_n} \cup J'_n \cup A_n \cup \widehat{A_n}$ and $E \cap F = J'_n$. Let $c \in \Omega'_n$ be a valid configuration. The positions of tiles from E in c are contiguous rows; that is, there exists $B \subset \mathbb{Z}$ such that $c^{-1}(E) = \mathbb{Z} \times B$. The positions of tiles from F in c are contiguous columns; that is, there exists $A \subset \mathbb{Z}$ such that $c^{-1}(F) = A \times \mathbb{Z}$. Therefore, the set of positions of junction tiles in c is given by the Cartesian product of A and B:

$$c^{-1}(J'_n) = c^{-1}(E \cap F) = c^{-1}(E) \cap c^{-1}(F) = (\mathbb{Z} \times B) \cap (A \times \mathbb{Z}) = A \times B.$$

The fact that the sets A and B are the images of increasing maps $\mathbb{Z} \to \mathbb{Z}$ follows from observations (2) and (3) proved below.

(2) From Lemma 6.1, the distance between two consecutive occurrences of junction tiles in the same row is n, $n+1$ or $n+2$. From Lemma 6.2, the distance between two consecutive occurrences of a vertical stripe tile (blue, green, yellow or antigreen) in the same row is $n-1$, n or $n+1$. Since vertical strips and junction tiles are vertically aligned, the difference between two consecutive elements of $A \subset \mathbb{Z}$ is n or $n+1$. Also, if $a \in A$, then $a+n \in A$ or $a+n+1 \in A$. Also $a-n \in A$ or $a-n-1 \in A$. Thus, A is the image of an increasing map $A : \mathbb{Z} \to \mathbb{Z}$ such that $A(k+1) - A(k) \in \{n, n+1\}$ for every $k \in \mathbb{Z}$.

(3) From the symmetry of the set $\mathcal{T}'_n$ of tiles, the same observation holds for the distance between consecutive junction tiles in the same column. □

Lemma 6.3 means that we can subdivide valid configurations in Ω'_n by rectangular patterns containing a unique junction tile at their bottom left corners; see Figure 22.

https://doi.org/10.1017/fms.2025.10069 Published online by Cambridge University Press

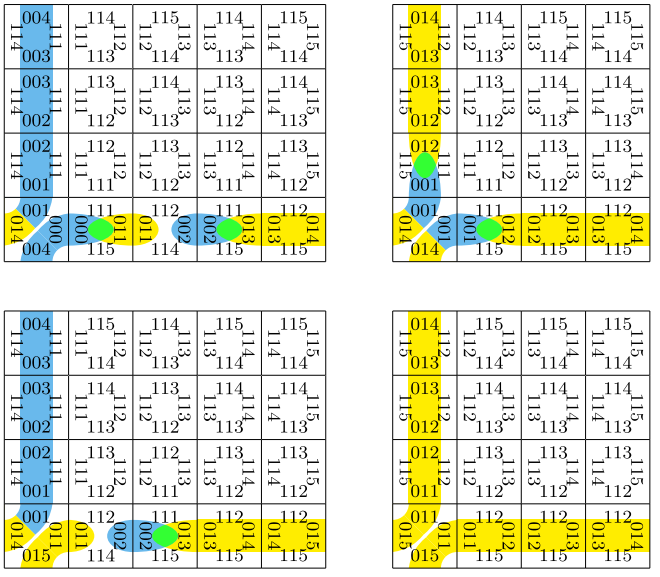

Figure 22. *Return blocks appearing in Figure 19. Each return block contains a unique junction tile at its bottom left corner.*

Proposition 6.4. *Every configuration in Ω'_n can be divided uniquely into rectangular blocks of sizes $n \times n$, $n \times \overline{n}$, $\overline{n} \times n$ and $\overline{n} \times \overline{n}$ with a unique junction tile at their bottom left corners.*

Proof. Let $c \in \Omega'_n$ be a configuration. Let $A, B : \mathbb{Z} \to \mathbb{Z}$ be the two increasing maps from Lemma 6.3 such that $c^{-1}(J'_n) = A(\mathbb{Z}) \times B(\mathbb{Z})$. For every $\boldsymbol{\ell} = (\ell_1, \ell_2) \in \mathbb{Z}^2$, the pattern appearing in c at support $[A(\ell_1), A(\ell_1+1)-1] \times [B(\ell_2), B(\ell_2+1)-1]$ is a rectangular pattern containing a unique junction tile at its bottom left corner. □

We call such a rectangular pattern described in Proposition 6.4 a **return block** (to a junction tile) (see Figure 23), following the terminology of return words in combinatorics on words [16, 64]. While the classical notion of return word is to a single pattern, here the notion of return block is to a subset of tiles – namely, the junction tiles. From Proposition 6.4, the **width** (and **height**) of these blocks is n or $n+1$. On the right of the junction tile within a return block is the **bottom row** where horizontal blue, green, yellow or antigreen tiles appear. Similarly, above the junction tile within a return block is the **left column** where vertical blue, green, yellow or antigreen tiles appear.

We may observe that the sequences of bottom labels of a return block made of tiles in $\mathcal{T}'_4$ appearing completely in Figure 19 and in Figure 22 are in the set

$$\left\{ \begin{array}{l} 004 \cdot 114 \cdot 115 \cdot 114 \cdot 115, \\ 004 \cdot 115 \cdot 114 \cdot 115 \cdot 115, \\ 015 \cdot 114 \cdot 115 \cdot 115 \cdot 115, \\ 014 \cdot 114 \cdot 115 \cdot 115, \\ 014 \cdot 115 \cdot 115 \cdot 115, \\ 015 \cdot 115 \cdot 115 \cdot 115 \end{array} \right\} \not\subset \tau_n(V_n). \tag{6.1}$$

In particular, $004 \cdot 114 \cdot 115 \cdot 114 \cdot 115$ does not belong to the image of τ_n when $n = 4$. But the sequence of bottom labels of a return block has a particular structure for configurations in Ω_n. This is the subject of the next section.

https://doi.org/10.1017/fms.2025.10069 Published online by Cambridge University Press

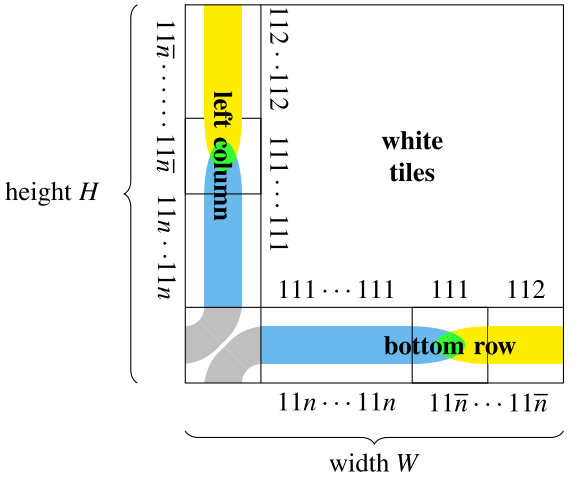

Figure 23. *A return block is split into four disjoint parts: the junction tile, the left column, the bottom row and the white tiles. Both its width W and its height H take values in the set $\{n, n+1\}$.*

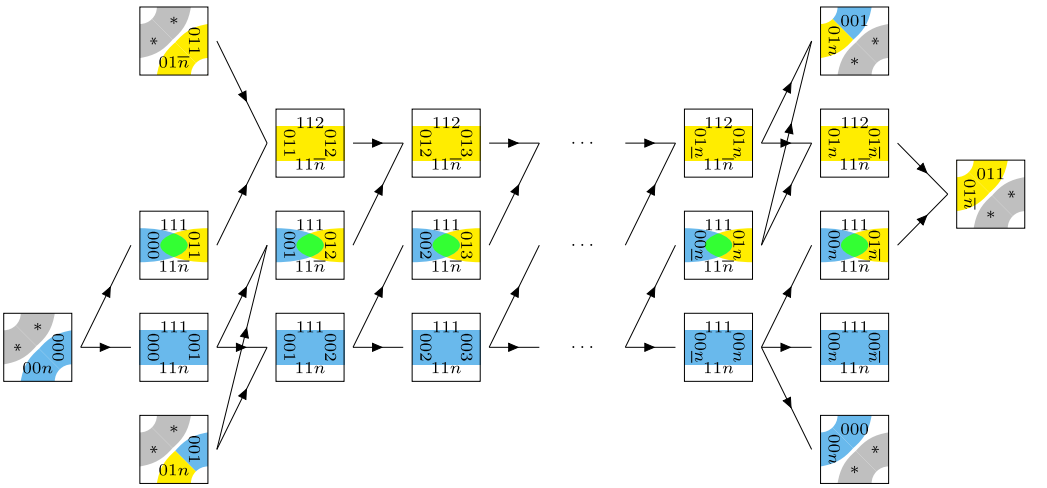

Figure 24. *Combinatorial structure between two consecutive junction tiles on the same horizontal row within a configuration of Ω_n. The nodes of the graph are placed such that any two tiles appearing in the same column have the same last digit for its left or right labels.*

6.2. Return blocks in the Wang shift Ω_n

When considering configurations in Ω_n instead of Ω'_n, there are no antigreen tiles in the row between two consecutive junction tiles. Thus, Figure 20 simplifies to Figure 24. In particular, in the bottom row of a return block within a configuration in Ω_n, the horizontal blue, green and yellow stripes appear in this order (when they appear). The same observation holds for the left column of a return block ordered from bottom to top.

Surprisingly, when the tiles are restricted to the set $\mathcal{T}_n$, the boundary of the return blocks can be decoded using the map τ_n defined in Section 5.

Lemma 6.5. *Let r be a return block appearing in a configuration $c \in \Omega_n$. The sequences of bottom labels of tiles in the bottom row of the return block r (from left to right) belong to the set*

https://doi.org/10.1017/fms.2025.10069 Published online by Cambridge University Press

$$\begin{aligned}\tau_n(V_n) = &\{01\overline{n}\cdot(11\overline{n})^i \mid n-1 \le i \le n\}\\ &\cup \{01n\cdot(11n)^i(11\overline{n})^j \mid i,j\ge 0, n-1\le i+j\le n\}\\ &\cup \{00n\cdot(11n)^i(11\overline{n})^j \mid i,j\ge 0, i+j=n\}.\end{aligned}$$

Proof. From Lemma 6.1, the sequence of bottom labels of the tiles between two consecutive junction tiles (including the left junction tile but not the right one) belongs to $\{00n, 01n, 01\overline{n}\}\cdot\{11n, 11\overline{n}\}^*$.

In the bottom row of every return block within a configuration in Ω_n, there is no antigreen stripe tile, and the horizontal blue, green and yellow stripe tiles appear in this order: blue → green → yellow. Since the bottom label of a blue horizontal stripe tile is $11n$ and the bottom label of a green or yellow horizontal stripe tile is $11\overline{n}$, the sequence of bottom labels of tiles in a horizontal row starting from a junction tile and ending before the next occurrence of a junction tile is in the set

$$\{00n, 01n, 01\overline{n}\}\cdot(11n)^*(11\overline{n})^*.$$

Some more restrictions are imposed:

- If it starts with $00n$, the length of the sequence is $n+1$. Indeed, if the bottom label of a junction tile is $00n$, then its right label is 000 with last digit 0. From Figure 24, the width of the return block containing this junction tile must be $n+1$ or $n+2$. A return block of width $W = n+2$ is impossible from Proposition 6.4. Thus, the width of the return bock is $W = n+1$.
- Also, if it starts with $01\overline{n}$, the next label is not $11n$ and has to be $11\overline{n}$. Indeed $01\overline{n}$ is the bottom label of a junction tile with right label 011, and 011 must be the left label of a yellow horizontal stripe tile with bottom label $11\overline{n}$; see Figure 24.

Restricting the sequences to those of lengths n or $\overline{n}$, we have that the sequence of bottom labels of tiles in the bottom row of the return block r (from left to right) belongs to the set

$$\begin{aligned}&\{01\overline{n}\cdot(11\overline{n})^i \mid n-1\le i\le n\}\\ &\cup\{01n\cdot(11n)^i(11\overline{n})^j \mid i,j\ge 0, n-1\le i+j\le n\}\\ &\cup\{00n\cdot(11n)^i(11\overline{n})^j \mid i,j\ge 0, i+j=n\}\\ =\ &\{\tau_n(111),\tau_n(000)\}\\ &\cup\{\tau_n(00i)\mid 1\le i\le n+1\}\cup\{\tau_n(11i)\mid 2\le i\le n+1\}\\ &\cup\{\tau_n(01i)\mid 1\le i\le n+1\}\\ =\ &\tau(V_n).\end{aligned}$$

□

6.3. *Desubstitution* $\Omega_n \leftarrow \Omega'_n$

In this section, we prove that every valid configuration with the tiles $\mathcal{T}_n$ can be desubstituted into a valid configuration over $\mathcal{T}'_n$ using the substitution ω'_n. It is based on the following lemma which relates return blocks in Ω_n to tiles of $\mathcal{T}'_n$.

Lemma 6.6. *Let $y \in \Omega_n$ be a configuration. For every return block r appearing in y, there exists a unique tile $t = \begin{smallmatrix}&\beta&\\ \gamma&\square&\alpha\\ &\delta&\end{smallmatrix} \in \mathcal{T}'_n$ such that $r = \omega'_n(t)$ with external labels $\begin{smallmatrix}&\tau_n(\beta)&\\ \tau_n(\gamma)&\square&\tau_n(\alpha)\\ &\tau_n(\delta)&\end{smallmatrix}$.*

Proof. Let $y \in \Omega_n$ be a configuration. From Proposition 6.4, the configuration y can be divided into return blocks, – that is, rectangular blocks of sizes $n\times n$, $n\times\overline{n}$, $\overline{n}\times n$ or $\overline{n}\times\overline{n}$ with a unique junction tiles at the bottom left corner; see Figure 23.

Let r be a return block appearing in y. From Lemma 6.5, the sequences of bottom labels of tiles in the bottom row of the return block r (from left to right) belong to the set $\tau_n(V_n)$. By symmetry and

https://doi.org/10.1017/fms.2025.10069 Published online by Cambridge University Press

since r is surrounded by returns blocks, this also holds for the right, top and left labels of r. Therefore, let $\alpha, \beta, \gamma, \delta \in V_n$ such that the right, top, left and bottom labels of the return block r are respectively $\tau_n(\alpha)$, $\tau_n(\beta)$, $\tau_n(\gamma)$ and $\tau_n(\delta)$. From Proposition 5.9, $t = \begin{smallmatrix} & \beta & \\ \gamma & \square & \alpha \\ & \delta & \end{smallmatrix} \in \mathcal{T}'_n$. From Lemma 5.3, there exists a unique rectangular pattern with these external labels. Thus, $r = \omega'_n(t)$. □

Proposition 6.7. *Let $n \geq 1$ be an integer. For every configuration $y \in \Omega_n$, there exist a unique configuration $x \in \Omega'_n$ and a unique vector $\boldsymbol{k} \in \{0, 1, \dots, n\}^2$ such that $y = \sigma^{\boldsymbol{k}}(\omega'_n(x))$.*

Proof. Let $\omega'_n : \Omega'_n \to \Omega'_n$ be the 2-dimensional substitution defined in (5.2).

Let $y \in \Omega_n$ be a configuration. From Lemma 6.3, there exist two strictly increasing sequences $A, B : \mathbb{Z} \to \mathbb{Z}$ such that the set of positions of junction tiles in the configuration y is the Cartesian product $A(\mathbb{Z}) \times B(\mathbb{Z})$. Also, the distance between two consecutive occurrences of junction tiles in the same row or the same column is n or $n+1$; that is, $A(\ell+1) - A(\ell) \in \{n, n+1\}$ and $B(\ell+1) - B(\ell) \in \{n, n+1\}$ for every $\ell \in \mathbb{Z}$. We may suppose without loss of generality that the sequences A and B are defined in such a way that the sequences take nonnegative values for nonnegative indices exclusively. In other words, $A(\ell) \geq 0$ if and only if $\ell \geq 0$ and $B(\ell) \geq 0$ if and only if $\ell \geq 0$.

For every $\boldsymbol{\ell} = (\ell_1, \ell_2) \in \mathbb{Z}^2$, consider the return block $y|_{S_{\boldsymbol{\ell}}}$ of support $S_{\boldsymbol{\ell}} = [A(\ell_1), A(\ell_1 + 1) - 1] \times [B(\ell_2), B(\ell_2 + 1) - 1]$. From Lemma 6.6, there exists a unique tile $x_{\boldsymbol{\ell}} \in \mathcal{T}'_n$ such that $y|_{S_{\boldsymbol{\ell}}} = \omega'_n(x_{\boldsymbol{\ell}})$. Let $\boldsymbol{k} = (-A(-1), -B(-1))$. The configuration $\sigma^{-\boldsymbol{k}}(y)$ has a junction tile at the origin $(0, 0)$. The configuration $x = (x_{\boldsymbol{\ell}})_{\boldsymbol{\ell} \in \mathbb{Z}^2}$ belongs to Ω'_n and satisfies that $\omega'_n(x) = \sigma^{-\boldsymbol{k}}(y)$. Thus, $y = \sigma^{\boldsymbol{k}}\omega'_n(x)$. □

Proposition 6.8. *For every integer $n \geq 1$, the 2-dimensional substitution $\omega'_n : \Omega'_n \to \Omega'_n$ satisfies $\Omega_n \subseteq \overline{\omega'_n(\Omega'_n)}^{\sigma}$.*

Proof. From Proposition 6.7, for every configuration $y \in \Omega_n$, there exist a unique configuration $x \in \Omega'_n$ and a unique vector $\boldsymbol{k} \in \{0, 1, \dots, n\}^2$ such that $y = \sigma^{\boldsymbol{k}}(\omega'_n(x))$. Therefore, $\Omega_n \subseteq \overline{\omega'_n(\Omega'_n)}^{\sigma}$. □

7. Tiles in $\mathcal{T}'_n \setminus \mathcal{T}_n$ are illegal so that $\Omega'_n = \Omega_n$

By definition $\mathcal{T}_n \subset \mathcal{T}'_n$, so that $\Omega_n \subseteq \Omega'_n$. In this section, we prove that in every configuration of the Wang shift Ω'_n defined from the set $\mathcal{T}'_n$, only the tiles from $\mathcal{T}_n$ appear; that is, $\Omega'_n \subseteq \Omega_n$.

7.1. Illegal tiles

Recall that the additional tiles are

$$\mathcal{T}'_n \setminus \mathcal{T}_n = A_n \cup \widehat{A_n} \cup \{j_n^{0,0,1,1}, j_n^{1,1,0,0}\} \cup \{b_n^n, \widehat{b_n^n}\}.$$

The proof that these tiles do not appear in any configuration in Ω'_n follows from the following lemmas. The easiest is to show that no configuration contains the last blue tile because the argument is very local.

Lemma 7.1. *A valid configuration in Ω'_n contains no blue tile in $\{b_n^n, \widehat{b_n^n}\}$.*

Proof. Let $c \in \Omega'_n$ be a valid configuration. The configuration c does not contain the tile $b_n^n = \begin{smallmatrix} & 111 & \\ 00n & \square & 00\overline{n} \\ & 11n & \end{smallmatrix}$ because no tile from $\mathcal{T}'_n$ has left label $00\overline{n}$. Similarly, the configuration c does not contain the tile $\widehat{b_n^n}$ because no tile from $\mathcal{T}'_n$ has bottom label $00\overline{n}$. □

Then, we show that no configuration of Ω'_n contains any antigreen tile. The argument is more difficult because antigreen tiles admit large surroundings; see Figure 19. As seen in the figure and proved in the

https://doi.org/10.1017/fms.2025.10069 Published online by Cambridge University Press

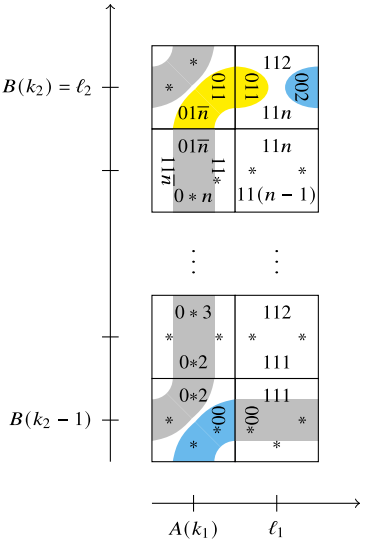

Figure 25. *The presence of the antigreen a_n^1 leads to a contradiction.*

next lemma, the presence of an antigreen tile forces the presence of another antigreen tile a few rows below that is closer to the left to a junction tile.

Lemma 7.2. *A valid configuration in Ω'_n contains no antigreen tile from the set $A_n \cup \widehat{A_n}$.*

$a_n^i =$ 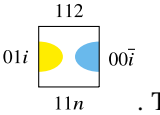

Proof. Let $c \in \Omega'_n$ be a valid configuration. Recall that . The configuration c does not contain the tile a_n^n because a_n^n has left label $00\overline{n}$, but no tile from $\mathcal{T}'_n$ has left label $00\overline{n}$. Similarly, the configuration c does not contain the tile $\widehat{a_n^n}$ because $\widehat{a_n^n}$ has top label $00\overline{n}$, but no tile from $\mathcal{T}'_n$ has top label $00\overline{n}$.

Suppose by contradiction that a_n^i appears in the configuration c for some integer i such that $1 \le i \le n-1$. Let $A, B : \mathbb{Z} \to \mathbb{Z}$ be the two increasing maps from Lemma 6.3 such that $c^{-1}(J'_n) = A(\mathbb{Z}) \times B(\mathbb{Z})$. Suppose that a_n^i appears at position $\boldsymbol{\ell} = (\ell_1, \ell_2) \in \mathbb{Z}^2$. Let $\boldsymbol{k} = (k_1, k_2) \in \mathbb{Z}^2$ be such that $A(k_1) \le \ell_1 < A(k_1+1)$ and $B(k_2) \le \ell_2 < B(k_2+1)$. Note that we must have $B(k_2) = \ell_2$. Suppose that the occurrence $\boldsymbol{\ell}$ is chosen such that $\ell_1 - A(k_1)$ is the minimum among all occurrences of the tile a_n^i in c – in other words, such that the distance to the nearest junction tile to its left on the same row is minimal. Since the bottom and top labels of a_n^i start with 1, the column ℓ_1 in the configuration c contains no junction tile; thus, $A(k_1) \ne \ell_1$ and $\ell_1 - A(k_1) \ge 1$. There are two cases to consider.

Case $\ell_1 - A(k_1) = 1$. In this case, the tile at position $(A(k_1), B(k_2))$ is a junction tile with right label 011 and bottom label $01\overline{n}$. Also, the antigreen tile at position (ℓ_1, ℓ_2) is a_n^1. Below the antigreen tile are white tiles, and below the junction tile is a yellow or green tile that we show in gray in Figure 25.

So the unit parts of horizontal edge labels decrease by one at each level from top to bottom until we reach the white tile at position $(\ell_1, B(k_2 - 1) + 1)$ with bottom label 111 and a tile at position $(A(k_1), B(k_2 - 1) + 1)$ with bottom label 0∗2. The tile at position $(\ell_1, B(k_2 - 1))$ must be a green or blue tile with left label 00∗. The tile at position $(A(k_1), B(k_2 - 1)$ must be a junction tile, but there are no junction tiles with top label 0∗2. So this case leads to a contradiction.

Case $\ell_1 - A(k_1) > 1$. This means that tiles in the column to the left of a_n^i do not contain junction tiles. On Figure 20, we observe that only the yellow tile y_n^{i-1} has right label $01i$. Thus, the tile to the left of a_n^i at position $(\ell_1 - 1, \ell_2)$ needs to be the yellow tile y_n^{i-1}. For every integer j such that $B(k_2 - 1) < j < B(k_2)$, the tiles at positions $(\ell_1 - 1, j)$ and (ℓ_1, j) are white tiles. So the unit parts of the horizontal edge labels

https://doi.org/10.1017/fms.2025.10069 Published online by Cambridge University Press

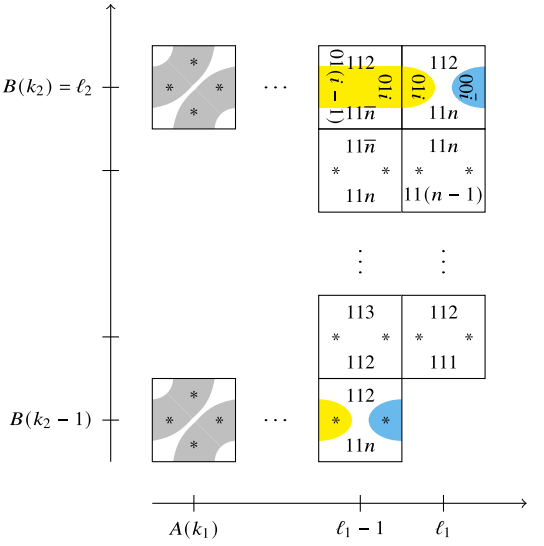

Figure 26. *The presence of the antigreen a_n^i leads to a contradiction.*

decrease by one at each level from top to bottom. Thus, the tile at position $(\ell_1 - 1, B(k_2 - 1))$ has top label 112, and the tile at position $(\ell_1, B(k_2 - 1))$ has top label 111. The situation is illustrated in Figure 26.

Since 112 and 111 are the labels of consecutive horizontal edges, we deduce from Figure 20 that the tile at position $(\ell_1 - 1, B(k_2 - 1))$ must be an antigreen tile as well. We observe that this antigreen tile is closer in distance to a junction tile to its left on the same row. This is a contradiction with the minimality of $\ell_1 - A(k_1)$. Thus, the configuration c does not contain the antigreen tile a_n^i.

Finally, by contradiction, suppose that the tile $\widehat{a_n^i}$ appears in the configuration c. Since $\mathcal{T}_n'$ is symmetric – that is, $\widehat{\mathcal{T}_n'} = \mathcal{T}_n'$ – the symmetric configuration $\widehat{c}$ is also a valid configuration in Ω_n'. Thus, the configuration c contains the tile a_n^i which contradicts the conclusion of the previous paragraph. □

The previous lemma implies that the pattern shown in Figure 19 cannot be extended to a valid configuration in Ω_n'.

Lemma 7.3. *A valid configuration in Ω_n' contains no junction tile from the set $\{j_n^{0,0,1,1}, j_n^{1,1,0,0}\}$.*

Proof. Recall that

$$j_n^{0,0,1,1} = \begin{array}{ccc} & 011 & \\ 01\overline{n} & \times & 000 \\ & 00n & \end{array} \quad \text{and} \quad \widehat{j_n^{0,0,1,1}} = j_n^{1,1,0,0} = \begin{array}{ccc} & 000 & \\ 00n & \times & 011 \\ & 01\overline{n} & \end{array}.$$

Let $x \in \Omega_n'$ be a valid configuration. We first prove that x does not contain the tile $j_n^{0,0,1,1}$. By contradiction, suppose that the tile $j_n^{0,0,1,1}$ appears in the configuration x at some position $\boldsymbol{\ell} \in \mathbb{Z}^2$. Consider the return block containing this junction tile and let W be its width and H be its height.

The bottom label of the junction tile $j_n^{0,0,1,1}$ is $00n$, and its right label is 000 with last digit 0. From Figure 20, the width of the return block containing this junction tile must be $n+1$ or $n+2$. A return block of width $W = n+2$ is impossible from Proposition 6.4. Thus, the width of the return bock is $W = n+1$.

If $n > 1$, then we have $W = n$, which is a contradiction. Indeed, the tile appearing above the junction tile $j_n^{0,0,1,1}$ must be a vertical stripe tile with right label 112, either yellow or antigreen. From the observation made in Figure 18, the width of this return block is $W = n$.

https://doi.org/10.1017/fms.2025.10069 Published online by Cambridge University Press

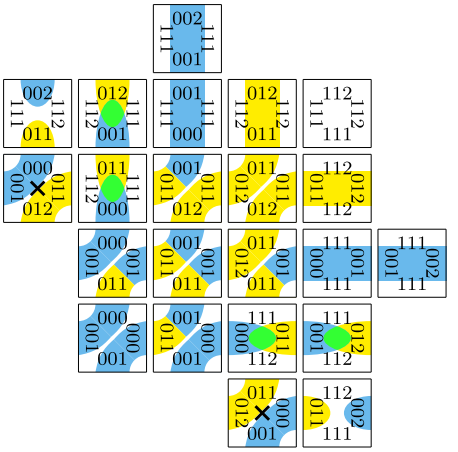

Figure 27. *Extended metallic mean Wang tile sets $\mathcal{T}'_n$ for $n = 1$.*

If $n = 1$, three different junction tiles can appear on top of $j_n^{0,0,1,1}$. All of them have right label 001. On the right of $j_n^{0,0,1,1}$, there may be a green or a blue tile, both of them having top label 111. We get the following picture where we illustrate the blue or green tile in gray.

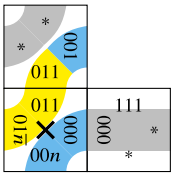

But no tiles from $\mathcal{T}'_1$ have left label 001 and bottom label 111; see Figure 27. Thus, no tile can be placed at position $\boldsymbol{\ell} + (1, 1)$. This is a contradiction.

Finally, by contradiction, suppose that the tile $j_n^{1,1,0,0} = \widehat{j_n^{0,0,1,1}}$ appears in the configuration x. Since $\mathcal{T}'_n$ is symmetric – that is $\widehat{\mathcal{T}'_n} = \mathcal{T}'_n$ – the symmetric configuration $\widehat{x}$ is also a valid configuration in Ω'_n. Thus, the configuration x contains the tile $j_n^{0,0,1,1}$, which contradicts the first part of the proof. □

We may now prove the following result.

Proposition 7.4. *For every integer $n \geq 1$, $\Omega'_n = \Omega_n$.*

Proof. Since $\mathcal{T}_n \subseteq \mathcal{T}'_n$, we have $\Omega_n \subseteq \Omega'_n$.

Let $c \in \Omega'_n$ be a valid configuration. From Lemma 7.1, the configuration c contains no blue tile in $\{b_n^n, \widehat{b_n^n}\}$. From Lemma 7.2, the configuration c contains no antigreen tile from $A_n \cup \widehat{A_n}$. From Lemma 7.3, the configuration c contains no junction tile from the set $\{j_n^{0,0,1,1}, j_n^{1,1,0,0}\}$. Thus, the range of c is $c(\mathbb{Z}^2) \subset \mathcal{T}_n$. Thus, $c \in \Omega_n$, from which we conclude that $\Omega'_n \subseteq \Omega_n$. □

8. Ω_n is self-similar and aperiodic

In this section, we show that Ω_n is self-similar and aperiodic. We prove Theorem A below after recalling its statement.

Theorem A. *For every integer $n \geq 1$, the set $\mathcal{T}_n$ containing $(n + 3)^2$ Wang tiles defines a Wang shift Ω_n which is self-similar. More precisely, there exists an expansive and recognizable 2-dimensional substitution $\omega_n : \Omega_n \to \Omega_n$ which is onto up to a shift – that is, such that $\Omega_n = \overline{\omega_n(\Omega_n)}^{\sigma}$.*

https://doi.org/10.1017/fms.2025.10069 Published online by Cambridge University Press

Proof. Let $n \geq 1$ be an integer. From Proposition 6.8, the 2-dimensional substitution $\omega'_n : \Omega'_n \to \Omega'_n$ defined in (5.2) satisfies $\Omega_n \subseteq \overline{\omega'_n(\Omega'_n)}^{\sigma}$. From Proposition 7.4, we have $\Omega'_n = \Omega_n$. The restriction of ω'_n to Ω_n is the 2-dimensional substitution $\omega_n : \Omega_n \to \Omega_n$ defined in (5.3). From Lemma 5.6, $\omega_n(\Omega_n) \subset \Omega_n$. Therefore, we have

$$\Omega_n \subseteq \overline{\omega'_n(\Omega'_n)}^{\sigma} = \overline{\omega'_n(\Omega_n)}^{\sigma} = \overline{\Omega_n(\omega_n)}^{\sigma} \subseteq \Omega_n.$$

Therefore, ω_n is in fact a 2-dimensional substitution $\Omega_n \to \Omega_n$ satisfying $\Omega_n = \overline{\omega_n(\Omega_n)}^{\sigma}$. The 2-dimensional substitution ω_n is recognizable following Proposition 6.4 since every configuration in Ω_n can be uniquely divided into return blocks. The 2-dimensional substitution ω_n is expansive (the image of every tile contains a junction tile and the image of every junction tile has a height and width at least 2). Hence, the Wang shift Ω_n is self-similar with respect to the substitution ω_n. □

Proof of Corollary B. From Theorem A, we have that the Wang shift Ω_n is self-similar, satisfying $\Omega_n = \overline{\omega_n(\Omega_n)}^{\sigma}$. Since the substitution ω_n is expansive and recognizable, it follows from Proposition 3.5 that Ω_n is aperiodic. □

9. The self-similarity is primitive

Substitutive shifts obtained from expansive and primitive morphisms are interesting for their properties. As in the 1-dimensional case, we say that ω is **primitive** if there exists $m \in \mathbb{N}$ such that for every $a, b \in \mathcal{A}$, the letter b occurs in $\omega^m(a)$. In this section, we show that the 2-dimensional substitution ω_n is primitive.

Lemma 9.1. *For every integer $n \geq 1$, the 2-dimensional substitution $\omega_n : \Omega_n \to \Omega_n$ is primitive.*

Proof. The proof follows from the following observations about the substitution ω_n:

- in the image of every tile in $\mathcal{T}_n$ under ω_n, there is some junction tile;
- in the image of every junction tile, there is a white tile $w_n^{1,1}$;
- in the image of the white tile $w_n^{1,1}$, there is the junction tile $j_n^{1,1,1,1}$;
- in the image of the junction tile $j_n^{1,1,1,1}$, there are the junction tile $j_n^{0,0,0,0}$, all white tiles W_n including the white tile $w_n^{1,1}$, and all blue tiles $B_n \cup \widehat{B_n}$ including the blue tiles $\{b_n^0, \widehat{b_n^0}\}$ (all blue tiles appear in the image because the left and bottom label of $j_n^{1,1,1,1}$ is $01\overline{n}$; see Lemma 5.2 and Figure 13);
- in the image of the blue tiles $\{b_n^0, \widehat{b_n^0}\}$, there are all yellow tiles $Y_n \cup \widehat{Y_n}$ including the yellow tiles $\{y_n^1, \widehat{y_n^1}\}$ (all yellow tiles appear in the images because the left label of b_n^0 is 000 and the bottom label of $\widehat{b_n^0}$ is 000; see Lemma 5.2 and Figure 12);
- in the image of yellow tiles $Y_n \cup \widehat{Y_n}$, there are the junction tiles $\{j_n^{0,1,0,0}, j_n^{0,0,0,1}\}$;
- in the image of $Y_n \cup \widehat{Y_n} \cup \{j_n^{0,0,0,0}\}$, there are all green tiles $G_n \cup \widehat{G_n}$:
  - green tiles g_n^n and $\widehat{g_n^n}$ appear in the image of $j_n^{0,0,0,0}$ because the left and bottom label of $j_n^{0,0,0,0}$ is $00n$; see Lemma 5.2 and Figure 12;
  - green tiles g_n^i and $\widehat{g_n^i}$ for $0 \leq i < n$ appear in the images of the yellow tiles because the bottom label of $\widehat{y_n^{\bar{i}}}$ is $01\bar{i}$; see Lemma 5.2 and Figure 13);
- in the image of $j_n^{0,0,0,0}$, there is the junction tile $j_n^{0,1,0,1}$;
- in the image of the blue tiles $\{y_n^1, \widehat{y_n^1}\}$, there are the green tiles $\{g_n^0, \widehat{g_n^0}\}$;
- in the image of the green tiles $\{g_n^0, \widehat{g_n^0}\}$, there are the junction tiles $\{j_n^{0,1,1,1}, j_n^{1,1,0,1}\}$.

The tiles that can be obtained from the successive application of the substitution ω_n are shown in Figure 28. The graph in the figure shows that every tile appears at distance 7 of every tile in $\mathcal{T}_n$. Thus, for every tile $t \in \mathcal{T}_n$, the pattern $(\omega_n)^7(t)$ contains all tiles of $\mathcal{T}_n$. Therefore, we conclude that ω_n is primitive. □

https://doi.org/10.1017/fms.2025.10069 Published online by Cambridge University Press

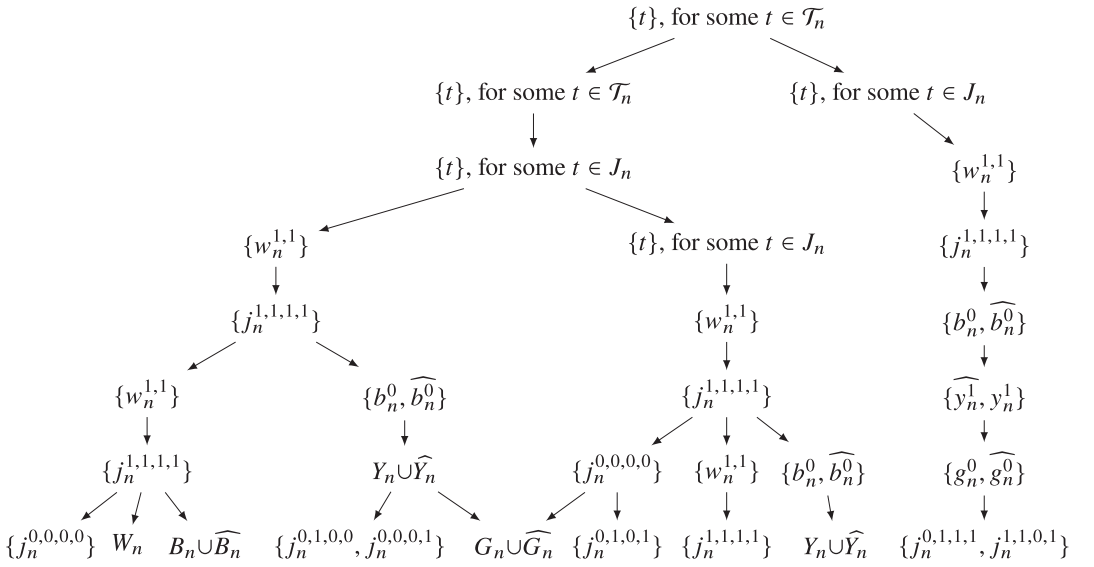

Figure 28. *When an arrow appears linking sets of tiles $S \to T$ and vertex T has in-degree one, it means that $T \subseteq \bigcup_{s\in S}\{t \in \mathcal{T}_n \mid t \text{ occurs in } \omega_n(s)\}$; that is, every tile $t \in T$ appears in the image of some tile $s \in S$ under the substitution ω_n. When two arrows $S \to T$ and $S' \to T$ appear, it means that every tile $t \in T$ appears in the image of some tile $s \in S \cup S'$ under the substitution ω_n. The figure illustrates that for every tile $t \in \mathcal{T}_n$, the pattern $(\omega_n)^7(t)$ contains every tile of $\mathcal{T}_n$. This shows the primitivity of the substitution ω_n.*

The exponent 7 deduced in the previous proof is not sharp, as computations illustrate that for every integer $n \geq 2$, the incidence matrix of $(\omega_n)^4$ is already positive, while the incidence matrix of $(\omega_1)^5$ is positive.

Lemma 9.2. *The Perron–Frobenius dominant eigenvalue of the incidence matrix of ω_n is β_n^2, the square of the n^{th} metallic mean number, and the inflation factor of ω_n is β_n.*

Proof. We may deduce the dominant eigenvalue of the incidence matrix of ω_n from that of a simpler substitution. For every integer $n \geq 1$, let ρ_n be the following 1-dimensional substitution:

$$\begin{array}{rccc} \rho_n : & \{\mathsf{a},\mathsf{b}\}^* & \to & \{\mathsf{a},\mathsf{b}\}^* \\ & \mathsf{a} & \mapsto & \mathsf{ab}^n \\ & \mathsf{b} & \mapsto & \mathsf{ab}^{n-1} \end{array}.$$

The incidence matrix of ρ_n is

$$\begin{pmatrix} 1 & 1 \\ n & n-1 \end{pmatrix}$$

whose characteristic polynomial is $x^2 - nx - 1$. The Perron–Frobenius dominant eigenvalue of the incidence matrix of ρ_n is the positive root β_n of the polynomial $x^2 - nx - 1$. Since ρ_n is primitive, the growth rate of $|\rho_n^k(u)|$ is independent of $u \in \{\mathsf{a},\mathsf{b}\}$ and is equal to β_n [51, Corollary 5.2]. In other words, for every $u \in \{\mathsf{a},\mathsf{b}\}$, we have

$$\lim_{k\to\infty} |\rho_n^k(u)|^{\frac{1}{k}} = \beta_n. \tag{9.1}$$

https://doi.org/10.1017/fms.2025.10069 Published online by Cambridge University Press

We observe that the 2-dimensional substitution ω_n is an extension of the direct product $\rho_n \times \rho_n$ of the 1-dimensional substitution ρ_n with itself. By extension, we mean the existence of a map

$$\zeta : \mathcal{T}_n \to \{\mathtt{a},\mathtt{b}\} \times \{\mathtt{a},\mathtt{b}\}$$
$$t \mapsto \begin{cases} (\mathtt{a},\mathtt{a}) & \text{if } t \in J_n, \\ (\mathtt{b},\mathtt{a}) & \text{if } t \in B_n \cup Y_n \cup G_n, \\ (\mathtt{a},\mathtt{b}) & \text{if } t \in \widehat{B_n} \cup \widehat{Y_n} \cup \widehat{G_n}, \\ (\mathtt{b},\mathtt{b}) & \text{if } t \in W_n, \end{cases}$$

such that $(\rho_n \times \rho_n) \circ \zeta = \zeta \circ \omega_n$.

Since ω_n is primitive, the dominant eigenvalue λ of the incidence matrix of the substitution ω_n is equal to the growth rate of $\text{AREA}(\omega_n^k(t))$ as $k \to \infty$, where $t \in \mathcal{T}_n$ is any tile and $\text{AREA}(p)$ denotes the cardinality of the support of a rectangular pattern $p \in (\mathcal{T}_n)^{*^2}$. Let $t \in \mathcal{T}_n$ such that $\zeta(t) = (t_1, t_2)$ for some $t_1, t_2 \in \{\mathtt{a},\mathtt{b}\}$. Since ζ is a tile to tile map, it preserves the area. Thus, we have

$$\begin{aligned} \lambda &= \lim_{k\to\infty} \text{AREA}(\omega_n^k(t))^{\frac{1}{k}} = \lim_{k\to\infty} \text{AREA}(\zeta \circ \omega_n^k(t))^{\frac{1}{k}} = \lim_{k\to\infty} \text{AREA}((\rho_n \times \rho_n)^k \circ \zeta(t))^{\frac{1}{k}} \\ &= \lim_{k\to\infty} \text{AREA}((\rho_n \times \rho_n)^k(\zeta(t)))^{\frac{1}{k}} = \lim_{k\to\infty} \text{AREA}((\rho_n \times \rho_n)^k(t_1, t_2))^{\frac{1}{k}} \\ &= \lim_{k\to\infty} \left(|\rho_n^k(t_1)| \cdot |\rho_n^k(t_2)|\right)^{\frac{1}{k}} = \lim_{k\to\infty} |\rho_n^k(t_1)|^{\frac{1}{k}} \cdot \lim_{k\to\infty} |\rho_n^k(t_2)|^{\frac{1}{k}} \overset{(9.1)}{=} \beta_n \cdot \beta_n = \beta_n^2. \end{aligned}$$

Therefore, the incidence matrices of the substitutions ω_n and $\rho_n \times \rho_n$ have the same Perron-Frobenius dominant eigenvalue, and it is equal to β_n^2.

The inflation factor is the factor of the homogeneous dilation associated with the stone inflation constructed from the direct product $\rho_n \times \rho_n$ [5, §5.6] (for example, a stone inflation for $\rho_4 \times \rho_4$ is shown in Figure 30 when $n = 4$). The inflation factor of the stone inflation of $\rho_n \times \rho_n$ is β_n as it multiplies distances between points by β_n and the areas by β_n^2. □

Theorem C. *For every integer $n \geq 1$, the 2-dimensional substitution $\omega_n : \Omega_n \to \Omega_n$ is primitive. The Perron–Frobenius dominant eigenvalue of the incidence matrix of ω_n is β_n^2, the square of the n^{th} metallic mean number, and the inflation factor of ω_n is β_n.*

Proof. From Lemma 9.1, ω_n is primitive. The Perron–Frobenius dominant eigenvalue of the incidence matrix of ω_n and its inflation factor is computed in Lemma 9.2. □

From Perron–Frobenius theorem, the primitivity of the substitution ω_n implies that every Wang tile in $\mathcal{T}_n$ appears with positive frequency in a configuration in the substitutive subshift $\mathcal{X}_{\omega_n}$ generated by the substitution ω_n. The frequencies of the tiles are given by the entries of the right-eigenvector of the incidence matrix of ω_n normalized so that the sum of its entries is 1.

10. Ω_n is minimal

The goal of this section is to prove that Ω_n is minimal. To prove minimality, we need more notions. We use the method proposed in [37, §3.3].

10.1. A criterion for minimality of a self-similar subshift

Recall that a subshift X is self-similar if $X = \overline{\omega(X)}^{\sigma}$ for some expansive d-dimensional substitution; see Definition 3.2 and Definition 3.3. First we recall Lemma 3.8 from [37].

https://doi.org/10.1017/fms.2025.10069 Published online by Cambridge University Press

Lemma 10.1. *Let $\omega : \mathcal{A} \to \mathcal{A}^{*^d}$ be an expansive and primitive d-dimensional morphism. Let $X \subseteq \mathcal{A}^{\mathbb{Z}^d}$ be a nonempty subshift such that $X = \overline{\omega(X)}^{\sigma}$. Then $\mathcal{X}_\omega \subseteq X$.*

Proof. The language of X is also self-similar satisfying $\mathcal{L}(X) = \mathcal{L}(\omega(\mathcal{L}(X)))$. Recursively, $\mathcal{L}(X) = \mathcal{L}(\omega^m(\mathcal{L}(X)))$ for every $m \geq 1$. Since X is nonempty, there exists a letter $a \in \mathcal{A}$ such that for all $m \geq 1$, the d-dimensional word $\omega^m(a)$ is in the language $\mathcal{L}(X)$. From the primitivity of ω, there exists $m \geq 1$ such that $\omega^m(a)$ contains an occurrence of every letter of the alphabet $\mathcal{A}$. Therefore, every letter is in $\mathcal{L}(X)$, and the d-dimensional word $\omega^m(a)$ is in the language $\mathcal{L}(X)$ for all letters $a \in \mathcal{A}$ and all $m \geq 1$. So we conclude that $\mathcal{L}(\mathcal{X}_\omega) \subseteq \mathcal{L}(X)$ and $\mathcal{X}_\omega \subseteq X$. □

Proving that a self-similar d-dimensional subshift X satisfying $X = \overline{\omega(X)}^{\sigma}$ is equal to $\mathcal{X}_\omega$ can be tricky. As illustrated in the following example, it depends on the combinatorics of the substitution.

Example 10.2. Consider the following 2-dimensional substitution ν over alphabet $\{a, b, c\}$:

$$\nu : a \mapsto \begin{pmatrix} c & c & c & c & c \\ c & c & c & c & c \\ c & c & a & c & c \end{pmatrix}, \quad b \mapsto \begin{pmatrix} c & c & b & c & a \\ c & c & c & c & c \\ c & c & c & c & c \end{pmatrix}, \quad c \mapsto \begin{pmatrix} c & c & a & c & c \\ c & c & c & b & c \\ c & c & c & c & c \end{pmatrix}.$$

We may observe that the vertical domino $\left(\begin{smallmatrix} a \\ b \end{smallmatrix}\right)$ does not belong to the language of the substitutive subshift $\mathcal{X}_\nu$ since it does not appear in any of the k-th image of any letter under the substitution. But one can see that the vertical domino $\left(\begin{smallmatrix} a \\ b \end{smallmatrix}\right)$ is preserved by the substitution. Therefore, there exists a configuration x containing a single vertical domino $\left(\begin{smallmatrix} a \\ b \end{smallmatrix}\right)$ which is fixed by the substitution. Thus, we have

$$\varnothing \neq \mathcal{X}_\nu \subsetneq \mathcal{X}_\nu \cup \{\sigma^n(x) \mid n \in \mathbb{Z}^2\}.$$

The subshift $\mathcal{X}_\nu \cup \{\sigma^n(x) \mid n \in \mathbb{Z}^2\}$ is self-similar, but it is not minimal because it contains a proper nonempty subshift.

Therefore, to conclude that we have the equality $\mathcal{X}_\omega = X$ for a self-similar subshift X, it is convenient to consider the domino patterns of size 1×2 and 2×1 straddling the images of the two letters of a domino as well as the 2×2 patterns straddling the images of the four letters of 2×2 pattern. More precisely, we need to consider the following directed graphs:

- Let $G_\omega^{2\times 2} = (V_\omega^{2\times 2}, E_\omega^{2\times 2})$ be the directed graph whose vertices and edges are

$$V_\omega^{2\times 2} = \left\{ \left(\begin{smallmatrix} a & b \\ c & d \end{smallmatrix}\right) \in \mathcal{A}^{2\times 2} \mid a \equiv_1 b, c \equiv_1 d, a \equiv_2 c, b \equiv_2 d \right\},$$

$$E_\omega^{2\times 2} = \left\{ \left(\begin{smallmatrix} e & f \\ g & h \end{smallmatrix}\right) \to \left(\begin{smallmatrix} a & b \\ c & d \end{smallmatrix}\right) \middle| \begin{array}{l} a \text{ is the bottom right letter of } \omega(e), \\ b \text{ is the bottom left letter of } \omega(f), \\ c \text{ is the top right letter of } \omega(g), \\ d \text{ is the top left letter of } \omega(h) \end{array} \right\}.$$

- Let $G_\omega^{2\times 1} = (V_\omega^{2\times 1}, E_\omega^{2\times 1})$ be the directed graph whose vertices and edges are

$$V_\omega^{2\times 1} = \left\{ \left(\begin{smallmatrix} a & b \end{smallmatrix}\right) \in \mathcal{A}^{2\times 1} \mid a \equiv_1 b \right\},$$

$$E_\omega^{2\times 1} = \left\{ \left(\begin{smallmatrix} e & f \end{smallmatrix}\right) \to \left(\begin{smallmatrix} a & b \end{smallmatrix}\right) \middle| \begin{array}{l} \text{there exists an integer } j \text{ such that } 0 \leq j < \textsc{height}(\omega(e)) \text{ and} \\ a \text{ is the letter in the } j\text{-th row in the right-most column of } \omega(e), \\ b \text{ is the letter in the } j\text{-th row in the left-most column of } \omega(f) \end{array} \right\}.$$

https://doi.org/10.1017/fms.2025.10069 Published online by Cambridge University Press

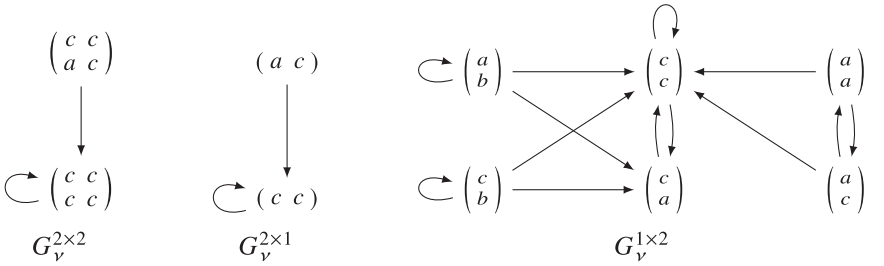

Figure 29. *The graphs $G_\nu^{2\times2}$, $G_\nu^{2\times1}$ and $G_\nu^{1\times2}$ for the substitution ν.*

- Let $G_\omega^{1\times2} = (V_\omega^{1\times2}, E_\omega^{1\times2})$ be the directed graph whose vertices and edges are

$$V_\omega^{1\times2} = \left\{ \begin{pmatrix} a \\ c \end{pmatrix} \in \mathcal{A}^{1\times2} \mid a \equiv_2 c \right\},$$

$$E_\omega^{1\times2} = \left\{ \begin{pmatrix} e \\ g \end{pmatrix} \to \begin{pmatrix} a \\ c \end{pmatrix} \middle| \begin{array}{l} \text{there exists an integer } i \text{ such that } 0 \le i < \text{WIDTH}(\omega(e)) \text{ and} \\ a \text{ is the letter in the } i\text{-th column in the bottom-most row of } \omega(e), \\ c \text{ is the letter in the } i\text{-th column in the top-most row of } \omega(g) \end{array} \right\}.$$

Finally, for every directed graph $G = (V, E)$, we define the set of **recurrent** vertices – that is, those belonging to a cycle of the graph:

$$\text{RECURRENTVERTICES}(G) = \{v \in V \mid v \text{ belongs to a cycle of } G\}.$$

Example 10.3. The graphs $G_\nu^{2\times2}$, $G_\nu^{2\times1}$ and $G_\nu^{1\times2}$ for the 2-dimensional substitution ν defined in Example 10.2 are shown in Figure 29. The recurrent vertices of the graphs are as follows:

$$\begin{aligned} \text{RECURRENTVERTICES}(G_\nu^{2\times2}) &= \left\{ \begin{pmatrix} c & c \\ c & c \end{pmatrix} \right\} \\ \text{RECURRENTVERTICES}(G_\nu^{2\times1}) &= \left\{ \begin{pmatrix} c & c \end{pmatrix} \right\} \\ \text{RECURRENTVERTICES}(G_\nu^{1\times2}) &= \left\{ \begin{pmatrix} a \\ b \end{pmatrix}, \begin{pmatrix} c \\ c \end{pmatrix}, \begin{pmatrix} a \\ a \end{pmatrix}, \begin{pmatrix} c \\ b \end{pmatrix}, \begin{pmatrix} c \\ a \end{pmatrix}, \begin{pmatrix} a \\ c \end{pmatrix} \right\} \end{aligned}$$

In particular, we observe that the vertical domino $\left(\begin{smallmatrix} a \\ b \end{smallmatrix}\right)$ belongs to a cycle of $G_\nu^{1\times2}$, even though it is not in the language $\mathcal{L}(\mathcal{X}_\nu)$.

The recurrent vertices of the three graphs $G_\omega^{2\times2}$, $G_\omega^{2\times1}$ and $G_\omega^{1\times2}$ provide a criteria for the minimality of a self-similar subshift $X = \overline{\omega(X)}^\sigma$. Lemma 3.7 and Lemma 3.9 from [37] gave hypothesis under which an expansive and primitive 2-dimensional substitution has a unique nonempty self-similar subshift. The following lemma is a relaxed version which allows to conclude that a self-similar subshift is minimal even when the 2-dimensional substitution admits more than one self-similar subshift (some made of configurations which are not uniformly recurrent).

Lemma 10.4. *Let $X = \overline{\omega(X)}^\sigma$ be a nonempty self-similar subshift where $\omega : \mathcal{A} \to \mathcal{A}^{*^d}$ is an expansive and primitive 2-dimensional morphism. The following are equivalent:*

(i) $\mathcal{L}(X) \cap \text{RECURRENTVERTICES}(G_\omega^s) \subset \mathcal{L}(\mathcal{X}_\omega)$ *for every size* $s \in \{2\times2, 2\times1, 1\times2\}$,
(ii) $X = \mathcal{X}_\omega$,
(iii) *X is minimal.*

An element $u \in \mathcal{A}^{\boldsymbol{n}}$ is called a ***d*-dimensional word** of **size** $\boldsymbol{n} = (n_1, \ldots, n_d) \in \mathbb{N}^d$ on the alphabet $\mathcal{A}$. We use the notation $\text{SIZE}(u) = \boldsymbol{n}$ when necessary.

https://doi.org/10.1017/fms.2025.10069 Published online by Cambridge University Press

Proof. Assume that $X = \overline{\omega(X)}^{\sigma}$ for some $\varnothing \neq X \subseteq \mathcal{A}^{\mathbb{Z}^d}$.

(i) $\implies$ (ii) From Lemma 10.1, we have $\mathcal{X}_\omega \subseteq X$. Let $z \in \mathcal{L}(X)$. We want to show that $z \in \mathcal{L}(\mathcal{X}_\omega)$. Since ω is expansive, let $m \in \mathbb{N}$ such that the image of every letter $a \in \mathcal{A}$ by ω^m is larger than z; that is, $\text{SIZE}(\omega^m(a)) \geq \text{SIZE}(z)$ for all $a \in \mathcal{A}$. We have $z \in \mathcal{L}(X) = \mathcal{L}(\omega^m(\mathcal{L}(X)))$. By the choice of m, z cannot overlap more than two blocks $\omega^m(a)$ in the same direction. Thus, there exists a word $u \in \mathcal{L}(X)$ of size 1×1, 2×1, 1×2 or 2×2 such that z is a subword of $\omega^m(u)$. If u is of size 1×1, then $z \in \mathcal{L}(\mathcal{X}_\omega)$. We may assume that the word u has the smallest possible rectangular size $s \in \{2\times1, 1\times2, 2\times2\}$.

We have $u \in V_\omega^s$. Since $u \in \mathcal{L}(X)$ and X is self-similar, there exists a sequence $(u_k)_{k\in\mathbb{N}}$ with $u_k \in V_\omega^s \cap \mathcal{L}(X)$ for all $k \in \mathbb{N}$ such that

$$\cdots \to u_{k+1} \to u_k \to \cdots \to u_1 \to u_0 = u$$

is a left-infinite path in the graph G_ω^s. Since V_ω^s is finite, there exist some $k, k' \in \mathbb{N}$ with $k < k'$ such that $u_k = u_{k'}$. Thus, $u_k \in \text{RECURRENTVERTICES}(G_\omega^s)$ and u is a subword of $\omega^k(u_k)$. From the hypothesis, we have $u_k \in \mathcal{L}(\mathcal{X}_\omega)$. Since ω is primitive, there exists ℓ such that u_k is a subword of $\omega^\ell(a)$ for every $a \in \mathcal{A}$. Therefore, z is a subword of $\omega^{m+k+\ell}(a)$ for every $a \in \mathcal{A}$. Then $z \in \mathcal{L}(\mathcal{X}_\omega)$ and $\mathcal{L}(X) \subseteq \mathcal{L}(\mathcal{X}_\omega)$. Thus, $X \subseteq \mathcal{X}_\omega$ and $X = \mathcal{X}_\omega$.

(ii) $\implies$ (i) If $X = \mathcal{X}_\omega$, then $\mathcal{L}(X) = \mathcal{L}(\mathcal{X}_\omega)$. Thus, $\mathcal{L}(X) \cap \text{RECURRENTVERTICES}(G_\omega^s) \subset \mathcal{L}(X) = \mathcal{L}(\mathcal{X}_\omega)$ for every size $s \in \{2\times2, 2\times1, 1\times2\}$.

(ii) $\implies$ (iii) The substitutive shift of ω is well defined since ω is expansive, and it is minimal since ω is primitive, using standard arguments [51, §5.2].

(iii) $\implies$ (ii) From Lemma 10.1, we have $\mathcal{X}_\omega \subseteq X$. Since X is minimal, we conclude that $\mathcal{X}_\omega = X$. □

10.2. The Wang shift Ω_n is minimal when $n \geq 2$

The proof that the Wang shift Ω_n is minimal needs to be split into two cases. When $n = 1$, configurations in Ω_1 have consecutive rows containing junction tiles, whereas this does not happen when $n \geq 2$. This affects the language of patterns of vertical domino support. In particular, a vertical domino made of two junction tiles may appear in the language of Ω_n when $n = 1$. In this section, we consider the case $n \geq 2$.

Lemma 10.5. *Let $n \geq 2$ be an integer. The following vertical dominoes appear in the language of the substitutive subshift $\mathcal{X}_{\omega_n}$:*

$$\begin{aligned}
\mathcal{L}_{1\times2}(\mathcal{X}_{\omega_n}) \supseteq\ & \left\{ \begin{pmatrix} j_n^{0,1,0,0} \\ \widehat{g_n^{n-1}} \end{pmatrix}, \begin{pmatrix} j_n^{0,1,0,1} \\ \widehat{g_n^{n-1}} \end{pmatrix}, \begin{pmatrix} j_n^{0,1,0,0} \\ \widehat{y_n^{n-1}} \end{pmatrix}, \begin{pmatrix} j_n^{0,1,0,1} \\ \widehat{y_n^{n-1}} \end{pmatrix}, \begin{pmatrix} j_n^{0,1,1,1} \\ \widehat{y_n^{n-1}} \end{pmatrix} \right\} \\
& \cup \left\{ \begin{pmatrix} j_n^{1,1,0,1} \\ \widehat{g_n^{n}} \end{pmatrix}, \begin{pmatrix} j_n^{1,1,0,1} \\ \widehat{y_n^{n}} \end{pmatrix}, \begin{pmatrix} j_n^{1,1,1,1} \\ \widehat{y_n^{n}} \end{pmatrix}, \begin{pmatrix} j_n^{0,0,0,0} \\ \widehat{b_n^{n-1}} \end{pmatrix}, \begin{pmatrix} j_n^{0,0,0,1} \\ \widehat{b_n^{n-1}} \end{pmatrix} \right\} \\
& \cup \left\{ \begin{pmatrix} g_n^{i-1} \\ w_n^{i,n} \end{pmatrix}, \begin{pmatrix} g_n^{i} \\ w_n^{i,n} \end{pmatrix} \middle| \ 1 \leq i \leq n \right\} \\
& \cup \left\{ \begin{pmatrix} b_n^{i-1} \\ w_n^{i,n-1} \end{pmatrix} \middle| \ 1 \leq i \leq n \right\} \cup \left\{ \begin{pmatrix} b_n^{i} \\ w_n^{i,n-1} \end{pmatrix} \middle| \ 1 \leq i \leq n-1 \right\} \\
& \cup \left\{ \begin{pmatrix} y_n^{i-1} \\ w_n^{i,n} \end{pmatrix} \middle| \ 2 \leq i \leq n \right\} \cup \left\{ \begin{pmatrix} y_n^{i} \\ w_n^{i,n} \end{pmatrix} \middle| \ 1 \leq i \leq n \right\}.
\end{aligned}$$

Proof. We show that every vertical domino listed above appears in the image of some tile under the application of the 2-dimensional substitution ω_n. Below, we use the notation $p \xrightarrow{\omega_n} q$ to denote that q

https://doi.org/10.1017/fms.2025.10069 Published online by Cambridge University Press

is a pattern appearing in the image $\omega_n(p)$. We have

$$j_n^{0,1,0,1} \xrightarrow{\omega_n} \begin{pmatrix} \widehat{b_n^0} \\ j_n^{0,0,0,0} \end{pmatrix} \xrightarrow{\omega_n} \begin{pmatrix} \mathbf{j_n^{1,1,0,1}} & y_n^1 & y_n^2 & \dots & y_n^n \\ \widehat{\mathbf{g_n^n}} & w_n^{1,n} & w_n^{2,n} & \dots & w_n^{n,n} \end{pmatrix},$$

$$j_n^{0,1,0,1} \xrightarrow{\omega_n} \begin{pmatrix} \widehat{w_n^{1,1}} \\ b_n^0 \end{pmatrix} \xrightarrow{\omega_n} \begin{pmatrix} \mathbf{j_n^{1,1,1,1}} & y_n^1 & y_n^2 & \dots & y_n^{n-1} \\ \widehat{\mathbf{y_n^n}} & w_n^{2,n} & w_n^{3,n} & \dots & w_n^{n,n} \end{pmatrix},$$

$$j_n^{0,1,0,1} \xrightarrow{\omega_n} \begin{pmatrix} \widehat{w_n^{1,1}} \\ b_n^0 \end{pmatrix} \xrightarrow{\omega_n} \begin{pmatrix} \widehat{j_n^{1,1,1,1}} \\ y_n^n \end{pmatrix} \xrightarrow{\omega_n} \begin{pmatrix} \mathbf{j_n^{0,0,0,0}} & b_n^0 & b_n^1 & \dots & b_n^{n-1} \\ \widehat{\mathbf{b_n^{n-1}}} & w_n^{1,n-1} & w_n^{2,n-1} & \dots & w_n^{n,n-1} \end{pmatrix},$$

$$g_n^0 \xrightarrow{\omega_n} \begin{pmatrix} \widehat{y_n^1} \\ j_n^{0,1,1,1} \end{pmatrix} \xrightarrow{\omega_n} \begin{pmatrix} \mathbf{j_n^{0,0,0,1}} \\ \widehat{\mathbf{b_n^{n-1}}} \end{pmatrix} \xrightarrow{\omega_n} \begin{pmatrix} \mathbf{j_n^{0,1,0,0}} & b_n^1 & b_n^2 & \dots & b_n^{n-1} \\ \widehat{\mathbf{g_n^{n-1}}} & w_n^{1,n-1} & w_n^{2,n-1} & \dots & w_n^{n-1,n-1} \end{pmatrix}.$$

Also,

$$g_n^1 \xrightarrow{\omega_n} \begin{pmatrix} \widehat{g_n^1} \\ j_n^{0,1,0,1} \end{pmatrix} \xrightarrow{\omega_n} \begin{pmatrix} \mathbf{j_n^{0,1,0,1}} \\ \widehat{\mathbf{g_n^{n-1}}} \end{pmatrix}.$$

Since $n \geq 2$, we have

$$j_n^{1,1,1,1} \xrightarrow{\omega_n} \begin{pmatrix} \widehat{b_n^0} \\ j_n^{0,0,0,0} \end{pmatrix} \xrightarrow{\omega_n} \begin{pmatrix} y_n^1 \\ w_n^{1,n} \end{pmatrix} \xrightarrow{\omega_n} \begin{pmatrix} \mathbf{j_n^{0,1,0,0}} \\ \widehat{\mathbf{y_n^{n-1}}} \end{pmatrix},$$

$$w_n^{1,1} \xrightarrow{\omega_n} \begin{pmatrix} w_n^{2,2} \\ y_n^1 \end{pmatrix} \xrightarrow{\omega_n} \begin{pmatrix} \mathbf{j_n^{0,1,0,1}} \\ \widehat{\mathbf{y_n^{n-1}}} \end{pmatrix},$$

$$g_n^0 \xrightarrow{\omega_n} \begin{pmatrix} w_n^{2,1} \\ \widehat{b_n^1} \end{pmatrix} \xrightarrow{\omega_n} \begin{pmatrix} \mathbf{j_n^{1,1,0,1}} \\ \widehat{\mathbf{y_n^n}} \end{pmatrix},$$

$$w_n^{1,1} \xrightarrow{\omega_n} \begin{pmatrix} \widehat{y_n^1} \\ j_n^{1,1,1,1} \end{pmatrix} \xrightarrow{\omega_n} \begin{pmatrix} g_n^0 \\ w_n^{1,n} \end{pmatrix} \xrightarrow{\omega_n} \begin{pmatrix} \mathbf{j_n^{0,1,1,1}} \\ \widehat{\mathbf{y_n^{n-1}}} \end{pmatrix}.$$

□

Lemma 10.6. *The following four* 2×2 *patterns belong to the language of the substitutive subshift* $\mathcal{L}(\mathcal{X}_{\omega_n})$*:*

$$\left\{ \begin{pmatrix} b_n^{n-1} & j_n^{0,0,0,0} \\ w_n^{n-1,n-1} & \widehat{b_n^{n-1}} \end{pmatrix}, \begin{pmatrix} g_n^{n-1} & j_n^{0,1,0,1} \\ w_n^{n,n} & \widehat{g_n^{n-1}} \end{pmatrix}, \begin{pmatrix} b_n^{n-1} & j_n^{0,1,0,0} \\ w_n^{n,n-1} & \widehat{g_n^{n-1}} \end{pmatrix}, \begin{pmatrix} g_n^{n-1} & j_n^{0,0,0,1} \\ w_n^{n-1,n} & \widehat{b_n^{n-1}} \end{pmatrix} \right\}$$

$$= \left\{ \begin{array}{|cc|cc|} \hline 111 & 000 & 000 & 000 \\ 00n & 00n & 00n & 00n \\ \hline 11n & & 00n & \\ \hline 11\bar{n} & 11\bar{n} & 111 & 111 \\ 11n & 11n & 11\bar{n} & 11\bar{n} \\ \hline \end{array}, \begin{array}{|cc|cc|} \hline 111 & 001 & 001 & 001 \\ 00n & 01n & 01n & 01n \\ \hline 11n & & 01n & \\ \hline 11\bar{n} & 11\bar{n} & 111 & 111 \\ 11n & 11n & 11\bar{n} & 11\bar{n} \\ \hline \end{array}, \begin{array}{|cc|cc|} \hline 111 & 000 & 000 & 000 \\ 00n & 00n & 00n & 00n \\ \hline 11n & & 01n & \\ \hline 11\bar{n} & 11\bar{n} & 111 & 111 \\ 11n & 11n & 11\bar{n} & 11\bar{n} \\ \hline \end{array}, \begin{array}{|cc|cc|} \hline 111 & 001 & 001 & 000 \\ 00n & 01n & 01n & 00n \\ \hline 11n & & 00n & \\ \hline 11\bar{n} & 11\bar{n} & 111 & 111 \\ 11n & 11n & 11\bar{n} & 11\bar{n} \\ \hline \end{array} \right\} \subset \mathcal{L}_{2\times 2}(\mathcal{X}_{\omega_n}).$$

Proof. We show that every pattern listed above appears in the image of some tile under some repeated application of the 2-dimensional substitution ω_n. Below, we use the notation $p \xrightarrow{\omega_n} q$ to denote that q is

https://doi.org/10.1017/fms.2025.10069 Published online by Cambridge University Press

a pattern appearing in the image $\omega_n(p)$. The four patterns can be obtained in a few steps when applying the substitution ω_n on the tiles $j_n^{1,1,1,1}$ and y_n^1. We have the following:

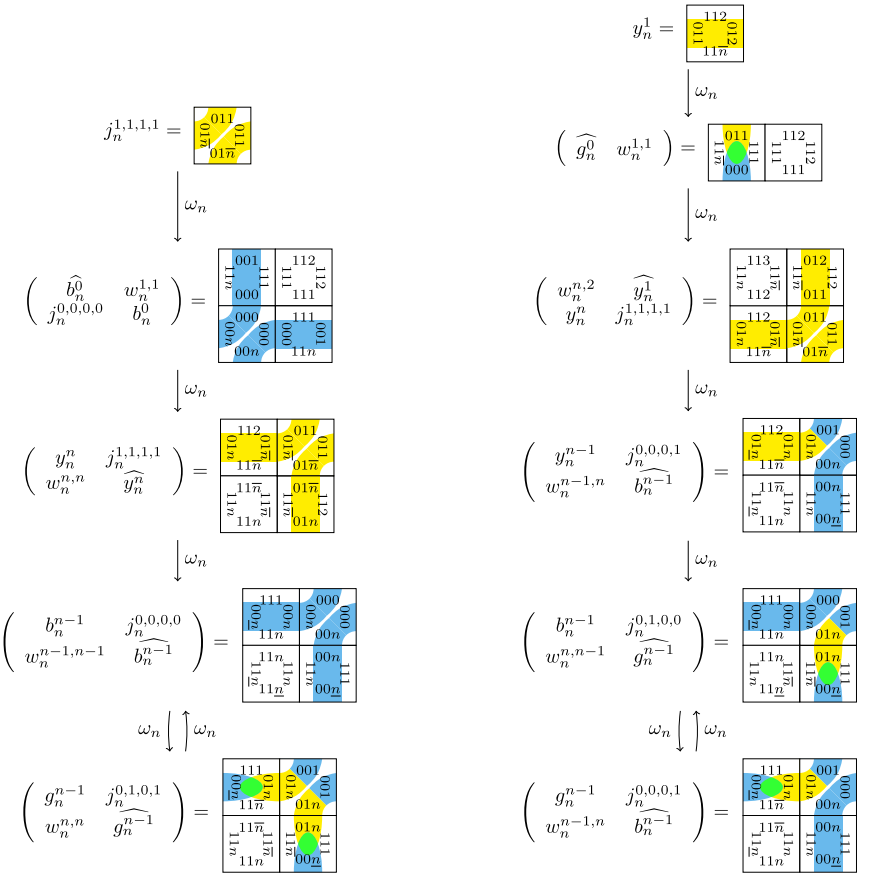

□

Lemma 10.7. *Let $n \geq 2$ be an integer. The following two vertical dominoes are illegal in Ω_n:*

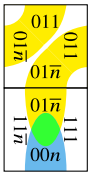
$= \begin{pmatrix} j_n^{1,1,1,1} \\ \widehat{g_n^n} \end{pmatrix} \notin \mathcal{L}(\Omega_n)$ *and*
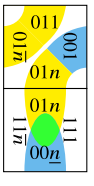
$= \begin{pmatrix} j_n^{0,1,1,1} \\ \widehat{g_n^{n-1}} \end{pmatrix} \notin \mathcal{L}(\Omega_n).$

Proof. Let $c \in \Omega_n$ be a valid configuration. Let $A, B : \mathbb{Z} \to \mathbb{Z}$ be the two increasing maps from Lemma 6.3 such that $c^{-1}(J_n) = A(\mathbb{Z}) \times B(\mathbb{Z})$.

Suppose that $j_n^{1,1,1,1}$ appears at position $\boldsymbol{\ell} = (\ell_1, \ell_2) \in \mathbb{Z}^2$ and that $\widehat{g_n^n}$ appears at position $(\ell_1, \ell_2 - 1)$ in c. Let $\boldsymbol{k} = (k_1, k_2) \in \mathbb{Z}^2$ be such that $A(k_1) \leq \ell_1 < A(k_1+1)$ and $B(k_2) \leq \ell_2 < B(k_2+1)$. Since $j_n^{1,1,1,1}$ is a junction tile, we must have $A(k_1) = \ell_1$ and $B(k_2) = \ell_2$. At position $(\ell_1, \ell_2 - 2)$, there must be a blue tile $\widehat{b_n^{n-1}}$ since only this tile has top label $00n$ when $n \geq 2$. The current situation is illustrated below.

https://doi.org/10.1017/fms.2025.10069 Published online by Cambridge University Press

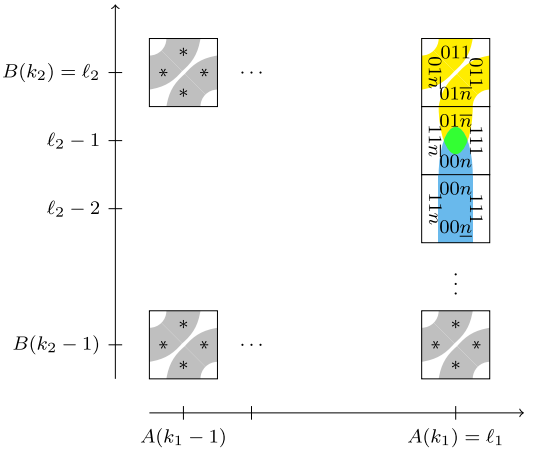

Consider the return block with support $[A(k_1 - 1), A(k_1)) \times [B(k_2), B(k_2 + 1))$. It has label $01\overline{n}$ at the far right of its bottom row. From Lemma 5.2, the width of this return block cannot be n, so it has to be

$$A(k_1) - A(k_1 - 1) = n + 1.$$

Now consider the return block with support $[A(k_1 - 1), A(k_1)) \times [B(k_2 - 1), B(k_2))$. The white tile at position $(A(k_1) - 1, \ell_2 - 2)$ has right label $11n$. From the observation made in Figure 18, the width of this return block is

$$A(k_1) - A(k_1 - 1) = n.$$

This is a contradiction. Thus, $\begin{pmatrix} j_n^{1,1,1,1} \\ \widehat{g_n^n} \end{pmatrix} \notin \mathcal{L}(\Omega_n)$.

The same contradiction is obtained if we suppose that $j_n^{0,1,1,1}$ appears at position $\boldsymbol{\ell} = (\ell_1, \ell_2) \in \mathbb{Z}^2$ and that $\widehat{g_n^{n-1}}$ appears at position $(\ell_1, \ell_2 - 1)$ in c. Indeed, a blue tile with left label $11n$ is also forced to appear at position $(\ell_1, \ell_2 - 2)$. □

Note that Lemma 10.7 cannot be extended to the case $n = 1$.

Proposition 10.8. *For every integer $n \geq 2$, the Wang shift Ω_n is minimal and is equal to the substitutive subshift $\Omega_n = \mathcal{X}_{\omega_n}$.*

Proof. Let $n \geq 2$ be an integer. From Theorem C, the 2-dimensional substitution ω_n is primitive. Also, ω_n is expansive. From Theorem A, the Wang shift Ω_n is self-similar, satisfying $\Omega_n = \overline{\omega_n(\Omega_n)}^{\sigma}$. Therefore, we may use Lemma 10.4 to show that the Wang shift Ω_n is minimal and $\mathcal{X}_{\omega_n} = \Omega_n$. From Lemma 10.4, our goal is show that

$$\mathcal{L}(\Omega_n) \cap \textsc{RecurrentVertices}(G^s_{\omega_n}) \subset \mathcal{L}(\mathcal{X}_{\omega_n})$$

for every size $s \in \{2 \times 2, 2 \times 1, 1 \times 2\}$.

https://doi.org/10.1017/fms.2025.10069 Published online by Cambridge University Press

Case $s = 1 \times 2$. We have

$$
\begin{aligned}
&\textsc{RecurrentVertices}(G_{\omega_n}^{1\times 2}) \\
&\subseteq \left\{ \begin{pmatrix} a \\ c \end{pmatrix} \middle| \begin{array}{l} \text{there exists } e, g \in \mathcal{A} \text{ such that } \textsc{width}(\omega_n(g)) = \textsc{width}(\omega_n(e)) \\ \text{there exists an integer } i \text{ such that } 0 \le i < \textsc{width}(\omega_n(e)) \text{ and} \\ a \text{ is the letter in the } i\text{-th column in the bottom-most row of } \omega_n(e), \\ c \text{ is the letter in the } i\text{-th column in the top-most row of } \omega_n(g) \end{array} \right\} \\
&= \left\{ \begin{pmatrix} a \\ c \end{pmatrix} \middle| \begin{array}{l} a \in \{j_n^{0,0,0,0}, j_n^{0,0,0,1}, j_n^{0,1,0,0}, j_n^{0,1,0,1}, j_n^{1,1,0,1}\} \\ c \in \{\widehat{b_n^{n-1}}, \widehat{g_n^{n-1}}, \widehat{g_n^n}\} \end{array} \right\} \\
&\quad \cup \left\{ \begin{pmatrix} a \\ c \end{pmatrix} \middle| \begin{array}{l} a \in \{j_n^{0,1,0,0}, j_n^{0,1,0,1}, j_n^{0,1,1,1}, j_n^{1,1,0,1}, j_n^{1,1,1,1}\} \\ c \in \{\widehat{y_n^{n-1}}, \widehat{y_n^n}, \widehat{g_n^{n-1}}, \widehat{g_n^n}\} \end{array} \right\} \\
&\quad \cup \left\{ \begin{pmatrix} g_n^{i-1} \\ w_n^{i,n} \end{pmatrix}, \begin{pmatrix} g_n^{i-1} \\ w_n^{i,n-1} \end{pmatrix}, \begin{pmatrix} g_n^{i} \\ w_n^{i,n} \end{pmatrix}, \begin{pmatrix} g_n^{i} \\ w_n^{i,n-1} \end{pmatrix} \middle| 1 \le i \le n \right\} \\
&\quad \cup \left\{ \begin{pmatrix} b_n^{i-1} \\ w_n^{i,n} \end{pmatrix}, \begin{pmatrix} b_n^{i-1} \\ w_n^{i,n-1} \end{pmatrix} \middle| 1 \le i \le n \right\} \cup \left\{ \begin{pmatrix} b_n^{i} \\ w_n^{i,n} \end{pmatrix}, \begin{pmatrix} b_n^{i} \\ w_n^{i,n-1} \end{pmatrix} \middle| 1 \le i \le n-1 \right\} \\
&\quad \cup \left\{ \begin{pmatrix} y_n^{i-1} \\ w_n^{i,n} \end{pmatrix}, \begin{pmatrix} y_n^{i-1} \\ w_n^{i,n-1} \end{pmatrix} \middle| 2 \le i \le n \right\} \cup \left\{ \begin{pmatrix} y_n^{i} \\ w_n^{i,n} \end{pmatrix}, \begin{pmatrix} y_n^{i} \\ w_n^{i,n-1} \end{pmatrix} \middle| 1 \le i \le n \right\}.
\end{aligned}
$$

However, we can estimate the set of vertical dominoes in $\mathcal{L}(\Omega_n)$ by the pair of tiles sharing the same label on the common horizontal edge excluding the two illegal dominoes from Lemma 10.7:

$$
\begin{aligned}
&\mathcal{L}_{1\times 2}(\Omega_n) \cap \left\{ \begin{pmatrix} a \\ c \end{pmatrix} \middle| a \text{ is a junction tile or a horizontal stripe tile} \right\} \\
&\subseteq \left\{ \begin{pmatrix} a \\ c \end{pmatrix} \middle| \begin{array}{l} a \in \{j_n^{0,1,0,0}, j_n^{0,1,0,1}, j_n^{0,1,1,1}\} \\ c \in \{\widehat{g_n^{n-1}}, \widehat{y_n^{n-1}}\} \end{array} \right\} \setminus \left\{ \begin{pmatrix} j_n^{0,1,1,1} \\ \widehat{g_n^{n-1}} \end{pmatrix} \right\} \qquad \text{(tiles sharing edge label } 01n\text{)} \\
&\quad \cup \left\{ \begin{pmatrix} a \\ c \end{pmatrix} \middle| \begin{array}{l} a \in \{j_n^{1,1,0,1}, j_n^{1,1,1,1}\} \\ c \in \{\widehat{g_n^n}, \widehat{y_n^n}\} \end{array} \right\} \setminus \left\{ \begin{pmatrix} j_n^{1,1,1,1} \\ \widehat{g_n^n} \end{pmatrix} \right\} \qquad \text{(tiles sharing edge label } 01\overline{n}\text{)} \\
&\quad \cup \left\{ \begin{pmatrix} a \\ c \end{pmatrix} \middle| \begin{array}{l} a \in \{j_n^{0,0,0,0}, j_n^{0,0,0,1}\} \\ c \in \{\widehat{b_n^{n-1}}\} \end{array} \right\} \qquad \text{(tiles sharing edge label } 00n\text{)} \\
&\quad \cup \left\{ \begin{pmatrix} b_n^{i} \\ w_n^{k,n-1} \end{pmatrix} \middle| \begin{array}{l} 0 \le i \le n-1, \\ 1 \le k \le n \end{array} \right\} \qquad \text{(tiles sharing edge label } 11n\text{)} \\
&\quad \cup \left\{ \begin{pmatrix} y_n^{i} \\ w_n^{k,n} \end{pmatrix} \middle| \begin{array}{l} 1 \le i \le n, \\ 1 \le k \le n \end{array} \right\} \qquad \text{(tiles sharing edge label } 11\overline{n}\text{)} \\
&\quad \cup \left\{ \begin{pmatrix} g_n^{i} \\ w_n^{k,n} \end{pmatrix} \middle| \begin{array}{l} 0 \le i \le n, \\ 1 \le k \le n \end{array} \right\} \qquad \text{(tiles sharing edge label } 11\overline{n}\text{)}.
\end{aligned}
$$

Note that

$$
\textsc{RecurrentVertices}(G_{\omega_n}^{1\times 2}) \subset \left\{ \begin{pmatrix} a \\ c \end{pmatrix} \middle| a \text{ is a junction tile or a horizontal stripe tile} \right\}.
$$

https://doi.org/10.1017/fms.2025.10069 Published online by Cambridge University Press

Thus, we can compute the intersection of the two sets, and using Lemma 10.5, we obtain

$$\begin{aligned}
&\textsc{RecurrentVertices}(G_{\omega_n}^{1\times 2}) \cap \mathcal{L}(\Omega_n)\\
&= \textsc{RecurrentVertices}(G_{\omega_n}^{1\times 2}) \cap \mathcal{L}_{1\times 2}(\Omega_n)\\
&= \left\{ \begin{pmatrix} a \\ c \end{pmatrix} \middle| \begin{matrix} a \in \{j_n^{0,1,0,0}, j_n^{0,1,0,1}, j_n^{0,1,1,1}\} \\ c \in \{\widehat{g_n^{n-1}}, \widehat{y_n^{n-1}}\} \end{matrix} \right\} \setminus \left\{ \begin{pmatrix} j_n^{0,1,1,1} \\ \widehat{g_n^{n-1}} \end{pmatrix} \right\}\\
&\quad \cup \left\{ \begin{pmatrix} a \\ c \end{pmatrix} \middle| \begin{matrix} a \in \{j_n^{1,1,0,1}, j_n^{1,1,1,1}\} \\ c \in \{\widehat{g_n^{n}}, \widehat{y_n^{n}}\} \end{matrix} \right\} \setminus \left\{ \begin{pmatrix} j_n^{1,1,1,1} \\ \widehat{g_n^{n}} \end{pmatrix} \right\}\\
&\quad \cup \left\{ \begin{pmatrix} a \\ c \end{pmatrix} \middle| \begin{matrix} a \in \{j_n^{0,0,0,0}, j_n^{0,0,0,1}\} \\ c \in \{\widehat{b_n^{n-1}}\} \end{matrix} \right\}\\
&\quad \cup \left\{ \begin{pmatrix} g_n^{i-1} \\ w_n^{i,n} \end{pmatrix}, \begin{pmatrix} g_n^{i} \\ w_n^{i,n} \end{pmatrix} \middle| 1 \le i \le n \right\}\\
&\quad \cup \left\{ \begin{pmatrix} b_n^{i-1} \\ w_n^{i,n-1} \end{pmatrix} \middle| 1 \le i \le n \right\} \cup \left\{ \begin{pmatrix} b_n^{i} \\ w_n^{i,n-1} \end{pmatrix} \middle| 1 \le i \le n-1 \right\}\\
&\quad \cup \left\{ \begin{pmatrix} y_n^{i-1} \\ w_n^{i,n} \end{pmatrix} \middle| 2 \le i \le n \right\} \cup \left\{ \begin{pmatrix} y_n^{i} \\ w_n^{i,n} \end{pmatrix} \middle| 1 \le i \le n \right\}\\
&\subset \mathcal{L}_{1\times 2}(\mathcal{X}_{\omega_n}) \subset \mathcal{L}(\mathcal{X}_{\omega_n}).
\end{aligned}$$

Case $s = 2 \times 1$. The condition is satisfied because this case is symmetric to the case $s = 1 \times 2$.

Case $s = 2 \times 2$. The tiles appearing on the corners of images of letters under ω_n are quite restricted. Therefore, we have the following inclusion:

$$\begin{aligned}
&\textsc{RecurrentVertices}(G_{\omega_n}^{2\times 2})\\
&\subseteq \left\{ \begin{pmatrix} a & b \\ c & d \end{pmatrix} \middle| \begin{matrix} \text{there exist } e, f, g, h \in \mathcal{T}_n \text{ such that} \\ a \text{ is the bottom right letter of } \omega(e), \\ b \text{ is the bottom left letter of } \omega(f), \\ c \text{ is the top right letter of } \omega(g), \\ d \text{ is the top left letter of } \omega(h) \end{matrix} \right\}\\
&= \left\{ \begin{pmatrix} a & b \\ c & d \end{pmatrix} \middle| \begin{matrix} a \in \{b_n^{n-1}, g_n^{n-1}\} \\ b \in \{j_n^{0,1,0,0}, j_n^{0,1,0,1}, j_n^{0,0,0,1}, j_n^{0,0,0,0}\} \\ c \in \{w_n^{n-1,n-1}, w_n^{n,n-1}, w_n^{n-1,n}, w_n^{n,n}\} \\ d \in \{\widehat{b_n^{n-1}}, \widehat{g_n^{n-1}}\} \end{matrix} \right\}.
\end{aligned}$$

The above set has size $2 \times 4 \times 4 \times 2 = 64$. Of those, only four belong to $\mathcal{L}(\Omega_n)$ because the choice made for the tile b imposes a unique choice for the tiles a, d and c. Thus, using Lemma 10.6, we obtain

$$\begin{aligned}
&\mathcal{L}(\Omega_n) \cap \textsc{RecurrentVertices}(G_{\omega_n}^{2\times 2})\\
&= \mathcal{L}_{2\times 2}(\Omega_n) \cap \textsc{RecurrentVertices}(G_{\omega_n}^{2\times 2})\\
&\subseteq \left\{ \begin{pmatrix} b_n^{n-1} & j_n^{0,0,0,0} \\ w_n^{n-1,n-1} & \widehat{b_n^{n-1}} \end{pmatrix}, \begin{pmatrix} g_n^{n-1} & j_n^{0,1,0,1} \\ w_n^{n,n} & \widehat{g_n^{n-1}} \end{pmatrix}, \begin{pmatrix} b_n^{n-1} & j_n^{0,1,0,0} \\ w_n^{n,n-1} & \widehat{g_n^{n-1}} \end{pmatrix}, \begin{pmatrix} g_n^{n-1} & j_n^{0,0,0,1} \\ w_n^{n-1,n} & \widehat{b_n^{n-1}} \end{pmatrix} \right\}
\end{aligned}$$

https://doi.org/10.1017/fms.2025.10069 Published online by Cambridge University Press

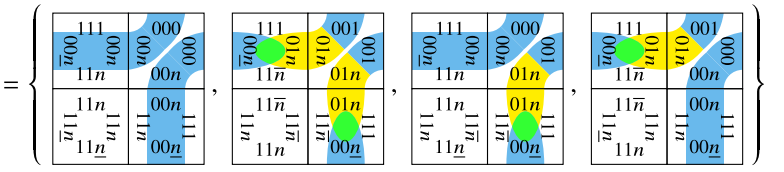

$\subset \mathcal{L}_{2\times 2}(\mathcal{X}_{\omega_n}) \subset \mathcal{L}(\mathcal{X}_{\omega_n})$.

From Lemma 10.4, we conclude that the Wang shift Ω_n is minimal and $\Omega_n = \mathcal{X}_{\omega_n}$. □

10.3. The Wang shift Ω_n is minimal when $n = 1$

From Theorem E, $\mathcal{T}_n$ is equivalent to the 16 Ammann Wang tiles when $n = 1$. We know from [24] that the 16 Ammann Wang tiles are self-similar and that the self-similarity is recognizable (the decomposition of every configuration into the 16 supertiles shown in [24, Figure 11.1.6] is unique). This corresponds to the case $n = 1$ of Theorem A proved here. Therefore, from Lemma 10.1, we have $\mathcal{X}_{\omega_1} \subseteq \Omega_1$. The goal of this section is to prove that the equality holds and therefore that Ω_1 is minimal. Note that minimality of Ω_1 was not proved in [24], neither in the more recent works about Ammann A2 tilings [1, 15].

The proof made in the previous section for $n \geq 2$ does not directly work for $n = 1$ because it is not true anymore that next to a junction tile is never a junction tile. Indeed, when $n = 1$, two junction tiles can be adjacent horizontally or vertically. This observation changes the description of vertical and horizontal dominoes that appear in the language.

Adapting the proof made above for $n \geq 2$ to the case $n = 1$ is possible. But, instead of doing this, we have chosen to provide a proof based on computer experiments in order to check that the criterion provided in Lemma 10.4 is satisfied. We hope that it may be useful to study other examples.

Lemma 10.9. *The Wang shift Ω_1 is minimal and $\Omega_1 = \mathcal{X}_{\omega_1}$.*

Proof. From Theorem C, the 2-dimensional substitution ω_1 is primitive. Also, ω_1 is expansive. From Theorem A, the Wang shift Ω_1 is self-similar, satisfying $\Omega_1 = \overline{\omega_1(\Omega_1)}^{\sigma}$. Therefore, we may use Lemma 10.4 to show the minimality of Ω_1.

We compute below the patterns in $\mathcal{L}_s(\Omega_1)$ and $\mathcal{L}_s(\mathcal{X}_{\omega_1})$ for every size $s \in \{2\times 2, 2\times 1, 1\times 2\}$. As we observe below, these sets are equal. Therefore, it is not necessary to compute RecurrentVertices$(G^s_{\omega_1})$. We define ω_1 as a 2-dimensional substitution over the alphabet $\{0, 1, 2, \ldots, 15\}$ according to the labeling of the tiles shown in Figure 31. We compute the patterns of size $s \in \{2\times 2, 2\times 1, 1\times 2\}$ in the substitutive subshift $\mathcal{X}_{\omega_1}$:

```
sage: from slabbe import Substitution2d                                          1
sage: omega1 = Substitution2d({0: [[9], [15]], 1: [[6], [7]], 2: [[13], [14]], 3: [[6]], 4:  2
      [[5], [7]], 5: [[12, 4], [11, 3]], 6: [[12, 1], [11, 3]], 7: [[8, 4]], 8: [[13, 0],
     [14, 3]], 9: [[12, 4], [14, 3]], 10: [[12, 1], [14, 3]], 11: [[6, 2]], 12: [[9, 0],
     [15, 3]], 13: [[8, 4], [15, 3]], 14: [[10, 2]], 15: [[9, 0]]})
sage: patterns_1x2_in_subst_shift = set((a,b) for [[a,b]] in omega1.list_dominoes(direction  3
     ="vertical", output_format="list_of_lists"))
sage: len(patterns_1x2_in_subst_shift)                                           4
30                                                                               5
sage: min(patterns_1x2_in_subst_shift) # show some minimal element               6
(0, 5)                                                                           7
sage: patterns_2x1_in_subst_shift = set((a,b) for [[a],[b]] in omega1.list_dominoes(  8
     direction="horizontal", output_format="list_of_lists"))
sage: len(patterns_2x1_in_subst_shift)                                           9
30                                                                               10
sage: min(patterns_2x1_in_subst_shift) # show some minimal element               11
(0, 1)                                                                           12
sage: patterns_2x2_in_subst_shift = sorted(omega1.list_2x2_factors())            13
sage: len(patterns_2x2_in_subst_shift)                                           14
```

https://doi.org/10.1017/fms.2025.10069 Published online by Cambridge University Press

```
51
sage: min(patterns_2x2_in_subst_shift) # show some minimal element
[[0, 5], [3, 7]]
```

We choose a solver to compute the dominoes and 2×2 patterns below. Three reductions are available: to a mixed-integer linear program, to a SAT instance or to an exact cover problem solved with Knuth's dancing links algorithm [31]. We use Knuth's algorithm because it performs well and it is in SageMath by default.

```
sage: solver = "dancing_links" # other options are: solver="gurobi" or solver="kissat"
```

We define the set $\mathcal{T}_1$ of Wang tiles in an order consistent with the labeling of the tiles with the indices in the set $\{0, 1, 2, \ldots, 15\}$ as shown in Figure 31. We compute the patterns of size $s \in \{2\times2, 2\times1, 1\times2\}$ in the Wang shift Ω_1:

```
sage: from slabbe import WangTileSet
sage: tiles = [("111", "012", "112", "001"), ("111", "001", "111", "000"), ("112", "012", "
    112", "011"), ("112", "112", "111", "111"), ("111", "011", "112", "000"), ("011", "001
    ", "011", "012"), ("011", "011", "012", "012"), ("012", "112", "011", "112"), ("001",
    "000", "001", "011"), ("001", "001", "011", "011"), ("001", "011", "012", "011"), ("
    001", "111", "000", "111"), ("000", "000", "001", "001"), ("000", "001", "011", "001")
    , ("011", "111", "000", "112"), ("012", "111", "001", "112")]
sage: T1 = WangTileSet(tiles)
sage: T1
Wang tile set of cardinality 16
sage: patterns_1x2_in_sft = T1.dominoes_with_surrounding(i=2, radius=1, solver=solver)
sage: len(patterns_1x2_in_sft)
30
sage: min(patterns_1x2_in_sft) # show some minimal element
(0, 5)
sage: patterns_2x1_in_sft = T1.dominoes_with_surrounding(i=1, radius=1, solver=solver)
sage: len(patterns_2x1_in_sft)
30
sage: min(patterns_2x1_in_sft) # show some minimal element
(0, 1)
sage: patterns_2x2_in_sft = T1.tilings_with_surrounding(2,2, radius=3, solver=solver)
sage: patterns_2x2_in_sft = sorted(pattern.table() for pattern in patterns_2x2_in_sft)
sage: len(patterns_2x2_in_sft)
51
sage: min(patterns_2x2_in_sft) # show some minimal element
[[0, 5], [3, 7]]
```

We compare the sets of horizontal dominoes, vertical dominoes and 2×2 patterns computed above within the language of the substitutive subshift $\mathcal{X}_{\omega_1}$ and within the language of the Wang shift Ω_1. We observe their equality:

```
sage: patterns_1x2_in_subst_shift == patterns_1x2_in_sft
True
sage: patterns_2x1_in_subst_shift == patterns_2x1_in_sft
True
sage: patterns_2x2_in_subst_shift == patterns_2x2_in_sft
True
```

Therefore, the above computations prove that we have the following equality:

$$\mathcal{L}_s(\Omega_1) = \mathcal{L}_s(\mathcal{X}_{\omega_1})$$

for every size $s \in \{2\times2, 2\times1, 1\times2\}$. Thus, for every size $s \in \{2\times2, 2\times1, 1\times2\}$, we have

$$\mathcal{L}(\Omega_1) \cap \textsc{RecurrentVertices}(G^s_{\omega_1}) \subset \mathcal{L}_s(\Omega_1) = \mathcal{L}_s(\mathcal{X}_{\omega_1}) \subset \mathcal{L}(\mathcal{X}_{\omega_1}).$$

From Lemma 10.4, we conclude that Ω_1 is minimal and $\Omega_1 = \mathcal{X}_{\omega_1}$. □

https://doi.org/10.1017/fms.2025.10069 Published online by Cambridge University Press

10.4. Proof of Theorem D

Theorem D. *For every integer $n \geq 1$, the Wang shift Ω_n is minimal and is equal to the substitutive subshift $\Omega_n = \mathcal{X}_{\omega_n}$.*

Proof. If $n = 1$, then Ω_1 is minimal and $\Omega_1 = \mathcal{X}_{\omega_1}$ from Lemma 10.9. If $n \geq 2$, then Ω_n is minimal and $\Omega_n = \mathcal{X}_{\omega_n}$ from Proposition 10.8. □

11. Open questions

Note that the n^{th} metallic mean is a quadratic Pisot unit; that is, it is an algebraic unit of degree two, and all its algebraic conjugates have modulus strictly less than one. The other quadratic Pisot units are the positive roots of $x^2 - nx + 1$ for $n \geq 3$. The family of quadratic Pisot units has nice properties [10, 32, 41]; see also [3]. The continued fraction expansion of the positive root of $x^2 - nx + 1$ is $[n-1; (1, n-2)^\infty]$. In particular, it is not purely periodic.

Question 1. Let β be a positive quadratic Pisot unit which is not a metallic mean. Can we construct a self-similar set of Wang tiles whose inflation factor is β?

An alternative question is about those quadratic integers whose continued fraction expansion is purely periodic.

Question 2. Let β be a positive quadratic integer whose continued fraction expansion is purely periodic. Does there exist a set of Wang tiles such that the shift is self-similar with inflation factor equal to β?

The procedure explained in [24, p.594–598] starts from the Ammann A2 shapes shown in Figure 1 and constructs a set of 16 Wang tiles which we show in Theorem E to be equivalent to the set $\mathcal{T}_1$. A question we can ask is whether this construction can be inverted. More precisely, starting from the Ammann set of 16 Wang tiles, can we recover the two Ammann shapes shown in Figure 1 with their Ammann bars? In general, we ask the following question.

Question 3. For every integer $n \geq 1$, can we find geometrical shapes with Ammann bars on them such that encoding their tilings by rhombi along a pair of Ammann bars is equivalent to the tiles $\mathcal{T}_n$?

Theorem E together with the discussion [24, p.594–598] is an answer to Question 3 when $n = 1$. An answer to Question 3 would shed light on Mr. Ammann's remarkable insights [57].

Relation to the work of Mozes

Let $n \geq 1$ be an integer and recall the 1-dimensional substitution

$$\rho_n = \begin{cases} \mathtt{a} \mapsto \mathtt{a}\mathtt{b}^n \\ \mathtt{b} \mapsto \mathtt{a}\mathtt{b}^{n-1} \end{cases}$$

over alphabet $\{\mathtt{a}, \mathtt{b}\}$ defined in the proof of Lemma 9.2. The incidence matrix of ρ_n is $\left(\begin{smallmatrix} 1 & 1 \\ n & n-1 \end{smallmatrix}\right)$ whose characteristic polynomial is $x^2 - nx - 1$, and whose Perron–Frobenius dominant eigenvalue is the n^{th} metallic mean. A right dominant eigenvector is $\left(\begin{smallmatrix} 1 \\ \beta_n - 1 \end{smallmatrix}\right)$ and a left dominant eigenvector is $\left(\begin{smallmatrix} n & \beta_n - 1 \end{smallmatrix}\right)$. Following the theory on inflation tilings [5, §6], a stone inflation associated with the substitution ρ_n gives a volume of n to the letter $\mathtt{a}$ and a volume of $\beta_n - 1$ to the letter $\mathtt{b}$. The stone inflation induced by the direct product $\rho_n \times \rho_n$ of the substitution ρ_n with itself in the sense of [43, §6] is shown in Figure 30; see also [5, Example 5.9]. Note that another substitution with same inflation factor and often used in examples illustrating metallic means is $\mathtt{a} \mapsto \mathtt{a}^n\mathtt{b}, \mathtt{b} \mapsto \mathtt{a}$ [5, Remark 4.7].

From the work of Mozes [43], we know that there exists a tiling system given by a finite set of tiles and a finite set of matching rules such that the tiling system is a symbolic extension of the substitutive dynamical system generated by the 2-dimensional substitution $\rho_n \times \rho_n$ over a four-letter alphabet. Since

https://doi.org/10.1017/fms.2025.10069 Published online by Cambridge University Press

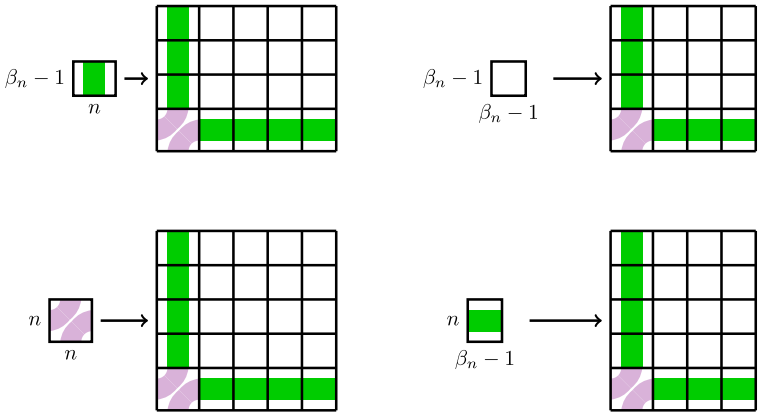

Figure 30. *Stone inflation associated with the direct product of the substitution ρ_n with itself with inflation factor equal to β_n, the n^{th} metallic mean. The size of the rectangles are given by the entries of a Perron–Frobenius dominant left-eigenvector of the incidence matrix of ρ_n. The figure is drawn with parameter $n = 4$. Color is added to the tiles to differentiate them and visually link them to the tiles in $\mathcal{T}_n$.*

the substitution $\rho_n \times \rho_n$ is recognizable (or has 'unique derivation', using the vocabulary of Mozes), the tiling system constructed by Mozes is even measure-theoretically isomorphic to the substitutive dynamical system. Note that the construction of an equivalent tiling system out of a substitution was extended to geometric substitutions [23].

In this contribution, we provide an explicit construction of a tiling system Ω_n which is a symbolic extension of the 2-dimensional substitutive subshift defined by $\rho_n \times \rho_n$. The set of Wang tiles deduced from [43] when applied on $\rho_n \times \rho_n$ would be much larger than $(n+3)^2$. This raises a question about the optimality of a tiling system for 2-dimensional substitutions.

Question 4. Is the size of $\mathcal{T}_n$ optimal? In other words, does there exist a set $\mathcal{T}$ of Wang tiles of cardinality $\#\mathcal{T} < (n+3)^2$ such that the Wang shift $\Omega_{\mathcal{T}}$ is isomorphic to the 2-dimensional substitutive subshift $\mathcal{X}_{\rho_n \times \rho_n}$?

A. Appendix A: The substitutions ω_n for $1 \le n \le 5$

Figure 31. *Substitution ω_1.*

https://doi.org/10.1017/fms.2025.10069 Published online by Cambridge University Press

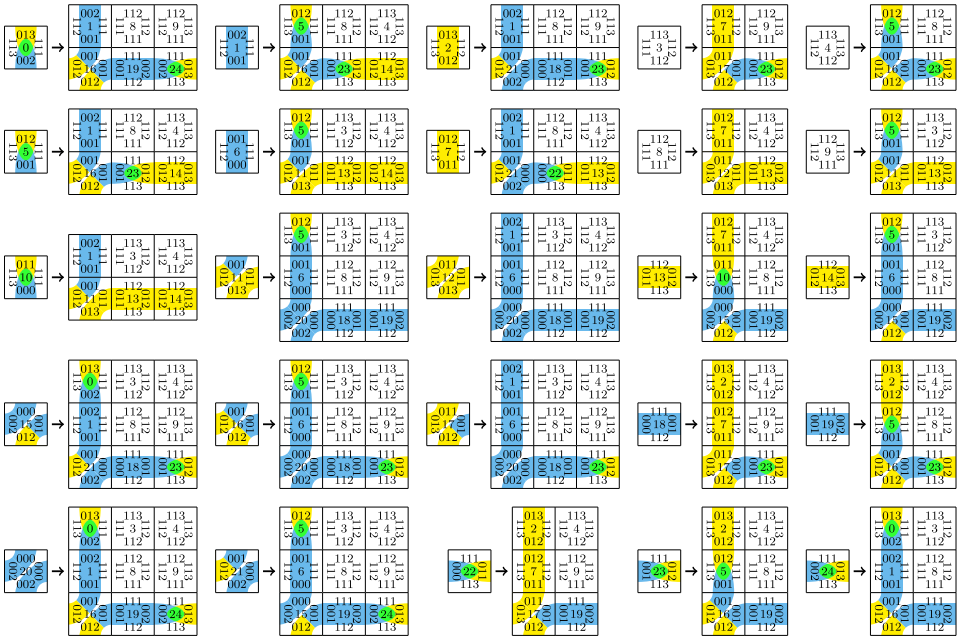

Figure 32. *Substitution ω_2.*

https://doi.org/10.1017/fms.2025.10069 Published online by Cambridge University Press

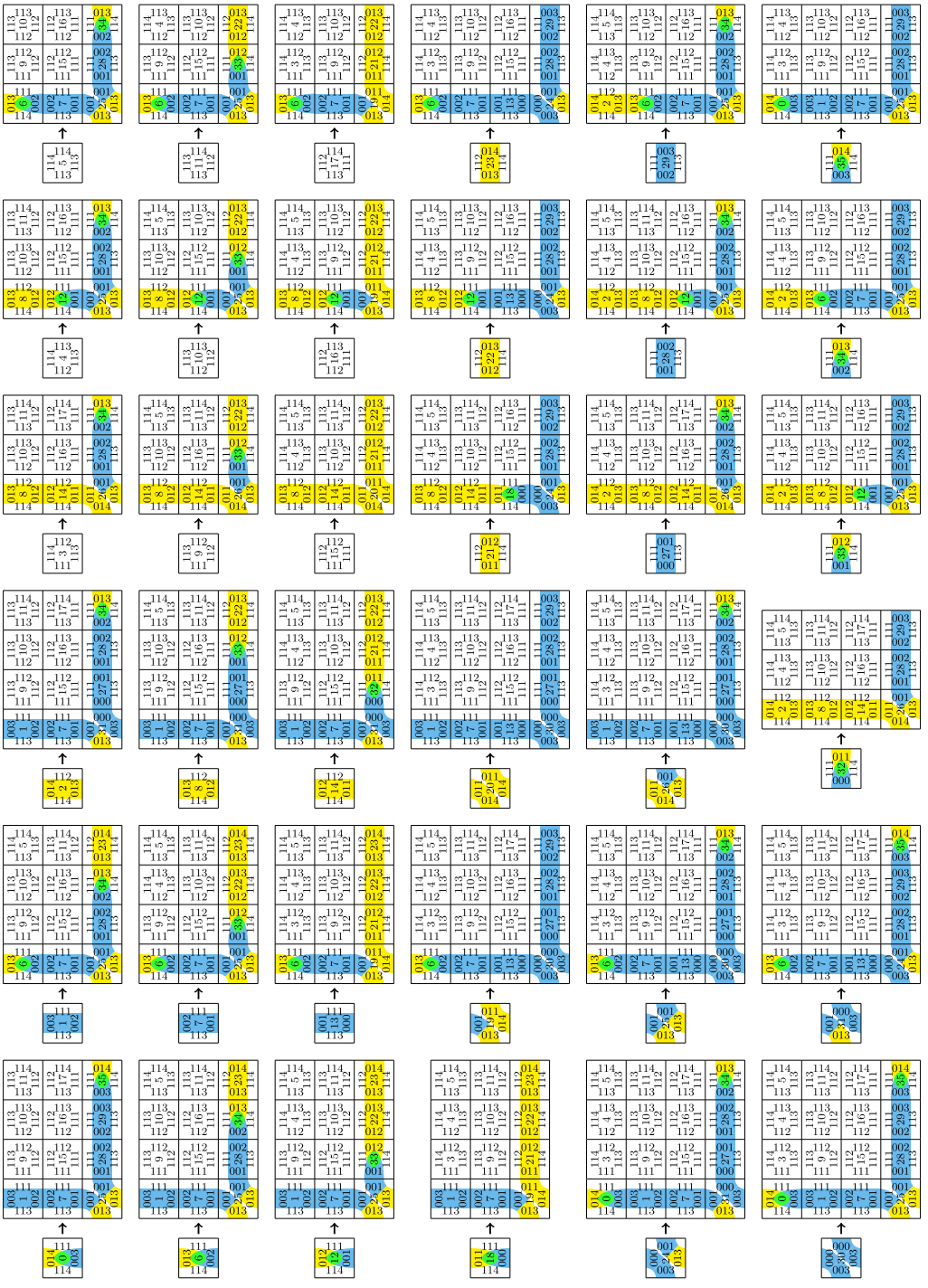

Figure 33. *Substitution ω_3 (rotated 90 degrees counterclockwise).*

https://doi.org/10.1017/fms.2025.10069 Published online by Cambridge University Press

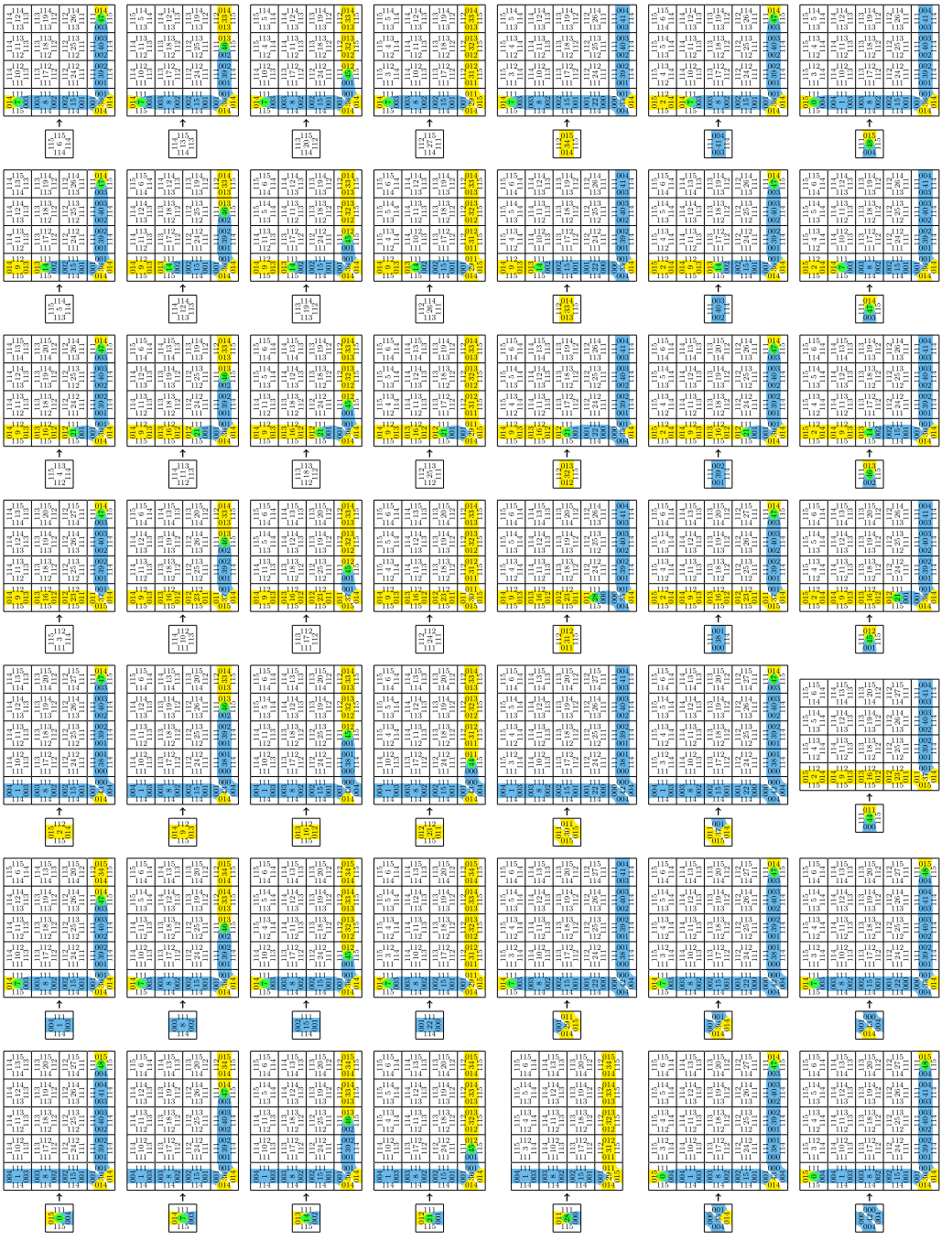

Figure 34. *Substitution ω_4 (rotated 90 degrees counterclockwise).*

https://doi.org/10.1017/fms.2025.10069 Published online by Cambridge University Press

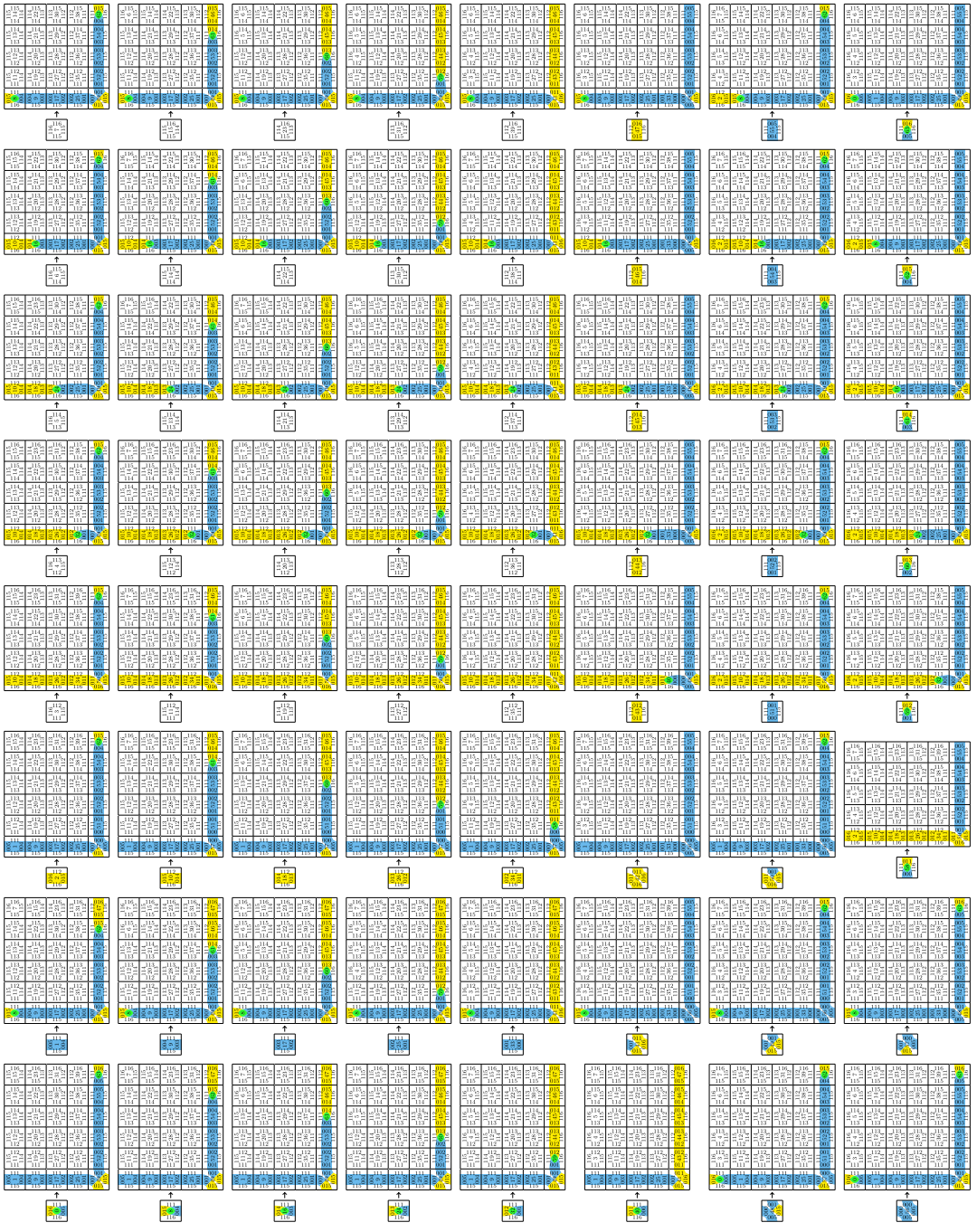

Figure 35. *Substitution ω_5 (rotated 90 degrees counterclockwise).*

https://doi.org/10.1017/fms.2025.10069 Published online by Cambridge University Press

B. Appendix B: Proving the self-similarity of Ω_2 in SageMath

In this section, we illustrate how Theorem A can be proved in SageMath for a specific but not too big integer $n \geq 1$. Since the proof of Theorem A given in this article was deduced from such computer experiments performed for small values of n, we hope that the approach shown below can be used to study and show the self-similarity of other aperiodic set of Wang tiles.

We use here a method proposed in [35] to study the substitutive structure of the Jeandel–Rao Wang shift [26]. The method is based on the notion of marker tiles (not to be confused with the notion of marker used in Lemma 10.1.8 from [40]). A nonempty subset $M \subset \mathcal{A}$ is called **markers for the direction $\boldsymbol{e}_2$** within a subshift $X \subset \mathcal{A}^{\mathbb{Z}^2}$ if for every configuration $x \in X$, the positions of the markers are nonadjacent rows; that is, $x^{-1}(M) = \mathbb{Z} \times P$ for some set $P \subset \mathbb{Z}$ such that $1 \notin P - P$. A symmetric definition holds for **markers for the direction $\boldsymbol{e}_1$**. It was proved that the existence of marker tiles allows to decompose uniquely a Wang shift. Informally, marker tiles are merged with the tiles that appear just on top of (or just below) them. Remaining tiles are kept unchanged. The search for markers and the construction of the substitution is performed by two algorithms FindMarkers and FindSubstitution. Their pseudocode can be found in [35]; see also the chapter [37] where a simpler example is considered.

Below, we prove the self-similarity of Ω_n when $n = 2$ using SageMath [54] with optional package `slabbe` [38]. The algorithms FindMarkers and FindSubstitution are used twice horizontally and then twice vertically. The computations show that every configuration in Ω_2 can be decomposed uniquely into 25 supertiles. The 25 supertiles are equivalent to the original set of 25 tiles. Thus, the Wang shift Ω_2 is self-similar and we compute the self-similarity.

We choose a solver to search for markers and desubstitutions below.

```
sage: solver = "dancing_links" # other options are: solver="gurobi" or solver="kissat"
```

First, we define the set $\mathcal{T}_2$ of Wang tiles.

```
sage: from slabbe import WangTileSet
sage: tiles = [("111", "013", "113", "002"), ("111", "002", "112", "001"), ("112", "013", "
    113", "012"), ("112", "113", "111", "112"), ("113", "113", "112", "112"), ("111", "012
    ", "113", "001"), ("111", "001", "112", "000"), ("112", "012", "113", "011"), ("112",
    "112", "111", "111"), ("113", "112", "112", "111"), ("111", "011", "113", "000"), ("
    011", "001", "012", "013"), ("011", "011", "013", "013"), ("012", "112", "011", "113")
    , ("013", "112", "012", "113"), ("001", "000", "002", "012"), ("001", "001", "012", "
    012"), ("001", "011", "013", "012"), ("001", "111", "000", "112"), ("002", "111", "001
    ", "112"), ("000", "000", "002", "002"), ("000", "001", "012", "002"), ("011", "111",
    "000", "113"), ("012", "111", "001", "113"), ("013", "111", "002", "113")]
sage: T2 = WangTileSet(tiles)
sage: T2_tikz = T2.tikz(ncolumns=10, scale=1.2, label_shift=.15)
```

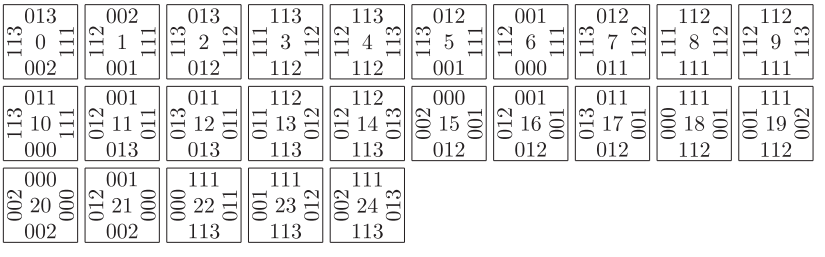

Then, we search for markers for the direction $\boldsymbol{e}_1$ (such markers appear on nonadjacent columns). We fusion the markers with the possible tiles appearing on their right (thus the marker appear on the left side of each pair).

```
sage: T2.find_markers(i=1, radius=1, solver=solver)
[[0, 1, 2, 5, 6, 7, 10, 11, 12, 15, 16, 17, 20, 21]]
sage: M = [0, 1, 2, 5, 6, 7, 10, 11, 12, 15, 16, 17, 20, 21]
```

https://doi.org/10.1017/fms.2025.10069 Published online by Cambridge University Press

```
sage: U1, s1 = T2.find_substitution(M=M, i=1, radius=2, solver=solver, side="left")
sage: s1_tikz = s1.wang_tikz(domain_tiles=U1, codomain_tiles=T2, ncolumns=5, scale=1.2,
    label_shift=.15, direction="left", extra_space=1.2)
```

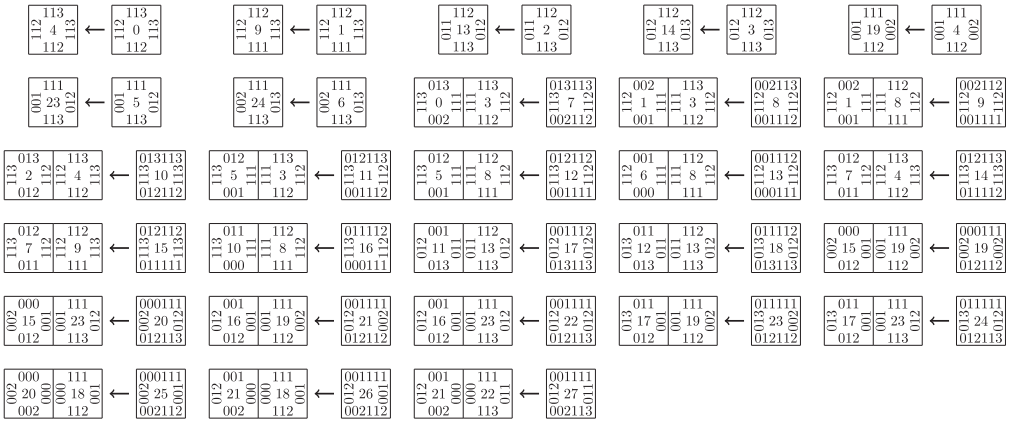

The resulting set of Wang tiles (shown above at the source of the arrows) is obtained by concatenating the top and bottom labels of the merged pairs:

```
sage: U1_tikz = U1.tikz(scale=1.4, label_shift=0.15)
```

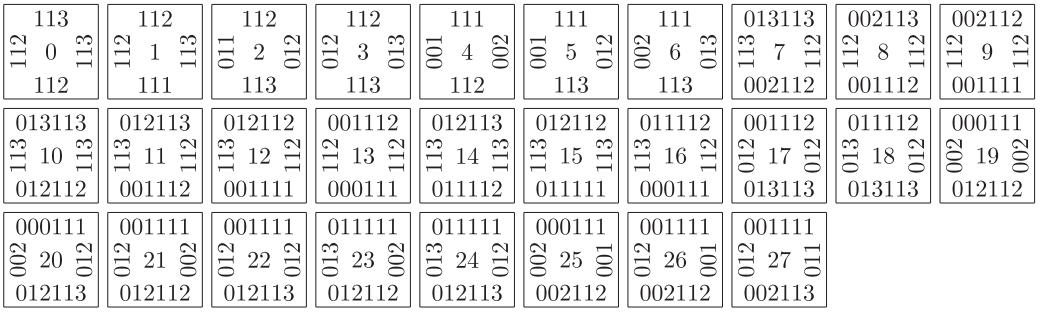

```
sage: U1.find_markers(i=1, radius=1, solver=solver)
[[0, 1, 2, 3, 4, 5, 6]]
sage: M = [0, 1, 2, 3, 4, 5, 6]
sage: U2, s2 = U1.find_substitution(M=M, i=1, radius=1, solver=solver)
sage: U2_tikz = U2.tikz(scale=1.7, label_shift=0.15, ncolumns=12)
```

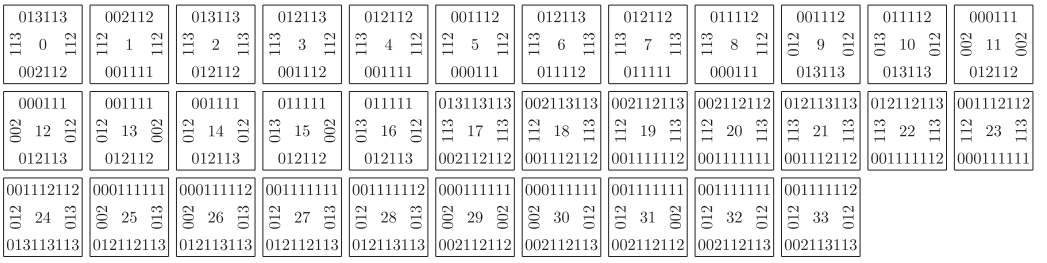

https://doi.org/10.1017/fms.2025.10069 Published online by Cambridge University Press

```
sage: U2.find_markers(i=2, radius=1, solver=solver)                                    62
[[9, 10, 11, 12, 13, 14, 15, 16, 24, 25, 27, 28, 29, 30, 31, 32, 33]]                  63
sage: M = [9, 10, 11, 12, 13, 14, 15, 16, 24, 25, 27, 28, 29, 30, 31, 32, 33]          64
sage: U3, s3 = U2.find_substitution(M=M, i=2, radius=1, solver=solver, side="left")     65
sage: U3_tikz = U3.tikz(scale=1.9, label_shift=0.1)                                    66
```

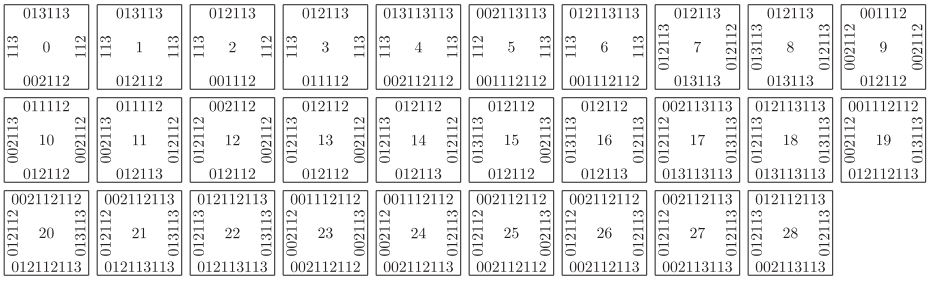


```
sage: U3.find_markers(i=2, radius=1, solver=solver)                                    67
[[0, 1, 2, 3, 4, 5, 6]]                                                                68
sage: M = [0, 1, 2, 3, 4, 5, 6]                                                        69
sage: U4, s4 = U3.find_substitution(M=M, i=2, radius=1, solver=solver)                 70
sage: U4_tikz = U4.tikz(scale=2.2, label_shift=.1)                                     71
```

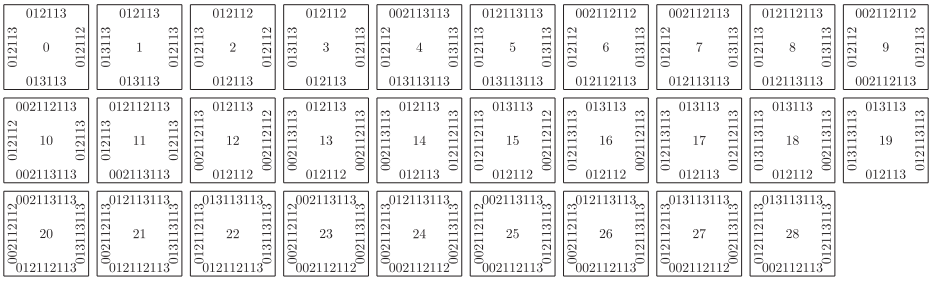

It turns out that tiles with indices 11, 14, 20, 27 are not needed within the above set of tiles as they do not have a surrounding of radius 2 as confirmed by the following computation. Thus, they cannot appear in any tiling. In fact, they correspond to antigreen tiles and other tiles proved to be illegal in Section 7. We compute the remaining twenty five tiles below.

```
sage: U5 = U4.tiles_allowing_surrounding(radius=2, solver=solver)                      72
sage: U5_tikz = U5.tikz(scale=2.1, label_shift=.1)                                     73
```

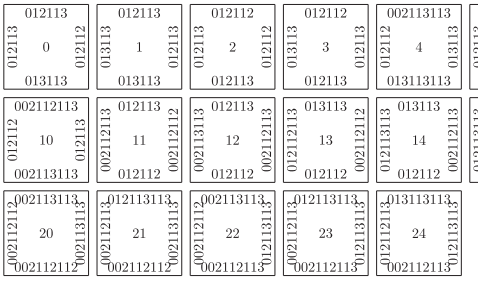

https://doi.org/10.1017/fms.2025.10069 Published online by Cambridge University Press

```
sage: U4_tiles = U4.tiles()                                                    74
sage: U5_tiles = U5.tiles()                                                    75
sage: d = {i:U4_tiles.index(U5_tiles[i]) for i in range(len(U5))}              76
sage: from slabbe import Substitution2d                                        77
sage: s5 = Substitution2d.from_permutation(d)                                  78
```

We confirm that the set U_5 is equivalent to the set $\mathcal{T}_n$ of Wang tiles we started with. We extract the bijection `s6` between the indices of the tiles. Also, it gives a bijection for the horizontal edge labels and vertical edge labels. Both are equal. This bijection corresponds to the map τ_n when $n = 2$ defined in Section 5.1.

```
sage: T2.is_equivalent(U5)                                                     79
True                                                                           80
sage: _,vert_bijection,horiz_bijection,s6 = T2.is_equivalent(U5, certificate=True)  81
sage: vert_bijection == horiz_bijection                                        82
True                                                                           83
sage: vert_bijection                                                           84
{'113': '012112', '111': '013113', '112': '012113', '012': '002112113', '011': '002113113',  85
 '013': '002112112', '001': '012113113', '000': '013113113', '002': '012112113'}
```

One may compare the bijection computed above with the map τ_n defined in Section 5. The only difference is that the image of the label 003 does not appear in the computed bijection above because it is does not appear as an edge label in the set $\mathcal{T}_2$.

The self-similarity is:

```
sage: self_similarity = s1*s2*s3*s4*s5*s6                                      86
sage: self_similarity                                                          87
```

$$0 \mapsto \begin{pmatrix} 1 & 8 & 9 \\ 16 & 19 & 24 \end{pmatrix}, \quad 1 \mapsto \begin{pmatrix} 5 & 8 & 4 \\ 16 & 23 & 14 \end{pmatrix}, \quad 2 \mapsto \begin{pmatrix} 1 & 8 & 9 \\ 21 & 18 & 23 \end{pmatrix}, \quad 3 \mapsto \begin{pmatrix} 7 & 9 \\ 17 & 23 \end{pmatrix}, \quad 4 \mapsto \begin{pmatrix} 5 & 8 \\ 16 & 23 \end{pmatrix},$$
$$5 \mapsto \begin{pmatrix} 1 & 8 & 4 \\ 16 & 23 & 14 \end{pmatrix}, \quad 6 \mapsto \begin{pmatrix} 5 & 3 & 4 \\ 11 & 13 & 14 \end{pmatrix}, \quad 7 \mapsto \begin{pmatrix} 1 & 8 & 4 \\ 21 & 22 & 13 \end{pmatrix}, \quad 8 \mapsto \begin{pmatrix} 7 & 4 \\ 12 & 13 \end{pmatrix}, \quad 9 \mapsto \begin{pmatrix} 5 & 3 \\ 11 & 13 \end{pmatrix},$$
$$10 \mapsto \begin{pmatrix} 1 & 3 & 4 \\ 11 & 13 & 14 \end{pmatrix}, 11 \mapsto \begin{pmatrix} 5 & 3 & 4 \\ 6 & 8 & 9 \\ 20 & 18 & 19 \end{pmatrix}, 12 \mapsto \begin{pmatrix} 1 & 3 & 4 \\ 6 & 8 & 9 \\ 20 & 18 & 19 \end{pmatrix}, 13 \mapsto \begin{pmatrix} 7 & 4 \\ 10 & 8 \\ 15 & 19 \end{pmatrix}, 14 \mapsto \begin{pmatrix} 5 & 3 \\ 6 & 8 \\ 15 & 19 \end{pmatrix},$$
$$15 \mapsto \begin{pmatrix} 0 & 3 & 4 \\ 1 & 8 & 9 \\ 21 & 18 & 23 \end{pmatrix}, 16 \mapsto \begin{pmatrix} 5 & 3 & 4 \\ 6 & 8 & 9 \\ 20 & 18 & 23 \end{pmatrix}, 17 \mapsto \begin{pmatrix} 1 & 3 & 4 \\ 6 & 8 & 9 \\ 20 & 18 & 23 \end{pmatrix}, 18 \mapsto \begin{pmatrix} 2 & 4 \\ 7 & 9 \\ 17 & 23 \end{pmatrix}, 19 \mapsto \begin{pmatrix} 2 & 4 \\ 5 & 8 \\ 16 & 23 \end{pmatrix},$$
$$20 \mapsto \begin{pmatrix} 0 & 3 & 4 \\ 1 & 8 & 9 \\ 16 & 19 & 24 \end{pmatrix}, 21 \mapsto \begin{pmatrix} 5 & 3 & 4 \\ 6 & 8 & 9 \\ 15 & 19 & 24 \end{pmatrix}, 22 \mapsto \begin{pmatrix} 2 & 4 \\ 7 & 9 \\ 17 & 19 \end{pmatrix}, \quad 23 \mapsto \begin{pmatrix} 2 & 4 \\ 5 & 8 \\ 16 & 19 \end{pmatrix}, 24 \mapsto \begin{pmatrix} 0 & 3 \\ 1 & 8 \\ 16 & 19 \end{pmatrix}.$$

The characteristic polynomial of the incidence matrix of the self-similarity is:

```
sage: matrix(self_similarity).charpoly().factor()                              88
```

$$(x-1)^3 \cdot (x+1)^5 \cdot x^{11} \cdot (x^2 - 6x + 1) \cdot (x^2 + 2x - 1)^2$$

The self-similarity shown with the associated Wang tiles:

```
sage: sim_tikz = self_similarity.wang_tikz(domain_tiles=T2, codomain_tiles=T2, ncolumns=5,  89
    scale=1.2, label_shift=.15)
```

https://doi.org/10.1017/fms.2025.10069 Published online by Cambridge University Press

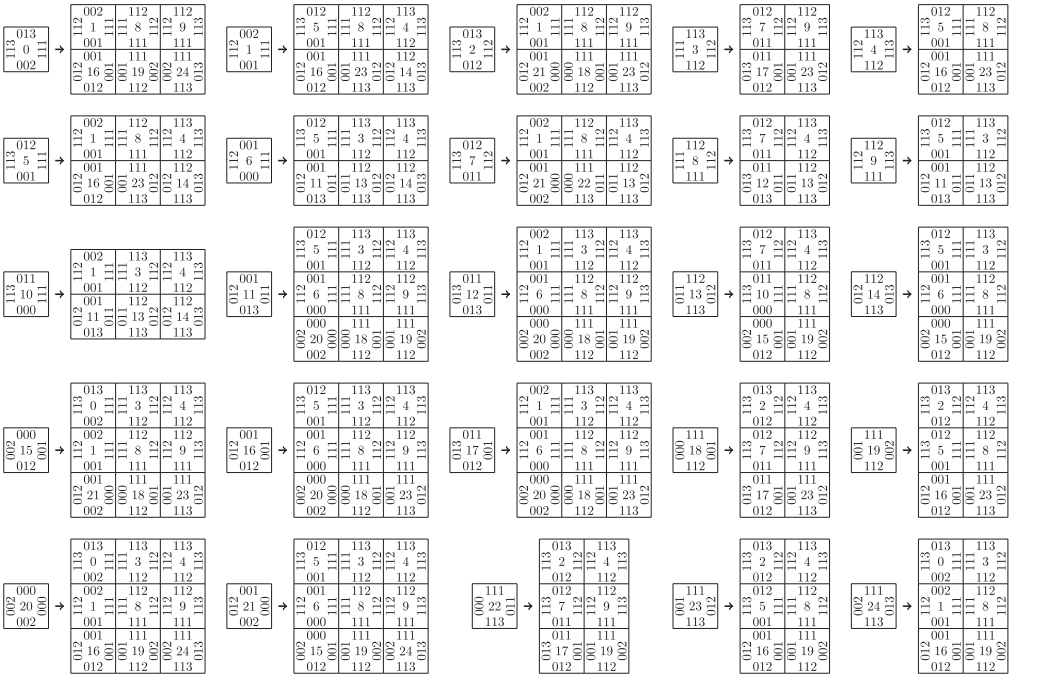

Acknowledgements. The author is thankful to the reviewers for their careful reading and remarks which led, in particular, to an improved and more formal proof of the self-similarity of ω_n. The author also wants to thank Dirk Frettlöh for making him aware of other existing aperiodic substitutive tilings involving metallic mean numbers, including the bronze mean [14].

Competing interest. The authors have no competing interests to declare.

Funding statement. This work was partly funded from France's Agence Nationale de la Recherche (ANR) projects CODYS (ANR-18-CE40-0007) and IZES (ANR-22-CE40-0011). It was also supported by grants from the *Symbolic Dynamics and Arithmetic Expansions* (SymDynAr) Project, co-funded by ANR (ANR-23-CE40-0024) and FWF (https://doi.org/10.55776/I6750), the Austrian Science Fund.

Reproducibility statement. All results proved in this article are proved by hand except the proof of Lemma 10.9 and the computations performed in Appendix B, which are based on the open-source mathematical software SageMath [54] and the optional package `slabbe` [38]. All SageMath input/output blocks in this article were created using the `sageexample` environment with SageTeX version `2021/10/16 v3.6` and with the following software versions:

```
sage: version()                                                          90
SageMath version 10.6.beta7, Release Date: 2025-02-21                    91
sage: import importlib.metadata                                          92
sage: importlib.metadata.version("slabbe")                               93
0.8.0                                                                    94
```

The fact that these software are open-source means that anyone is free to use, reproduce, verify, adapt for their own needs all of the computations performed therein according to the GNU General Public License (version 2, 1991, http://www.gnu.org/licenses/gpl.html).

The contents of all of the `sageexample` environments from the tex source are gathered in the file `demos/arXiv_2312_03652_doctest.sage` autogenerated by SageTeX when running `pdflatex`. This file is included in the `slabbe` package and available at https://gitlab.com/seblabbe/slabbe/. It allows to make sure that future releases of the package do not break the code included in this article. It is possible to reproduce all computations present in this article and check that all outputs are correct, by *doctesting* this file – that is, by running the command `sage -t demos/arXiv_2312_03652_doctest.sage`. It should output `All tests passed!` and `[67 tests, 31.02s wall]` (most probably with a different timing).

References

[1] S. Akiyama, 'A note on aperiodic Ammann tiles', *Discrete Comput. Geom.* **48**(3) (2012), 702–710.
[2] S. Akiyama and Y. Araki, 'An alternative proof for an aperiodic monotile', Preprint, 2023, arxiv:2307.12322.

[3] S. Akiyama and V. Komornik, 'Discrete spectra and Pisot numbers', *J. Number Theory* **133**(2) (2013), 375–390.
[4] R. Ammann, B. Grünbaum and G. C. Shephard, 'Aperiodic tiles', *Discrete Comput. Geom.* **8**(1) (1992), 1–25.
[5] M. Baake and U. Grimm. *Aperiodic Order. Vol. 1* (Encyclopedia of Mathematics and Its Applications) vol. 149 (Cambridge University Press, Cambridge, 2013).
[6] M. Baake, F. Gähler and L. Sadun, 'Dynamics and topology of the Hat family of tilings', Preprint, 2023, arxiv:2305.05639.
[7] F. P. M. Beenker, *Algebraic Theory of Non-Periodic Tilings of the Plane by Two Simple Building Blocks: A Square and a Rhombus* (EUT-Rep.) (Eindhoven 82-WSK-04, 1982).
[8] R. Berger, 'The undecidability of the domino problem', *Mem. Amer. Math. Soc. No.* **66** (1966), 72.
[9] V. Berthé, W. Steiner, J. M. Thuswaldner and R. Yassawi, 'Recognizability for sequences of morphisms', *Ergodic Theory Dynam. Systems* **39**(11) (2019), 2896–2931.
[10] P. Borwein and K. G. Hare, 'General forms for minimal spectral values for a class of quadratic Pisot numbers', *Bull. London Math. Soc.* **35**(1) (2003). 47–54.
[11] E. Charlier, T. Kärki and M. Rigo, 'Multidimensional generalized automatic sequences and shape-symmetric morphic words', *Discrete Math.* **310**(6–7) (2010), 1238–1252.
[12] N. Govert de Bruijn, 'Algebraic theory of Penrose's nonperiodic tilings of the plane, I, II', *Nederl. Akad. Wetensch. Indag. Math.* **43**(1) (1981), 39–52, 53–66.
[13] V. W. de Spinadel, 'The family of metallic means,' *Vis. Math.* **1**(3) (1999), 1 HTML document; approx. 16.
[14] T. Dotera, S. Bekku and P. Ziherl, 'Bronze-mean hexagonal quasicrystal', *Nature Materials* **16**(10) (2017), 987–992.
[15] B. Durand, A. Shen and N. Vereshchagin, 'On the structure of Ammann A2 tilings', *Discrete Comput. Geom.* **63**(3) (2020), 577–606.
[16] F. Durand, 'A characterization of substitutive sequences using return words', *Discrete Math.* **179**(1–3) (1998), 89–101.
[17] D. Frettlöh, A. L. D. Say-awen and M. L. A. N. De Las Peñas, 'Substitution tilings with dense tile orientations and n-fold rotational symmetry', *Indag. Math., New Ser.* **28**(1) (2017), 120–131.
[18] D. Frettlöh, 'More inflation tilings', In *Aperiodic order Vol. 2*. (Encyclopedia Math. Appl.) vol. 166 (Cambridge Univ. Press, Cambridge, 2017), 1–37.
[19] D. Frettlöh, A. Garber and N. Mañibo, 'Substitution tilings with transcendental inflation factor', *Discrete Anal.* (2024), Paper No. 11, 24.
[20] D. Frettlöh, E. Harriss and F. Gähler, 'Tilings encyclopedia: Bronze-mean tiling', 2023, https://tilings.math.uni-bielefeld.de/substitution/bronze-mean/.
[21] F. Gähler, A. Julien and J Savinien, 'Combinatorics and topology of the Robinson tiling', *C. R. Math. Acad. Sci. Paris* **350**(11–12) (2012), 627–631.
[22] F. Gähler, E. E. Kwan and G. R. Maloney, 'A computer search for planar substitution tilings with n-fold rotational symmetry', *Discrete Comput. Geom.* **53**(2) (2015), 445–465.
[23] C. Goodman-Strauss, 'Matching rules and substitution tilings', *Ann. of Math. (2)* **147**(1) (1998), 181–223.
[24] B. Grünbaum and G. C. Shephard, *Tilings and Patterns* (W. H. Freeman and Company, New York, 1987).
[25] M. Hochman, 'Multidimensional shifts of finite type and sofic shifts', in *Combinatorics, Words and Symbolic Dynamics (Encyclopedia Math. Appl.)* vol. 159 (Cambridge Univ. Press, Cambridge, 2016), 296–358.
[26] E. Jeandel and M. Rao, 'An aperiodic set of 11 Wang tiles', *Adv. Comb.* **2021** (2021), 37. Id/No 1.
[27] J. Kari and P. Papasoglu, 'Deterministic aperiodic tile sets', *Geom. Funct. Anal.* **9**(2) (1999), 353–369.
[28] J. Kari and V. H. Lutfalla, 'Substitution discrete plane tilings with $2n$-fold rotational symmetry for odd n', *Discrete Comput. Geom.* **69**(2) (2023), 349–398.
[29] J. Kari and M. Rissanen, 'Sub Rosa, a system of quasiperiodic rhombic substitution tilings with n-fold rotational symmetry', *Discrete Comput. Geom.* **55**(4) (2016), 972–996.
[30] D. E. Knuth, *The Art of Computer Programming. Vol. 1: Fundamental Algorithms*, second printing (Addison-Wesley Publishing Co., Reading, Mass.-London-Don Mills, Ont, 1969).
[31] D. E. Knuth, 'Dancing links', in *Millenial Perspectives in Computer Science* (Red Globe Press, London, 2000), 187–214, arxiv:cs/0011047.
[32] T. Komatsu, 'An approximation property of quadratic irrationals', *Bull. Soc. Math. France* **130**(1) (2002), 35–48.
[33] S. Labbé, 'A self-similar aperiodic set of 19 Wang tiles', *Geom. Dedicata* **201** (2019), 81–109.
[34] S. Labbé, 'Markov partitions for toral $\mathbb{Z}^2$-rotations featuring Jeandel-Rao Wang shift and model sets', *Ann. H. Lebesgue* **4** (2021), 283–324.
[35] S. Labbé, 'Substitutive structure of Jeandel-Rao aperiodic tilings', *Discrete Comput. Geom.* **65**(3) (2021), 800–855.
[36] S. Labbé, C. Mann and J. McLoud-Mann, 'Nonexpansive directions in the Jeandel-Rao Wang shift', *Discrete Contin. Dyn. Syst.* **43**(9) (2023), 3213–3250.
[37] S. Labbé, 'Three characterizations of a self-similar aperiodic 2-dimensional subshift', Preprint, 2020, arxiv:2012.03892.
[38] S. Labbé, Optional SageMath Package slabbe (Version 0.7.7), 2024, https://pypi.python.org/pypi/slabbe/.
[39] D. Lind, 'Multi-dimensional symbolic dynamics', in *Symbolic Dynamics and Its Applications* (Proc. Sympos. Appl. Math.) vol. 60 (Amer. Math. Soc., Providence, RI, 2004), 61–79.
[40] D. Lind and B. Marcus, *An Introduction to Symbolic Dynamics and Coding* (Cambridge University Press, Cambridge, 1995).
[41] Z. Masáková, K. Pastirčáková and E. Pelantová, 'Description of spectra of quadratic Pisot units', *J. Number Theory* **150** (2015), 168–190.

https://doi.org/10.1017/fms.2025.10069 Published online by Cambridge University Press

[42] B. Mossé, 'Puissances de mots et reconnaissabilité des points fixes d'une substitution', *Theoret. Comput. Sci.* **99**(2) (1992), 327–334.
[43] S. Mozes, 'Tilings, substitution systems and dynamical systems generated by them', *J. Analyse Math.* **53** (1989), 139–186.
[44] J. Nakakura, P. Ziherl, J. Matsuzawa and T. Dotera, 'Metallic-mean quasicrystals as aperiodic approximants of periodic crystals', *Nature Communications* **10**(1) (2019), Article number: 4235.
[45] OEIS Foundation Inc., 'Entry A352403 in the on-line encyclopedia of integer sequences', 2023, https://oeis.org/A352403.
[46] OEIS Foundation Inc., 'Metallic means', 2023, https://oeis.org/wiki/Metallic_means.
[47] S. Pautze, 'Cyclotomic aperiodic substitution tilings', *Symmetry* **9**(2) (2017), Article number: 19.
[48] R. Penrose, 'The rôle of aesthetics in pure and applied mathematical research', *Bull. Inst. Math. Appl.* **10**(Jul–Aug) (1974), 266–271.
[49] R. Penrose, 'Pentaplexity. A class of non-periodic tilings of the plane', *Math. Intell.* **2** (1979), 32–37.
[50] R. Penrose, 'Remarks on tiling: Details of a $(1+\varepsilon+\varepsilon^2)$-aperiodic set', in *The Mathematics of Long-Range Aperiodic Order. Proceedings of the NATO Advanced Study Institute, Waterloo, Ontario, Canada, August 21–September 1, 1995* (Kluwer Academic Publishers, Dordrecht, 1997), 467–497.
[51] M. Queffélec, *Substitution Dynamical Systems—Spectral Analysis* (Lecture Notes in Mathematics) vol. 1294, second edn. (Springer-Verlag, Berlin, 2010).
[52] E. A. Robinson, 'On the table and the chair', *Indag. Math., New Ser.* **10**(4) (1999), 581–599.
[53] R. M. Robinson, 'Undecidability and nonperiodicity for tilings of the plane', *Invent. Math.* **12** (1971), 177–209.
[54] Sage Developers, *SageMath, the Sage Mathematics Software System (Version 10.5)*, 2024, http://www.sagemath.org.
[55] K. Schmidt, 'Multi–dimensional symbolic dynamical systems', in *Codes, Systems, and Graphical Models (Minneapolis, MN, 1999)* (IMA Vol. Math. Appl.) vol. 123 (Springer, New York, 2001), 67–82.
[56] M. Schroeder, Fractals, Chaos, Power Laws. *Minutes from an Infinite Paradise* (W.H. Freeman and Company, New York, 1991).
[57] M. Senechal, 'The mysterious Mr. Ammann', *Math. Intelligencer* **26**(4) (2004), 10–21.
[58] D. Smith, J. S. Myers, C. S. Kaplan and C. Goodman-Strauss, 'An aperiodic monotile', *Comb. Theory* **4**(1) (2024), Paper No. 6, 91.
[59] D. Smith, J. S. Myers, C. S. Kaplan and C. Goodman-Strauss, 'A chiral aperiodic monotile', *Comb. Theory* **4**(2) (2024), Paper No. 13, 25.
[60] J. E. S. Socolar, 'Quasicrystalline structure of the hat monotile tilings', *Phys. Rev. B* **108** (2023), 224109.
[61] J. E. S. Socolar and J. M. Taylor, 'An aperiodic hexagonal tile', *J. Combin. Theory Ser. A* **118**(8) (2011), 2207–2231.
[62] B. Solomyak, 'Nonperiodicity implies unique composition for self-similar translationally finite tilings', *Discrete Comput. Geom.* **20**(2) (1998), 265–279.
[63] B. Solomyak, 'Dynamics of self-similar tilings', *Ergodic Theory Dynam. Systems* **17**(3) (1997), 695–738.
[64] L. Vuillon, 'A characterization of Sturmian words by return words', *European J. Combin.* **22**(2) (2001), 263–275.
[65] P. Walters, *An Introduction to Ergodic Theory (GTM)* vol. 79 (Springer-Verlag, New York-Berlin, 1982).
[66] H. Wang, 'Proving theorems by pattern recognition – II', *Bell System Technical Journal* **40**(1) (1961), 1–41.

https://doi.org/10.1017/fms.2025.10069 Published online by Cambridge University Press